

สารที่มีฤทธิ์ยับยั้งเอนไซม์แอลฟาไกลูโคซิเดสจากต้น

GYNURA PROCUMBENS



นางสาว จิรานุช มิ่งเมือง

สภามหาวิทยาลัยบูรพา
วิทยานิพนธ์นี้เป็นส่วนหนึ่งของการศึกษาตามหลักสูตรปริญญาเภสัชศาสตรมหาบัณฑิต

สาขาวิชาเภสัชเวช ภาควิชาเภสัชเวช
คณะเภสัชศาสตร์ จุฬาลงกรณ์มหาวิทยาลัย

ปีการศึกษา 2550

ลิขสิทธิ์ของจุฬาลงกรณ์มหาวิทยาลัย

α -GLUCOSIDASE INHIBITORS FROM
GYNURA PROCUMBENS

Miss Jiranuch Mingmuang



A Thesis Submitted in Partial Fulfillment of the Requirements
for the Degree of Master of Science in Pharmacy Program in Pharmacognosy

Department of Pharmacognosy
Faculty of Pharmaceutical Sciences

Chulalongkorn University

Academic Year 2007

Copyright of Chulalongkorn University

Thesis Title α -GLUCOSIDASE INHIBITORS FROM *GYNURA PROCUMBENS*
By Miss Jiranuch Mingmuang
Field of Study Pharmacognosy
Thesis Advisor Associate Professor Surattana Amnuoypol, Ph.D.
Thesis Co-advisor Khanit Suwanborirux, Ph.D

Accepted by the Faculty of Pharmaceutical Sciences, Chulalongkorn University in
Partial Fulfillment of the Requirements for the Master's Degree.

Pornpen Pramyoeth Dean of the Faculty of Pharmaceutical Sciences
(Associate Professor Pornpen Pramyoethin, Ph.D.)

THESIS COMMITTEE

K. Likhit Chairman
(Associate Professor Kittisak Likhitwitayawuid, Ph.D.)

S. Amnuoypol Thesis Advisor
(Associate Professor Surattana Amnuoypol, Ph.D.)

Khanit Suwanborirux Thesis Co-advisor
(Khanit Suwanborirux, Ph.D.)

Thatree Phadungcharoen Member
(Associate Professor Thatree Phadungcharoen)

Suree Jianmongkol Member
(Assistant Professor Suree Jianmongkol, Ph.D.)

จิราหนู มิ่งเมือง : สารที่มีฤทธิ์ยับยั้งเอนไซม์แอลฟาไกลูโคซิเดสจากต้น *GYNURA PROCUMBENS* (α -GLUCOSIDASE INHIBITORS FROM *GYNURA PROCUMBENS*.) อ.ที่ปรึกษา: รศ.ดร. สุรัตนา อำนวยผล อ.ที่ปรึกษาร่วม: อ.ดร. คณิต สุวรรณบริรักษ์; 116 หน้า.

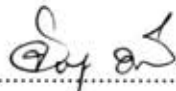
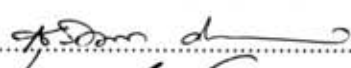
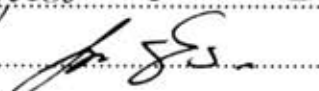
แอลฟาไกลูโคซิเดสเป็นเอนไซม์ที่ใช้ในขั้นตอนสุดท้ายของการย่อยสลายคาร์โบไฮเดรต สารที่มีฤทธิ์ยับยั้งเอนไซม์ดังกล่าวได้นำมาใช้ในการยับยั้งการเกิดกลูโคส และช่วยให้ระดับน้ำตาลในเลือดลดลง

จากการศึกษาเบื้องต้นพบว่า สารสกัดด้วยน้ำจากต้น *Gynura procumbens* (Lour.) Merr. มีฤทธิ์ยับยั้งการทำงานของเอนไซม์ดังกล่าว เมื่อทำการแยกสารสกัดด้วยน้ำ ควบคู่กับการทดสอบฤทธิ์การยับยั้งการทำงานของเอนไซม์พบว่า สารสกัดแยกส่วนมีฤทธิ์ยับยั้งเอนไซม์ได้ร้อยละ 82.93, 59.41, และ 64.21 ที่ความเข้มข้น 1 มิลลิกรัมต่อมิลลิลิตร ตามลำดับ เมื่อศึกษา จลนศาสตร์ของเอนไซม์พบว่า สารสกัดแยกส่วนที่มีฤทธิ์สูงสุดมีฤทธิ์ยับยั้งเอนไซม์แบบแข่งขัน

เมื่อนำสารสกัดแยกส่วนดังกล่าวมาทำปฏิกิริยา acetylation กับ acetic anhydride ใน pyridine ได้สารอนุพันธ์อะเซทิลของน้ำตาลโมเลกุลคู่ 3 ชนิดคือ GP1, GP2, และ GP3 ตามลำดับ หลังจากทำการพิสูจน์โครงสร้างทางเคมีของสารประกอบที่แยกได้โดยการวิเคราะห์เชิงสเปกตรัมของ NMR, IR, และ MS พบสารดังกล่าวเป็นอนุพันธ์อะเซทิลของน้ำตาลโมเลกุลคู่ 3 ชนิดคือ α -D-glucopyranosyl-(1 \rightarrow 2)-O-psicofuranoside, α -D-glucopyranosyl-(1 \rightarrow 2)-O-fructofuranoside, และ α -D-galactopyranosyl-(1 \rightarrow 2)-O-tagatofuranoside, ตามลำดับ

สถาบันวิทยบริการ จุฬาลงกรณ์มหาวิทยาลัย

ภาควิชาเภสัชเวท
สาขาวิชาเภสัชเวท
ปีการศึกษา 2550

ลายมือนิสิต..... 
ลายมือชื่ออาจารย์ที่ปรึกษา..... 
ลายมือชื่ออาจารย์ที่ปรึกษาร่วม..... 

4876560533 : MAJOR PHARMACOGNOSY

KEY WORD : *GYNURA PROCUMBENS* α -GLUCOSIDASE INHIBITORS

JIRANUCH MINGMUANG: α -GLUCOSIDASE INHIBITORS FROM *GYNURA*

PROCUMBENS. THESIS ADVISOR: ASSOC. PROF. SURATTANA

AMNUOYPOL, Ph.D., THESIS CO-ADVISOR: KHANIT SUWANBORIRUX, Ph.D.,

116 pp.

α -Glucosidase is the key enzyme which catalyzes the final step in the digestive process of carbohydrates. Hence, α -glucosidase inhibitors can retard the liberation of D-glucose from complex dietary carbohydrates and delay glucose absorption, reducing plasma glucose levels.

In a preliminary examination of the extracts of *Gynura procumbens* (Lour.) Merr., the aqueous extract exhibited highest inhibitory activity on α -glucosidase. Further fractionation of the active aqueous extract by bioassay guidance furnished fractions showing 82.93, 59.41, and 64.21 % inhibition on α -glucosidase at concentration 1 mg/ml, respectively. Kinetic study on α -glucosidase suggested that the most active fractions showed competitive inhibition property.

The active fractions were treated with acetic anhydride in pyridine to give 3 acetyl derivatives, GP1, GP2, and GP3, respectively. The structures were determined by analyses of ^1H , ^{13}C , and 2D-NMR, IR, and mass spectrometry. The results suggested that the main components of the active fractions were α -D-glucopyranosyl-(1 \rightarrow 2)-O-psicofuranoside, α -D-glucopyranosyl-(1 \rightarrow 2)-O-fructofuranoside, and α -D-galactopyranosyl-(1 \rightarrow 2)-O-tagatofuranoside, respectively.

Department: Pharmacognosy

Field of study: Pharmacognosy

Academic Year: 2007

Student's signature.....*J. M.*.....

Advisor's signature.....*S. Amnuaypol*.....

Co-advisor's signature.....*Khanit Suwanborirux*.....

ACKNOWLEDGEMENTS

The author wishes to express her deepest gratitude to her thesis advisor, Associate Professor Dr. Surattana Amnouypol, for her guidance, suggestion and supervision throughout this work.

Her genuine gratefulness is particularly extended to her thesis co-advisor, Dr. Khanit Suwanborirux for his helpful suggestion, NMR knowledge, generosity and encouragement throughout this research study.

Her thankfulness is sincerely grateful to Dr. Chutima Petchprayoon, Dr. Kornvika Charupant, and Dr.Sarin Tadtong without their invaluable instruction and good encouragement, the completion of this work would not have been possible.

Her grateful appreciation is owed to all the members of the Center for Bioactive Natural Products from Marine Organism and Endophytic Fungi (BNPME), Department of Pharmacognosy, Chulalongkorn University, for their good suggestion, decent facilities and kindness.

Her sincere thank to Pharmaceutical Research Instrument Center of Faculty of Pharmaceutical Sciences, Chulalongkorn University, for the provision of laboratory facilities.

Her special thank is given to the thesis committee for their constructive suggestion and critical perusal and useful advice.

A large debt of her gratitude is deepest thankfulness to all teachers, staff members of the Department of Pharmacognosy, and all of her friends, who kindly offer their knowledge, assistance, encouragement and helpful comments throughout this research. Her appreciation is beyond the words.

Her most appreciation is presented to her family. They provide her with love, opportunity, support and encouragement to her destination.

CONTENTS

	Page
ABSTRACT (Thai).....	iv
ABSTRACT (English).....	v
ACKNOWLEDGEMENTS.....	vi
CONTENTS.....	vii
LIST OF TABLES.....	x
LIST OF FIGURES.....	xi
LIST OF SCHEMES.....	xiii
LIST OF ABBREVIATIONS.....	xiv
CHAPTER	
I INTRODUCTION.....	1
II LITETATURE REVIEW	
1. Characteristics of genus <i>Gynura</i> and <i>G. procumbens</i>	3
2. Uses	7
3. The chemical constituents and biological activities of plants in genus <i>Gynura</i>	8
4. The chemical constituents and biological activities of <i>G. procumbens</i> ..	12
5. Anti-diabetic agents.....	13
6. α -Glucosidase inhibitors.....	14
7. Natural products with α -glucosidase inhibitory activity.....	16
III EXPERIMENTAL	
1. Plant materials.....	22
2. General techniques.....	22

2.1 Solvents.....	22
2.2 Analytical thin layer chromatography.....	22
2.3 Column chromatography	
2.3.1 Flash column chromatography.....	23
2.3.2 Gel filtration chromatography.....	23
2.4 Spectroscopy	
2.4.1 Ultraviolet (UV) absorption spectroscopy.....	23
2.4.2 Infrared (IR) absorption spectroscopy.....	24
2.4.3 Mass spectroscopy.....	24
2.4.4 Proton and carbon nuclear magnetic resonance (¹ H and ¹³ C NMR) spectroscopy.....	24
2.5 Physical Properties	
Optical rotations.....	24
3. Extraction and isolation.....	24
3.1 Extraction and isolation <i>Gynura procumbens</i> (Lour.) Merr.	24
3.1.1 Extraction of the aerial part of <i>G. procumbens</i>	24
3.1.2 Isolation of compounds from aqueous extract.....	26
4. Acetylation of the active isolated fractions.....	29
4.1 Acetylation and isolation of acetylated F21.....	30
4.2 Acetylation and isolation of acetylated F11.....	31
4.3 Acetylation and isolation of acetylated F14.....	32
5. Physical and Spectral data of the acetylated compounds	
5.1 Compound GP1	33
5.2 Compound GP2	34

5.3 Compound GP3	34
6. α -Glucosidase Inhibitory Activity.....	34
6.1 Material and instruments.....	34
6.2 Preparation of the test sample.....	35
6.3 Determination of α -glucosidase inhibitory activity.....	35
6.4 Determination of IC_{50}	36
6.5 Determination of enzyme kinetics.....	37
IV RESULTS AND DISCUSSION	
1. Structure determination of the acetylated compounds from the aqueous extracts of <i>G. procumbens</i>	
1.1 Structure Determination of GP1	40
1.2 Structure Determination of GP2	45
1.3 Structure Determination of GP3	49
2. α -Glucosidase inhibitory activity.....	53
2.1 Screening for α -glucosidase inhibitory activity.....	53
2.2 Enzyme kinetics.....	56
V CONCLUSIONS AND RECOMMENDATION.....	64
REFERENCES.....	65
APPENDIX.....	69
VITA.....	113

TABLES

Table	Page
1. Ethnomedical use of <i>Gynura</i> species.....	7
2. The chemical constituents and biological activities of <i>G. procumbens</i>	12
3. Natural product compounds showing <i>in vitro</i> with α -glucosidase inhibitory activity.	16
4. Fractions obtained from the fractionation of F04.....	27
5. Fractions obtained from the fractionation of F13.....	27
6. Fractions obtained from the fractionation of F16.....	28
7. The ^1H and ^{13}C NMR assignments, ^1H - ^1H COSY, HMBC, and NOESY correlations of GP1 (acetylated part).....	44
8. The ^1H and ^{13}C NMR assignments, ^1H - ^1H COSY, HMBC, and NOESY correlations of GP2 (acetylated part).....	48
9. The ^1H and ^{13}C NMR assignments, ^1H - ^1H COSY, HMBC, and NOESY correlations of GP3 (acetylated part).....	52
10. The percent Inhibition of the isolated fractions from the aqueous extract.....	54
11. The $1/V$ value of 1-deoxynojirimycin with variety of substrate concentrations.....	57
12. The kinetics parameters of α -glucosidase in the presence of 1-deoxynojirimycin..	58
13. The $1/V$ value of F08 with variety of substrate concentrations.....	58
14. The kinetics parameters of α -glucosidase in the presence of F08.....	60
15. The $1/V$ value of F21 with variety of substrate concentrations.....	60
16. The kinetics parameters of α -glucosidase in the presence of F21.....	61

LIST OF FIGURES

Figure	Page
1. <i>Gynura procumbens</i> (Lour.) Merr.	6
2. Chemical constituents of genus <i>Gynura</i>	9
3. Processing of the oligosaccharide (Glc3Man9GlcNac2) portion of the immature N-glycoprotein by the action of glucosidases I and II.....	15
4. Structures of α -glucosidase inhibitors: disaccharides.....	18
5. Structures of α -glucosidase inhibitors: iminosugars.....	19
6. Structures of α -glucosidase inhibitors: acarbose, voglibose, and thiosugars.....	21
7. Type of inhibitors.....	38
8. The ^1H - ^{13}C long-range correlations in HMBC spectra of GP1.....	42
9. NOESY correlations of GP1.....	42
10. The structure of α -D-glucopyranosyl-(1 \rightarrow 2)-O-psicofuranoside.....	43
11. The structure of α -D-psicopyranoside.....	45
12. The ^1H - ^{13}C long-range correlations in HMBC spectra of GP2.....	46
13. NOESY correlations of GP2.....	47
14. The structure of α -D-glucopyranosyl-(1 \rightarrow 2)-O-fructofuranoside.....	47
15. The ^1H - ^{13}C long-range correlation in HMBC spectra of GP3.....	50
16. NOESY correlation spectra of GP3.....	50
17. The structure of α -D-galactosyl-(1 \rightarrow 2)-O- tagatoside.....	51
18. The percenti inhibition of the isolated fractions from the aqueous extract of <i>G. procumbens</i> on α -glucosidase at concentration 1 mg/ml.....	55
19. Dose-dependent inhibitory effect on α -glucosidase by F08.....	56
20. Lineweaver-Burk plot of α -glucosidase in presence of 1-Deoxynojirimycin.....	57
21. Lineweaver-Burk plot of α -glucosidase in presence of F08.....	59
22. Lineweaver-Burk plot of α -glucosidase in presence of F21.....	61
23. Parent compounds of GP1, GP2, and GP3, respectively	62

24. EI mass spectrum of GP1.....	71
25. FAB mass spectrum of GP1.....	71
26. IR spectrum of GP1.....	72
27. ¹ H NMR (500 MHz) spectrum of GP1 (CDCl ₃).....	73
28. ¹ H NMR (500 MHz) spectrum of GP1 (CDCl ₃).....	74
29. ¹ H NMR (500 MHz) spectrum of GP1 (CDCl ₃).....	75
30. ¹³ C NMR (75 MHz) spectrum of GP1 (CDCl ₃).....	76
31. ¹³ C NMR (75 MHz) spectrum of GP1 (CDCl ₃).....	77
32. COSY spectrum of GP1 (CDCl ₃).....	78
33. COSY spectrum of GP1 (CDCl ₃).....	79
34. HMQC spectrum of GP11 (CDCl ₃).....	79
35. HMQC spectrum of GP11 (CDCl ₃).....	80
36. HMBC spectrum of GP1 (CDCl ₃).....	80
37. HMBC spectrum of GP1 (CDCl ₃).....	81
38. NOESY NMR spectrum of GP1 (CDCl ₃).....	81
39. EI mass spectrum of GP2.....	82
40. FAB mass spectrum of GP2.....	82
41. IR spectrum of GP2.....	83
42. ¹ H NMR (500 MHz) spectrum of GP2 (CDCl ₃).....	84
43. ¹ H NMR (500 MHz) spectrum of GP2 (CDCl ₃).....	85
44. ¹³ C NMR (75 MHz) spectrum of GP2 (CDCl ₃).....	86
45. ¹³ C NMR (75 MHz) spectrum of GP2 (CDCl ₃).....	87
46. COSY spectrum of GP2 (CDCl ₃).....	88
47. COSY spectrum of GP2 (CDCl ₃).....	89

48. COSY spectrum of GP2 (CDCl ₃).....	90
49. HMQC spectrum of GP2 (CDCl ₃).....	91
50. HMBC spectrum of GP2 (CDCl ₃).....	92
51. HMBC spectrum of GP2 (CDCl ₃).....	93
52. NOESY NMR spectrum of GP2 (CDCl ₃).....	94
53. EI mass spectrum of GP3.....	95
54. FAB mass spectrum of GP.....	95
55. IR spectrum of GP3.....	96
56. ¹ H NMR (500 MHz) spectrum of GP3 (CDCl ₃).....	97
57. ¹ H NMR (500 MHz) spectrum of GP3 (CDCl ₃).....	98
58. ¹ H NMR (500 MHz) spectrum of GP3 (CDCl ₃).....	99
59. ¹³ C NMR (75 MHz) spectrum of GP3 (CDCl ₃).....	100
60. ¹³ C NMR (75 MHz) spectrum of GP3 (CDCl ₃).....	101
61. ¹³ C NMR (75 MHz) spectrum of GP3 (CDCl ₃).....	102
62. ¹³ C NMR (75 MHz) spectrum of GP3 (CDCl ₃).....	103
63. COSY spectrum of GP2 (CDCl ₃).....	104
64. COSY spectrum of GP2 (CDCl ₃).....	105
65. HMQC spectrum of GP3 (CDCl ₃).....	106
66. HMQC spectrum of GP3 (CDCl ₃).....	107
67. HMQC spectrum of GP3 (CDCl ₃).....	108
68. HMQC spectrum of GP3 (CDCl ₃).....	109
69. HMBC spectrum of GP3 (CDCl ₃).....	110
70. HMBC spectrum of GP3 (CDCl ₃).....	111
71. NOESY spectrum of GP3 (CDCl ₃).....	112

LIST OF SCHEMES

Scheme	Page
1. Extraction of <i>G. procumbens</i>	25
2. Isolation of F04.....	26
3. Isolation of F08.....	29
4. Isolation of GP1.....	31
5. Isolation of GP2.....	32
6. Isolation of GP3.....	33



สถาบันวิทยบริการ
จุฬาลงกรณ์มหาวิทยาลัย

LIST OF ABBREVIATIONS AND SYMBOLS

$[\alpha]_D^{25}$	=	Specific rotation at 25°C and sodium D line (589 nm)
α	=	Alpha
β	=	Beta
<i>br</i>	=	Broad (for NMR spectra)
°C	=	Degree Celsius
Calcd	=	Calculated
CHCl ₃	=	Chloroform
CDCl ₃	=	Deuterated chloroform
cm ⁻¹	=	Wave number
¹³ C NMR	=	Carbon-13 Nuclear Magnetic Resonance
COSY	=	Correlation Spectroscopy
1-D	=	One dimensional
2-D	=	Two dimensional
<i>d</i>	=	Doublet (for NMR spectra)
<i>dd</i>	=	Doublet of doublets (for NMR spectra)
<i>ddd</i>	=	Doublet of doublets of doublets (for NMR spectra)
DEPT	=	Distortionless Enhancement by Polarization Transfer
DMAP	=	4- <i>N,N</i> -dimethylaminopyridine
DMSO	=	Dimethyl sulfoxide
<i>dt</i>	=	Doublet of triplet (for NMR spectra)
δ	=	Chemical shift (in ppm)
EIMS	=	Electron Impact Mass Spectrometry
FABMS	=	Fast Atom Bombardment Mass Spectrometry

EtOAc	=	Ethyl acetate
g	=	Gram
^1H NMR	=	Proton Nuclear Magnetic Resonance
HMBC	=	^1H -detected Heteronuclear Multiple Bond Correlation
HMQC	=	^1H -detected Heteronuclear Multiple Quantum Correlation
Hz	=	Hertz
IC ₅₀	=	Median inhibitory concentration
IR	=	Infrared spectrum
J	=	Coupling constant
kg	=	Kilogram
l	=	Liter
λ_{max}	=	Wavelength at maximal absorption
m	=	Multiplet
cm	=	Centimeter
μg	=	Microgram
μl	=	Microliter
μM	=	Micromolar
M^+	=	Molecular ion
MeOH	=	Methanol
mg	=	Miligram
$(\text{M}+\text{H})^+$	=	Protonated molecular ion
MHz	=	megahertz
min	=	minute
ml	=	Mililiter

m/z	=	Mass to charge ratio
nm	=	Nanometer
NMR	=	Nuclear Magnetic Resonance
NOESY	=	Nuclear Overhauser Effect Correlation Spectroscopy
ppm	=	Part-per million
ν_{\max}	=	Wave number of maximal absorption
q	=	Quartet (for NMR spectra)
ROESY	=	Rotating frame Overhauser Enhancement Spectroscopy
s	=	Singlet (for NMR spectra)
t	=	Triplet (for NMR spectra)
td	=	Triplet of doublet (for NMR spectra)
TLC	=	Thin Layer Chromatography
UV	=	Ultraviolet



สถาบันวิทยบริการ
จุฬาลงกรณ์มหาวิทยาลัย

CHAPTER I

INTRODUCTION

Diabetes mellitus is a common disorder associated with increased morbidity, mortality rate. At the present time it is estimated that 150 million people worldwide have diabetes and that the member will increase to 220 million by 2010 and 300 million by 2025. Globally, the percentage of type 2 diabetes (non insulin dependent diabetes mellitus) is greater than 90% (Zimmet *et al.*, 2001). Patients with diabetes have an increased risk of cardiovascular disease (CVD). Recently, much attention has been paid to evidence that abnormalities of the postprandial state are an important contributing factor to the development of atherosclerosis, even in diabetes mellitus. Postprandial hyperglycemia is more important in a development of macrovascular disease (Ceriello *et al.*, 2000). Therefore, effective control of postprandial hyperglycemia is more strongly warranted than previously thought. To control postprandial hyperglycemia, α -glucosidase inhibitors are widely used, as monotherapy as well as combination therapy with other antidiabetic agents (Cornish *et al.*, 1997).

α -Glucosidase is a membrane-bound enzyme at the epithelium of the small intestine, that hydrolyses the cleavage of glucose from disaccharides and oligosaccharides. The inhibitors of this enzyme delay carbohydrate digestion, prolong the overall carbohydrate digestion time and thus cause a reduction in the rate of glucose absorption and lower postprandial rise in blood glucose. Therefore, inhibition of α -glucosidase is considered important in managing non insulin-dependent diabetes (Bischoff *et al.*, 1994).

Plants represent a valuable source of therapeutic agents of diverse chemical constituents and pharmacological properties. Ethnomedicinal use of plants is beneficial as a guideline for plant selection which may be further scientifically evaluated for their relevant medicinal values. The *in vitro* α -glucosidase inhibitory assay was examined

utilizing of *p*-nitrophenyl-D- α -glucopyranoside (PNP-G) as an enzyme substrate (Matsui *et al.*, 1996, Ikeda *et al.*, 1999). During the past decades, numerous plant constituents possessing *in vitro* α - glucosidase inhibitory activities have been reported. They are alkaloids (Soenei, 2000), flavonoids (Hong, 2004), and polysaccharides (Atsou *et al.*, 2003). Compounds with potent α - glucosidase inhibitory activity and less toxicity have undergone further investigation for their therapeutic potential.

Gynura species are claimed in Thai traditional medicine as the remedies for inflammation and skin diseases, including *Gynura pseudochina* for herpes viral infection. *Gynura procumbens* (Lour.) Merr are widely distributed in South East Asia, especially Indonesia, Malaysia, and Thailand. The plant is considerable medicinal value. The fresh leaves of *G. procumbens* (จิงเจียหม่าเยี้ย, Jing-Jia Moa Yea in Central and southern of Thailand) has been used traditionally as antidiabetes in China, Taiwan, South of Asia and Thailand (Kew *et al*, 2002, Lam *et al*, 1998 and Akowuah *et al*, 2002). Moreover, *G. procumbens* has been reported to have several biological activities as antilipidemia, antihypertensive (Ebraika *et al.* 2002 and Lam *et al.*, 1998), and antidiabetes (Zhang *et al.*, 2003 and Akowuah *et al.*, 2002).

Based on the Chinese - ethnomedicinal anti-diabetic claim of *G. procumbens*, a phytochemical investigation of the plant guided by *in vitro* α - glucosidase inhibitory bioactive assay has been carried out. These bioactive components will be beneficial for further development of anti-diabetic agents from *G. procumbens*.

The main objectives for this investigation are

1. To isolate and purify chemical compounds from the aerial part of *G. procumbens* (Lour.) Merr.
2. To determine chemical structures of the isolated compounds.
3. To evaluate the isolated compounds for α - glucosidase inhibitory activity.

CHAPTER II

LITERATURE REVIEW

1. Characteristics of Genus *Gynura* and *Gynura procumbens* (Lour.) Merr.

Gynura is a small genus of plants and belongs to family Asteraceae which consists of about 100 species widely distributed in the tropical and subtropical regions of the world. They are annual or perennial herbs. Leaves are alternate, dentate or pinnately divided, rarely entire, petiolate or sessile. Capitula are discoid homogamous, solitary or few to numerous corymbose. Involucres are campanulate or cylindrical, with many linear bracteoles at base phyllaries uniseriate, lanceolate, equal, and imbricate with scarious margin. Receptacle are flat, areolate or shortly fimbriate. All florets are hermaphroditic and fertile. The corolla is yellow or orange, rarely purplish, tubular, with slender tube and narrowly campanulate limb, lobes 5. Anthers are entire or subauriculate at base. Style arms are slender, appendages subulate, papillose. Achenes are cylindrical, 10-ribbed glabrous or puberulous, truncate at both ends. Pappus is white, sericeous (Chen *et al.*, 2007).

Flora of Thailand (Koyama *et al.*, 2008) describes *G. procumbens* (Lour.) Merr. or *Cacaia procumbens* (Lour.) as a scrambling or climbing shrubs over thickets. Its stems are slender or woody, to 5 mm across at lower stem, leafy, glabrous or sparsely pubescent and 4 m height from the root. Leaves are sessile or petiolate, sometimes auriculate, laminae ovate to narrowly ovate in outline, 3-10 cm long, 0.5-3 cm wide. Leaves have apex acuminate, base narrowed down petiole, margins variable from entire to toothed or lobed or dissected almost to the midrib, both surfaces often glabrous, but occasionally pubescent, petioles 0-2.5 cm long. Inflorescences in axillaries and terminal corymbs with 5-20 heads; peduncles slender, to 6 cm long, pubescent. The heads are discoid; receptacle slightly convex, somewhat fibrillate, involucres cylindrical to turbinate, 8-12 mm high and 8 mm wide; calyculate, calyculus 6, slender, to 5 mm long; phyllaries 8-13 in 1 series, linear- lanceolate, dark purple, 1-1.2 mm wide, apex gradually tapering, abaxial surfaces hairy, margins narrowly hyaline. Florets 21 per

head and corolla is orange-yellow, 10-12 mm long, apex with 5 lobed, lobes 1-1.5 mm long. Achenes are cylindric, 4-5 mm long, 10-ribbed, ribs pale brown grooves dark brown, glabrous. Pappus of capillary bristles and 10-11 mm long, white.

Five species of *Gynura* were found in Thailand (Smitinand, 2001) as follows:

1. *G. crepidoides* Benth. หญ้าดอกคำ, Yaa Dok Khao (Loei)
2. *G. integrifolia* Gegnep. ว่านแจ้, Waan Chaeng (Nakhon Sawan)
3. *G. procumbens* (Lour.) Merr. or *G. sarmentosa* DC. ประคำดีควาย, Pra-Kham dee Khwai (Pattani)
4. *G. pseudo-china* (L.) DC. ผักกาดกบ, Phakkaat Kop (Phetchabun)
5. *G. pseudo-china* var. *hispidula* Thwaites. ว่านมหาภาพ, Waan Mahakaan (Central)

Five species of *Gynura* were found in Thailand (Smitinand, 2004) as follows:

1. *G. crepidoides* Benth. หญ้าดอกขาว, Yaa Dok Khao (Loei)
2. *G. cusimbera* (S.) Moove. ฝอยทองอินทนนท์ Foi thong inthanon (Bangkok)
3. *G. integrifolia* Gegnep. ดาวเรืองโคก Dao rueang khok (Loei), ว่านแจ้, Waan Chaeng (Nakhon Sawan)
4. *G. procumbens* (Lour.) Merr. ประคำดีควาย, Pra-Kham dee Khwai (Pattani), มูมะแสง Mu maeng san (Chumphon)
5. *G. pseudo-china* (L.) DC. var. *pseudochina* คำโคก Kham khok (Khon kaen), ผักกาดกบ, Phakkaat Kop (Phetchabun)
- *G. pseudo-china* var. *hispidula* Thwaites. ว่านมหาภาพ, Waan Mahakaan (Central)

Koyama *et al.*, in 2008, reclassified the *Gynura* species in Thailand to 11 species including

1. *G. bicolor* (Roxb.) DC.
2. *G. calciphila* Kerr.
 - 2.1. *G. calciphila* var. *calciphila* Kerr.
 - 2.2. *G. calciphila* var. *dissecta* F.G.
3. *G. cusimbua* (S.) Moore.

4. *G. divaricata* (L.) DC
5. *G. hmopengensis* H.
6. *G. integrifolia* Gegnep.
7. *G. longifolia* Kerr.
8. *G. nepalensis* DC.
9. *G. procumbens* (Lour.) Merr.
10. *G. pseudochina* (L.) DC.
11. *G. truncate* Kerr.



สถาบันวิทยบริการ
จุฬาลงกรณ์มหาวิทยาลัย



Figure 1 *Gynura procumbens* (Lour.) Merr.

2. Uses

Plants in the genus *Gynura* have numerous uses. Some species are ornamental due to the violet color of the leaves such as *G. aurantiaca* DC. (Velvet plant), *G. pseudochina* DC. Moreover, the leaves of *G. procumbens* Merr. and *G. formosana* DC. have also been used as vegetables. Significantly, the ethnomedical uses of the plant among the Asian countries are numerous as shown in **Table 1**. It is noted that the topical remedies for the treatment of inflammation, pain, and allergic conditions are common among nearly all the species mentioned.

In Thailand, several members of *Gynura* species have been recognized as satisfying remedies for various skin diseases.

Table1: Ethnomedical use of *Gynura* species

Species	Uses
<i>G. aurantiaca</i> DC.	Java, leaves : poultice for ringworm (Perry <i>et al.</i> , 1980).
<i>G. crepidioides</i> Benth.	India, leaves : decoction for stomachic (Perry <i>et al.</i> , 1980).
<i>G. divaricata</i> DC.	China, dried whole plant : Decoction internally for bronchitis, pulmonary tuberculosis, pertussis, sore eye, toothache, rheumatic arthralgia (Perry <i>et al.</i> , 1980). China, fresh herb : macerate: externally for traumatic injury, fracture, wound bleeding, mastitis boils pyodermas, leg ulcer, burns (Roeder <i>et al.</i> , 1996).
<i>G. formosana</i> Kitam.	Taiwan, leaves and root : juice externally for wound and snake bite (Perry <i>et al.</i> , 1980).
<i>G. sagetum</i> (Lour.) Merr. (<i>G. japonica</i> (Thumb.) Juel).	China, root : hemostat, vulnerary for bleeding, bruises furunculosis. whole plant decocted or crushed in white wine for amenorrhea, epistaxis, hematemesis, hemoptysis mastitis and traumatic injuries. Indochina, fresh leaves : treatment of poisonous insect bite (Perry <i>et al.</i> , 1980).

Species	Uses
<i>G. procumbens</i> (Lour.) Merr.	China, dried leaves : rubbed with oil and mashed as a salve for rash (Perry <i>et al.</i> , 1980). Thailand, fresh leaves : as poultice to relief pain, inflammation, allergic response, treatment of poisonous animal bite (Pongboonrod, 1979).
<i>G. pseudo-china</i> DC.	Indo-china, leaf sap : gargle for throat inflammation (Kew <i>et al.</i> , 2002). Thailand, root : remedy for uterine hemorrhages, dysentery, and inflamed wounds (Pongboonrod, 1979). tuberous root : antipyretic leaves : anti-inflammatory for herpes viral infection (Kasipan, 1979).

3. The chemical constituents and biological activities of plants in genus *Gynura*

Previous chemical investigations on the genus *Gynura* are limited, although the chemical pattern of the Asteraceae is well recorded. Since many plants of this family possess diverse medicinal values, which it is deemed worthwhile to identify the active substances from these plants. The compounds commonly found in many genera are sesquiterpene lactones, triterpene monools and diols, polyacetylenes, methylated flavonols and flavones, caffeic esters, insulin-type fructans, cyclitols, L-inositol, and fatty oils in the seed. Essential oils and diterpenoids are also widely distributed. Alkaloids, cyanogenic glycosides, amides, coumarins, and several types of phenolic constituents have much more limited distribution. Polyacetylene, sesquiterpene lactones and fructans polysaccharides are regarded as the chemical characters of Asteraceae (Herout, 1971).

The chemical pattern on the subfamily level of the Senecioneae tribe, to which the genus *Gynura* belongs, indicates the presence of pyrrolizidine alkaloids chiefly in the genus *Senecio*. The sesquiterpenes with an eremophilane and furanoeremophilane skeletons are often found in many genera. Triterpenes are also widespread but are usually obtained as complex mixtures. Several *Senecio* species contain sitosterol.

Hydroxycinnamates are also widespread in the Senecioneae. Caffeoylquinic acids are found in both *Arnica* and *Senecio* species. Flavone and flavonol 3- or 7-glucosides are also commonly found in the Senecioneae (Heywood *et al.*, 1977).

The chemical studies on the genus *Gynura* have revealed the presence of pyrrolizidine alkaloids (Metheson *et al.*, 1992., Wiedenfeid *et al.*, 1982), phytosterol (Sadikun *et al.*, 1996), terpene-coumarins (Bohlmann *et al.*, 1977), steroids (Takahira *et al.*, 1997), chromones (Jong *et al.*, 1997), and proanthocyanidins (Yoshitama *et al.*, 1994), (Figure 2). However, there are only a few pharmacological studies on these plants. Only the anti-HSV activities of *G. procumbens* (Lour.) Merr. (แป๊ะตำปิ้ง, จักรนารายณ์) (Jarikasem, 2000), anti-inflammatory and antipyretic activities of *G. divaricata* DC., *G. integrifolia* Gagnap. (Chitcharonthum *et al.*, 1992), and local anesthetic activity of *G. segetum* (Lour.) Merr. (Xueshao and Xizhi, 1987) have so far been reported.

Chemical constituents in *Gynura*

1. Pyrrolizidine alkaloids



Gynuramine (R=H)

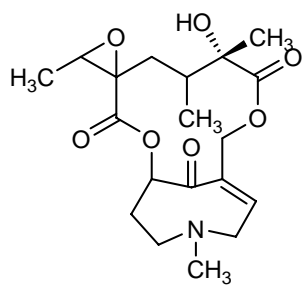
Senecionine

Acetylgynuramine (R=COCH₃)

(Liang and Roeder, 1984)

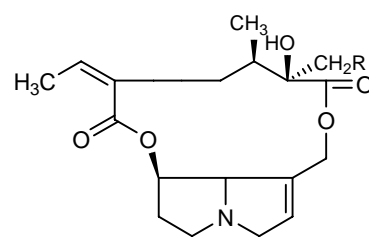
(Wiedenfeid, 1982)

Figure 2 Chemical constituents of genus *Gynura*



Otosenine

(Matheson and Robins, 1992)

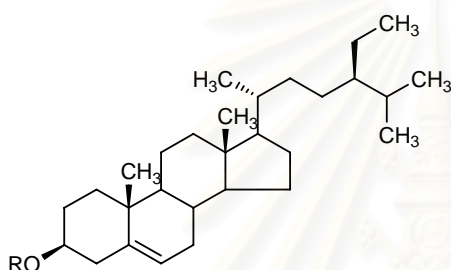
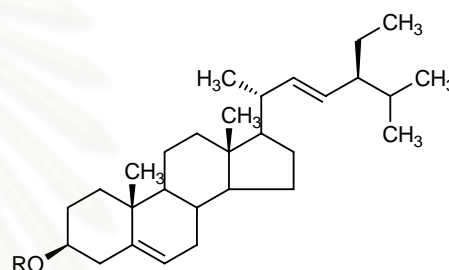


Intergerrimine (R=H)

Usaramine (R=OH)

(Roeder *et al.*, 1996)

2. Phytosterol

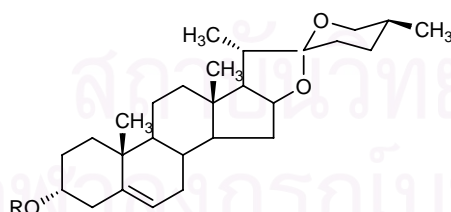
 β -Sitosterol (R=H) β -Sitosterol-glucoside(R = β -D-glucose)(Sadikun *et al.*, 1996)

Stigmasterol (R=H)

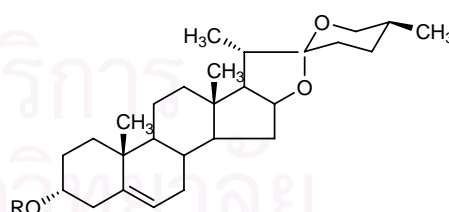
Stigmasterol-glucoside

(R = β -D-glucose)(Sadikun *et al.*, 1996)

3. Steroidal saponins

3-Epi-diosgenin-3- β -

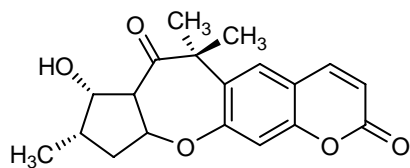
D-glucopyranoside

R = β -D-glucose(Takahira *et al.*, 1997)3-Epi-streptrogenin-3- β -

D-glucopyranoside

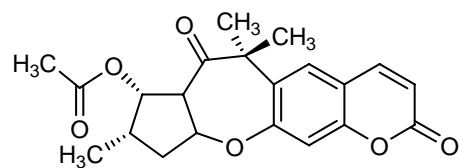
R = β -D-glucose(Takahira *et al.*, 1997)Figure 2 Chemical constituents of genus *Gynura* (continued)

4. Terpene-coumarins



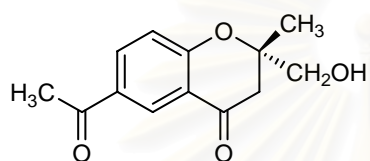
Gynurone

(Bohlmann, 1997)



Acetyl gynurone

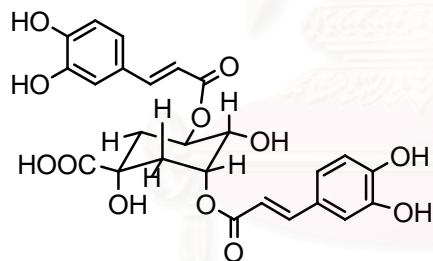
(Bohlmann, 1997)



Acetylchromanone

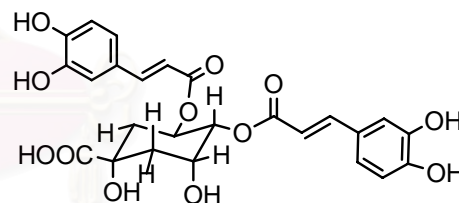
(Bohlmann, 1997)

5. Caffeic acid ester



3,5-di-O-Caffeoylquinic acid

(Jarikasem, 2000)



4,5-di-O-Caffeoylquinic acid

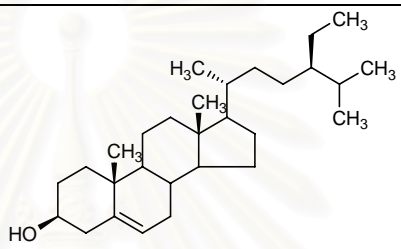
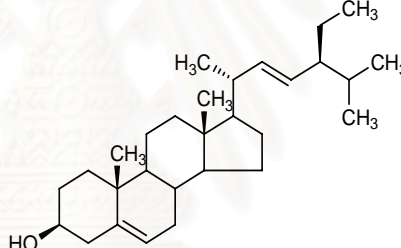
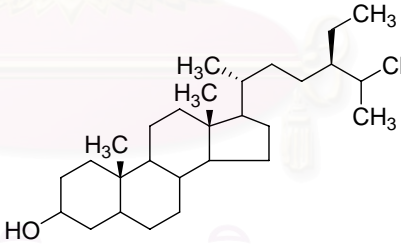
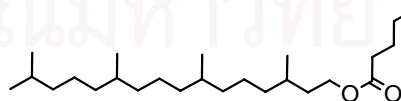
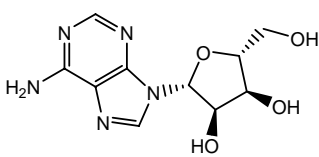
(Jarikasem, 2000)

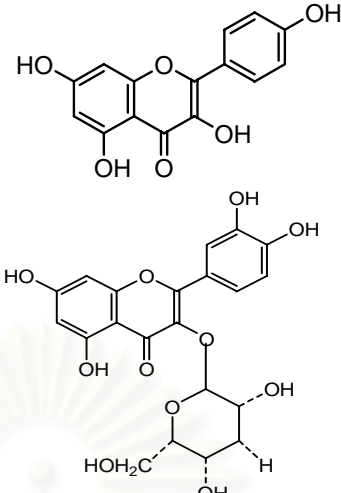
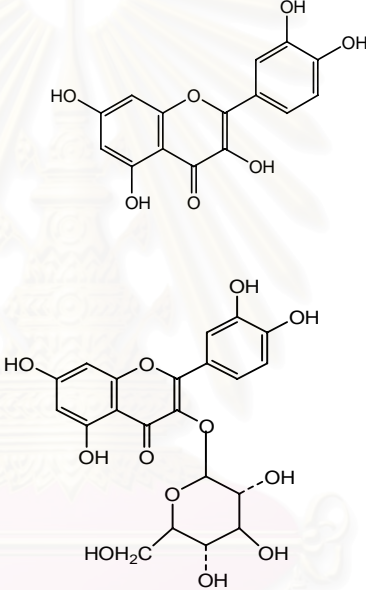
Figure 2 Chemical constituents of genus *Gynura* (continued)

4. The chemical constituents and biological activities of *G. procumbens*

The chemical constituents and biological activities of *G. procumbens* have been reported including sterols, phytol valerate, adenosine, flavonols and flavonol glycosides.

Table 2: The chemical constituents and biological activities of *G. procumbens*

No.	Compounds	Chemical structure	Activity/ References
1	β -sitosterol		- (Sadikun <i>et al.</i> , 1996)
2	Stigmasterol		- (Sadikun <i>et al.</i> , 1996)
3	Dihydrostigmasterol		Anti-hyperglycaemia (Akowuah <i>et al.</i> , 2002)
4	phytyl valerate		- (Lee <i>et al.</i> , 2002)
5	adenosine		- (Kew <i>et al.</i> , 2002)

No.	Compounds	Chemical structure	References
6	Kaempferol and kaempferol glycoside - Kaempferol - Kaempferol glucoside		Anti- hyperglycaemia (Akowuah <i>et al.</i> , 2002)
7	Quercetin and quercetin glycoside - Quercetin - Quercetin-3-O- rhamnoside		Anti- hyperglycaemia (Akowuah <i>et al.</i> , 2002)

5. Anti-diabetic agents

Diabetes mellitus (DM) is a group of metabolic diseases characterized by hyperglycemia, hypertriglyceridemia, and hypercholesterolemia, resulting from defects in insulin secretion or action or both (George and Ludvik, 2000; Nyholm *et al.*, 2000). One of the late complications of uncontrolled DM is the formation of advanced glycosylated end products (AGE) which can react with other proteins and are also capable of causing increased permeability and thickening of blood vessel walls with loss of elasticity (Dominiczak *et al.*, 1990).

Four groups of oral hypoglycemic drugs, sulphonylureas, biguanides, thiazolidinediones, and α -glucosidase inhibitors have been used in the treatment of DM. They act by lowering blood glucose levels thereby delaying or preventing the onset of diabetic complications. **Biguanides** may involve in the enhancement of insulin receptors (Uehara *et al.*, 2001; Zangeneh *et al.*, 2003) to increase the absorption of sugars whilst **sulphonylureas** involve in the augmentation of insulin secretion and are effective only when residual pancreatic cell activity is present (Guney *et al.*, 2002). **Thiazolidinediones** bind to nuclear peroxisome proliferators-activated receptor- γ (PPAR γ), which activates insulin-responsive genes that regulate carbohydrate metabolism and **α -glucosidase inhibitors** reduce intestinal absorption of starch, dextrin, and disaccharides (Laurence *et al.*, 2006).

6. α -Glucosidase inhibitors

Glycoside trimming enzymes are crucially important in a broad range of metabolic pathways, including glycoprotein and glycolipid processing and carbohydrate digestion in the intestinal tract. Amongst the large array of enzymes, glucosidases are postulated to be a powerful therapeutic target since they catalyze the cleavage of glycosidic bonds releasing glucose from the non-reducing end of a polysaccharide chain involved in glycoprotein biosynthesis. Glucosidase inhibitors have promising therapeutic potential in the treatment of disorders such as diabetes, human immunodeficiency virus (HIV) infection, metastatic cancer, and lysosomal storage diseases (Imperiali *et al.*, 2003).

Several glucosidase are specific for the cleavage of glycosidic bonds depending on the number, position, or configuration of the hydroxyl groups in the sugar molecule. Thus, α - and β -glucosidases are able to catalyze the cleavage of glycosidic bonds involving terminal glucose connected at the site of cleavage, respectively, through α - or β -linkages at anomeric center. The transition state structure for the substrates of these enzymes has a pseudoaxial orientation of the C-O bond and a skew conformation, suggesting that the main differences between α - and β -glucosidases are concerned with positioning of the catalytic nucleophile and the catalytic proton donor, represented by two carboxylic acids units (Heightman *et al.*, 2001)

The activity of glucosidases is fundamental to several biochemical processes such as degradation of diet polysaccharides to furnish monosaccharide units, which are then able to be metabolically absorbed and used by organism and glycoprotein processing, and biosynthesis of oligosaccharide units in glycoprotein or glycolipids (Lillelund *et al.*, 2002).

The enzymes glucosidases I and II are involved in the key steps of trimming of this N-linked oligosaccharide by cleaving Glc (1→2) Glc and Glc (1→3) Glc linkages, respectively, liberating the three glucose terminal residues of the $\text{Glc}_3\text{Man}_9\text{GlcNac}_2$ glycoprotein (Schweden *et al.*, 1986). (Figure. 3)

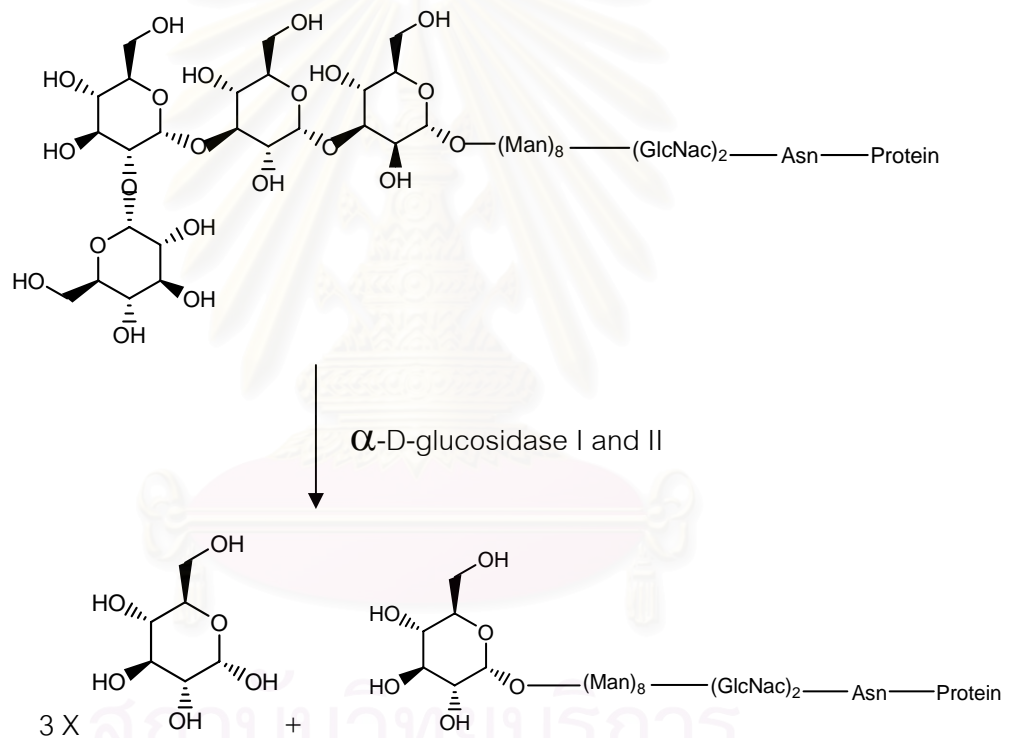


Figure 3 Processing of the oligosaccharide ($\text{Glc}_3\text{Man}_9\text{GlcNac}_2$) portion of the immature N-glycoprotein by the action of glucosidases I and II

Subsequently, this immature glycoprotein is processed by concomitant action of glycosidases and transferases to give specific glycol-conjugates, which play fundamental roles in the biological processes, such as the immune response, intercellular regulation, cellular differentiation, the stability and solubility of proteins, and

pathological processes, such as inflammation and cancer, since α -glucosidase may play a role in tumor cells for metastatic process. Inhibitors of glucosidases I and II have also been studied as potential anti-HIV agents (Mitsuya *et al.*, 1990).

The multiple functions of glucosidases in the organism warrant the search for potential therapeutic inhibitors to be used in diabetes (Hollender *et al.*, 1998), obesity (Kordik, 1999), glycosphingolipid lysosomal storage disease including Gaucher's disease (Platt *et al.*, 1999), HIV infections (Papandreou *et al.*, 2002) and tumors in general (Asano *et al.*, 2001). In support of the increasing interest in synthetic and natural glucosidase inhibitors as important tools for understanding biochemical processes and also as prospective therapeutic agents, the following review describes the chemical structural diversity of the main α - and β -glucosidase inhibitors that comprise disaccharides, iminosugars, carbasugars, thiosugars and non-glycosidic inhibitors (Melo *et al.*, 2006).

7. Natural products with α -glucosidase inhibitory activity

Several classes of natural product compounds have been reported to exhibit *in vitro* α -glucosidase inhibitory activity. A list of prominent *in vitro* α -glucosidase inhibitor compounds is given in Table 3, and chemical structures are shown in Figure 4.

Table 3: Natural product compounds showing *in vitro* α -glucosidase inhibitory activity

Types of compounds	Compounds	Natural origin	Applications
Phenolic compounds	cinnamic acid	<i>Kaempferia galanga</i> L.	Anti-diabetes and anti-HIV (Adisakwattana <i>et al.</i> , 2003)
Flavonoids	3-O - acylmesquitol and derivatives	<i>Dichrostachys cinerea</i> L.	Anti-diabetes and anti-HIV (Jagadeeshwar <i>et al.</i> ,

Types of compounds	Compounds	Natural origin	Applications
Flavones	6-hydroxyflavones and baicalein derivatives	<i>Origanum majorana</i> L.	Anti-diabetes and anti-HIV (Gao and Kawabata., 2004)
Polysaccharides	isoacarbose and acarviosine	<i>Saccharomyces cerevisiae</i> and <i>Actinomycetales</i> sp.	Anti-diabetes (Kimura <i>et al.</i> , 2003)
Triterpenoids	oleanolic acid and derivatives	<i>Tridax procumbens</i> L.	Anti-diabetes and anti-HIV (Shaiq <i>et al.</i> , 2002)
Alkaloids	homonojirimycin and analogue	<i>Lobelia sessilifolia</i> Lamb. and <i>Adenophora</i> sp.	Anti-diabetes and anti-HIV (Ikeda <i>et al.</i> , 1999)
N/A	crude extract	<i>Pinus densiflora</i> L.	Anti-diabetes (Kim <i>et al.</i> , 2004)
N/A	crude extract	<i>Cogniauxia podoleana</i> Baillon.	Anti-diabetes (Diatewa <i>et al.</i> , 2004)
N/A	crude extract	<i>Mangifera indica</i> L.	Anti-diabetes (Prashanth <i>et al.</i> , 2001)
N/A	crude extract	<i>Punica granatum</i> L.	Anti-diabetes (Li <i>et al.</i> , 2005)

Note : N/A = Not applicable

In 1953, α -glucosidase inhibitors comprised of **disaccharides** such as kojibiose and nigerose (Figure. 4) were shown to be inhibitors of α -D-glucosidase I and α -D-glucosidase II, respectively, and this opened up new perspectives for the

development of novel drugs, especially of pseudo-disaccharide class, for treatment of HIV infection. Kojibiose containing α -(1 \rightarrow 2) glycosidic bond was isolated from two sources, sake extracts and also from a product related to rice fermentation by *Aspergillus oryzae*. Nigerose, was produced from acid hydrolysis of amylopectin, which was shown α -(1 \rightarrow 3) glycosidic linkage. The importance of nigerose and nigerosylmalto-oligosaccharides has also been shown to influence the immune function and quality of life in the healthy elderly person as supplemental syrup on food.

Extracts of *Mormodica charantia* seeds and of *Grifola frondosa* fruits showing α -glucosidase inhibitory activity have also been investigated and D-(+)-trehalose was identified as the active component. Trehalose, constituted by two units of glucose link by an α -(1 \rightarrow 1) bond, is employed in the preparation of foods and manufacture of cosmetics. It was recently suggested as a drug to be used in treatment of osteoporosis, since it was shown to increase trabecular density in rat. Its inhibitory capacity compared with the model 1-deoxynojirimycin indicated that, while a concentration of 0.1 μ M of 1-deoxynojirimycin showed a 52% inhibition of α -glucosidase, trehalose at 2 mM showed only 42% of inhibitory activity. C-disaccharides constitute another class of glycosidic analogues with potential enzymatic inhibitory activity.

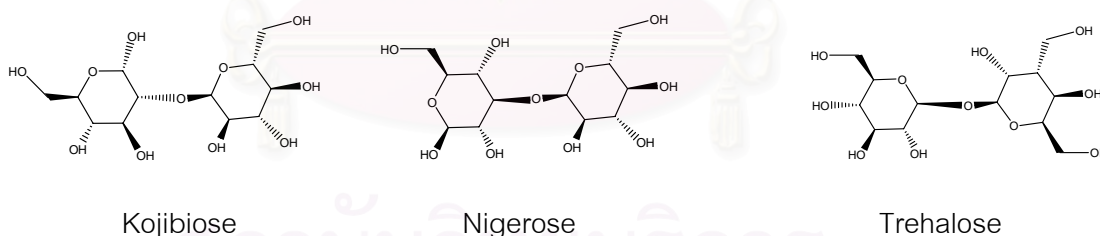


Figure 4 Structures of α -glucosidase inhibitors: disaccharides

Iminosugars, isolated from plants or microorganism, are considered to have a high potential therapeutic value and are of interest to be applied in the elucidation of biological recognition processes. In 1966, Nojirimycin is the first glucose analogue which comprises endocyclic nitrogen in place of oxygen pyranosidic atom. The polyhydroxypiperidine, initially isolated as an antibiotic from several strains of *Bacillus*, *Streptomyces*, and mulberry leaves, was shown to be a potent inhibitor of both α - and β -

glucosidases of differences origins. However, the presence of a hydroxyl group at C-1 adds instability that harms the biological assays. Reduction of nojirimycin by catalytic hydrogenation or sodium borohydride provides analogue 1-deoxynojirimycin, a more stable and a potent glucosidase inhibitor *in vitro*. Based on experiments involving cultured cells, nojirimycin inhibited the formation of complex-type oligosaccharides, leading to the accumulation of $\text{Glc}_{(1-3)}\text{Man}_{(7-9)}\text{GlcNac}_2$. However, its *in vivo* activity is only moderate. (Junge *et al.*, 1996 and Melo *et al.*, 2006). Therefore, a large number of deoxynojirimycin derivatives were prepared for increasing the *in vivo* activity. Miglitol was selected as the most favorable inhibitor out of a large number of *in vitro* active agents. In 1996, miglitol was granted clearance by the U.S. Food and Drug Administration (FDA) and was introduced onto the market in 1999 as a more potent second-generation α -glucosidase inhibitor with fewer gastrointestinal side effects (Figure 5).

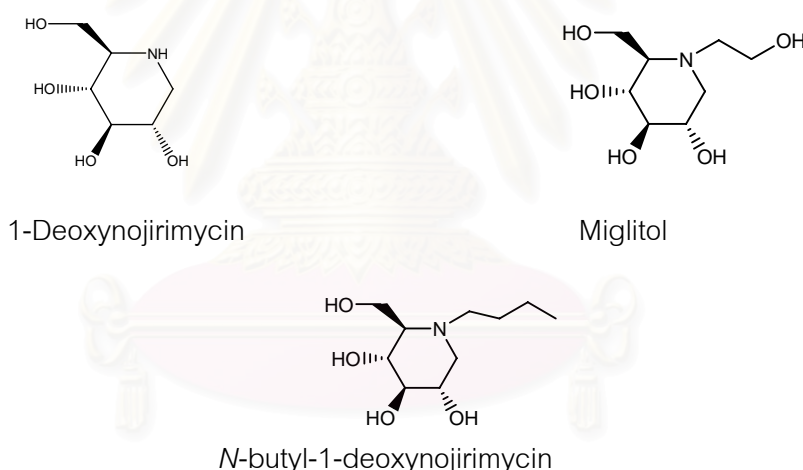


Figure 5 Structures of α -glucosidase inhibitors: iminosugars

Among aminocyclitols from natural products, acarbose is one of the most important clinical derivatives. It was found in 1970s, and it was realized that inhibition of all or some of the intestinal disaccharidases and pancreatic α -amylase by inhibitors could regulate the absorption of carbohydrate and these inhibitors could be used therapeutically in the oral treatment of the non-insulin dependent diabetes mellitus (type II diabetes). Acarbose has been produced as a secondary metabolite in a large scale from fermentation cultures of *Actinoplanes* sp. SE 50. It was a potent sucrase inhibitor,

which inhibits pig intestinal sucrase with IC_{50} value of 0.5 μM and was also effective in carbohydrate loading tests in rats and healthy volunteers, reducing postprandial blood glucose and increasing insulin secretion (Schmidt *et al.*, 1977 and Puls *et al.*, 1971).

Currently, three drugs are therapeutically used as anti-glucosidases. Miglitol and acarbose are used in the treatment of type II diabetes, since they reduce the postprandial hyperglycemia by interfering with the digestion of dietary carbohydrates. *N*-Butyl-1-deoxynojirimycin is employed for control of Gaucher's disease, related to disturbed lysosomal storage (Figure 5).

In 1984, the validamycin A-producing organism *Streptomyces hygroscopicus* var. *limoneus* was reported to co-produce **valiolamine**, which is a potent inhibitor of pig intestinal maltase and sucrase with IC_{50} values of 2.2 and 0.049 μM , respectively (Kameda *et al.*, 1984). Numerous *N*-substituted valiolamine derivatives were synthesized to enhance its α -glucosidase inhibitory activity *in vitro* and the very simple derivative voglibose which was obtained by reductive amination of valiolamine with dihydroxyacetone, was selected as the potential oral anti-diabetic agent (Horie *et al.*, 1986). The IC_{50} values toward maltase and sucrase were 0.015 μM and 0.046 μM , respectively. Voglibose has been commercially available for the treatment of diabetes since 1994.

The naturally occurring **thiosugars** are a class comprised of derivatives with a strong anti α -glucosidase activity. The parent compound is salacinol, which was isolated from the aqueous root and stem extract of *Salacia reticulata* Wight (Yuasa *et al.*, 2001). This tree is known as kothalahimbutu in Sinhalese and distributed in Sri Lanka and Indian forests, and has been used as a supplementary food in Japan to prevent obesity and diabetes. Traditionally, ayurvedic medicine advises that a person suffering from diabetes should drink water left overnight in a mug carved from kothalahimbutu wood. **Salacinol** and **Kotalanol** have been identified as α -glucosidase inhibiting components. The IC_{50} values of salacinol toward rat intestinal maltase, sucrase, and isomaltase are 3.2, 0.84, and 0.59 $\mu\text{g/ml}$, respectively (Yoshikawa *et al.*, 1998). The inhibitory activities toward maltase and sucrase are nearly equal to those of acarbose and that toward isomaltase is much more potent than that of acarbose. Kotalanol shows

a more potent inhibitory activity than salacinol and acarbose toward sucrase. Furthermore salacinol has been found to inhibit the increase of serum glucose levels in sucrose-loaded rat higher activity than acarbose (Asano, 2003).

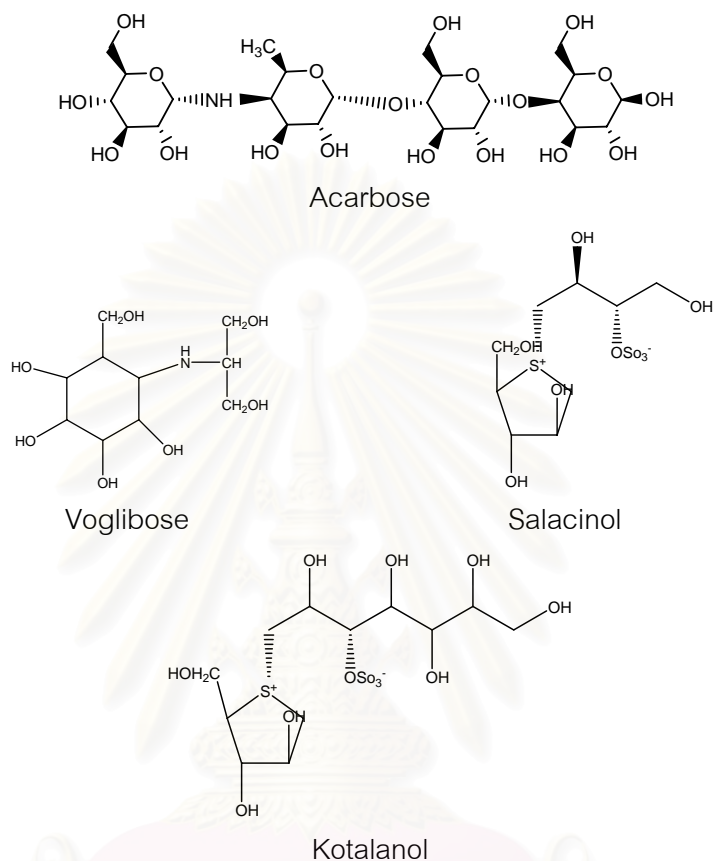


Figure 6 Structures of α -glucosidase inhibitors: acarbose, voglibose, and thiosugars

At present there is no report on α -glucosidase inhibitory activity of the plant extract or compounds from *G. procumbens*. Judging from many interesting biological activities of *Gynura* plants, *G. procumbens* has thus been selected for investigation in this study.

CHAPTER III

EXPERIMENT

1. Plants materials

Gynura procumbens (Lour.) Merr. was collected from Siriruckhacharti Medicinal Plant Garden, Mahidol University, Salaya campus in Nakhon-pathom province, Thailand. A plant specimen was identified by Dr. Kongkanda Chayamnant, Director of Bangkok Forest Herbarium (BKF), Royal Forest Department, Ministry of Agriculture and Cooperatives, Bangkok, Thailand. A voucher specimen has been deposited at the department of Pharmacognosy, Faculty of Pharmaceutical Sciences, Chulalongkorn University, Bangkok, Thailand.

2. General Techniques

2.1 Solvents

Throughout this work, all organic solvents were of commercial grade and redistilled prior to use.

2.2 Analytical Thin-Layer Chromatography

- Technique : One dimension, ascending
- Adsorbent : Silica gel F₂₅₄ coated on aluminium sheet and RP18
silica gel GF₂₅₄ coated on aluminium sheet (E. Merck)
- Layer thickness : 250 µm
- Developing distance : 5.0 cm
- Temperature : Laboratory room temperature (25-35°C)
- Detection : 1. Visual detection under ultraviolet light at
wavelengths of 254 nm and 365 nm
2. Visual detection under daylight after spray with
Anisaldehyde TS and heat the plate for 5-10 minutes

2.3. Column Chromatography

2.3.1 Flash column chromatography

- Adsorbent : Silica gel 60 (No.7734), particle size 0.063-0.200 mm.
(70-230 mesh ASTM) (E. Merck)
- : Silica gel 60 (No.9385), particle size 0.040-0.063 mm.
(230-400 mesh ASTM) (E. Merck)
- : Cosmosil[®] RP18, particle size 43-60 μm
(NACALAI TESQUE)
- Packing method : Wet packing: The adsorbent was suspended in an eluent, poured into the column, and then allowed to set tightly.
- Sample loading : The sample was dissolved in a small amount of eluent, and then applied gently on top of the column.
- Detection : Fractions were examined using TLC technique in the same manner as described in section 2.2.

2.3.2 Gel filtration chromatography

- Gel filter : Sephadex LH-20 (Pharmacia Biotech AB)
- Packing method : Gel filter was suspended in the eluent and left standing to swell for 24 hours prior to use. It was then poured into the column and then allowed to set tightly.
- Sample loading : The sample was dissolved in a small amount of eluent, and then applied gently on top of the column.
- Detection : Fractions were examined using TLC technique in the same manner as described in section 2.2.

2.4 Spectroscopy

2.4.1 Ultraviolet (UV) absorption spectroscopy

UV (in MeOH) spectra were obtained on a Shimadzu UV-160A spectrophotometer (Pharmaceutical Research Instrument Center, Faculty of Pharmaceutical Sciences, Chulalongkorn University)

2.4.2 Infrared (IR) absorption spectroscopy

IR spectra were recorded on a Jasco 4100 FT-IR spectrometer (Bureau of Drugs and Narcotics, Department of Medical Sciences)

2.4.3 Mass spectroscopy

EI and FAB mass spectra were obtained with a JEOL JMS-700 mass spectrometer with direct inlet, operating at 10 kV ionization voltages (Meiji Pharmaceutical University, Japan)

2.4.4 Proton and Carbon Nuclear Magnetic Resonance (^1H and ^{13}C -NMR) Spectroscopy

^1H -NMR (300 MHz) and ^{13}C -NMR (75 MHz) spectra were obtained with a Bruker Avance DPX-300 FT-NMR spectrometer (Pharmaceutical Research Instrument Center, Faculty of Pharmaceutical Sciences, Chulalongkorn University) and ^1H -NMR (500 MHz) and ^{13}C -NMR (125 MHz) spectra were obtained with an Inova 500 FT-NMR spectrometer (Scientific and Technological Research Equipment Center, Chulalongkorn University)

The solvents for NMR spectra were deuterated chloroform (CDCl_3), deuterated dimethyl sulfoxide ($\text{DMSO-}d_6$), or deuterated pyridine ($\text{pyridine-}d_5$). Chemical shifts were reported in ppm scale using the chemical shift of the solvent as the reference signal.

2.5 Physical Properties

Optical rotations

Optical rotation were measured on a Polax 2L polarimeter using a sodium Lamp operating at 589 nm (Medicinal Plant Quality Assurance Center, Institute's of Medicinal Plants research, Department of Medical Sciences).

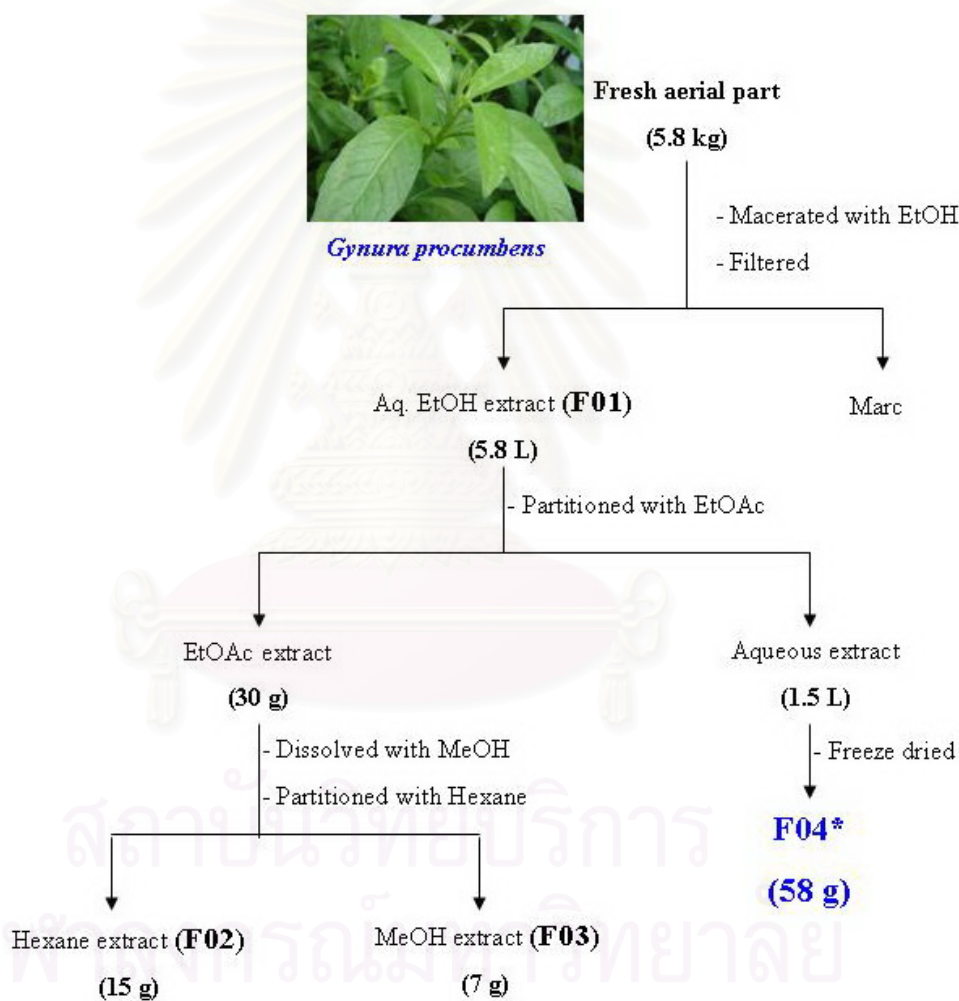
3. Extraction and Isolation

3.1 Extraction of the aerial part of *G. procumbens* (Lour.) Merr.

The fresh aerial parts of *G. procumbens* (5.8 kg) were blended and macerated with 28 L of 95% ethanol for 3 times. The obtained extract was filtered, combined and

concentrated under reduced pressure at 45°C to yield an aqueous ethanol extract (F01: 5.8 L).

The aqueous ethanol was partitioned with ethyl acetate for five times, and the ethyl acetate layer was concentrated to dryness under reduced pressure to yield 30 g of crude ethyl acetate extract (dark green syrupy mass). Crude ethyl acetate was dissolved in methanol (500 ml) and partitioned with hexane. Removal of organic solvents gave a crude hexane extract (F02: green mass, 15 g) and a crude methanol extract (F03: dark green mass, 7 g), respectively (Scheme 1).



Scheme 1. Extraction of *G. procumbens*

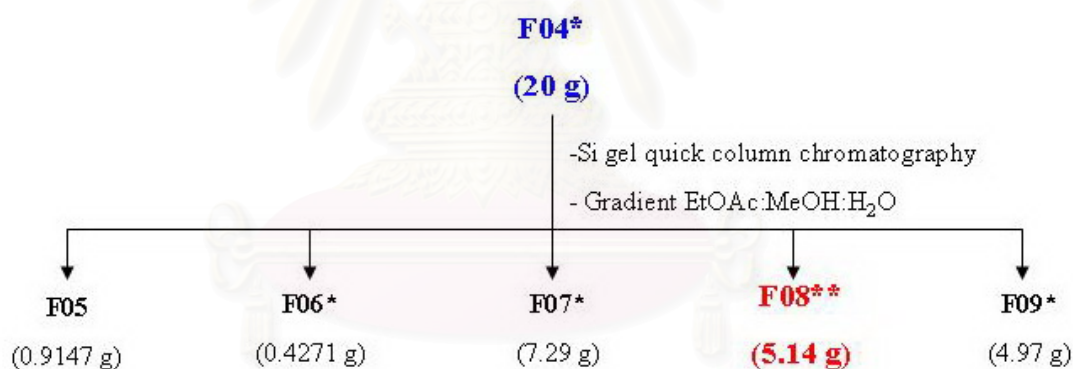
* show $\geq 50\%$ inhibition on *in vitro* α -glucosidase inhibitory activity

The remaining water extract was concentrated under reduced pressure and freeze-dried for 2 days to give 58 g of crude water extract (F04: yellow-brown mass) (Scheme 1). Each extract was subjected to *in vitro* α -glucosidase inhibitory assay (as

described in Section 6). The water extract, F04, was the most active fraction, as tested at concentration of 100 mg/ml and was further separated by chromatographic techniques.

3.2 Isolation of compounds from the aqueous extract

The separation of the extract from *G. procumbens* was performed by bioassay guided fractionation using α -glucosidase inhibitory assay. The aqueous extract (F04, 20 g) was chromatographed on a quick column (silica gel No. 7734, 100 g) by eluting stepwise with EtOAc, EtOAc-MeOH, MeOH, MeOH-H₂O. Each 500 ml fraction was collected and examined by TLC (Silica gel RP 18, MeOH:H₂O = 7:3) and detected under UV₂₅₄. Fractions with similar TLC pattern were combined and evaporated to dryness, to give 5 fractions, F05-F09 (Scheme 2, Table 5).



Scheme 2. Isolation of F04

* show $\geq 50\%$ inhibition on *in vitro* α -glucosidase inhibitory activity

** show highest activity

Table 4 Fractions obtained from the fractionation of F04

Fraction	Volume of eluate (ml)	Total weight (g)
F05	800	0.91
F06	1000	0.43
F07	1500	7.29
F08	1500	5.14
F09	2000	4.97

Each fraction was subjected to *in vitro* α -glucosidase inhibitory assay. Fractions F06, F07, F08, and F09 showed 50, 50, 60 and 55% inhibition, respectively, at concentration 1 mg/ml. The most active fraction F08 was further separated on a reversed phase column (Cosmosil[®] RP18, 3.6 g) and eluted with gradient 0-100% MeOH in H₂O, to give 3 fractions, F10-F12. The most polar fraction F12, was further separated, and examined by TLC on a silica gel, n-BuOH:MeOH:H₂O (3:5:2) to give three fractions, F13-F15.

F13, a light yellow mass, was repeatedly separated in the same manner as above to give F16-F19 (Table 6).

Table 5 Fractions obtained from the fractionation of F13

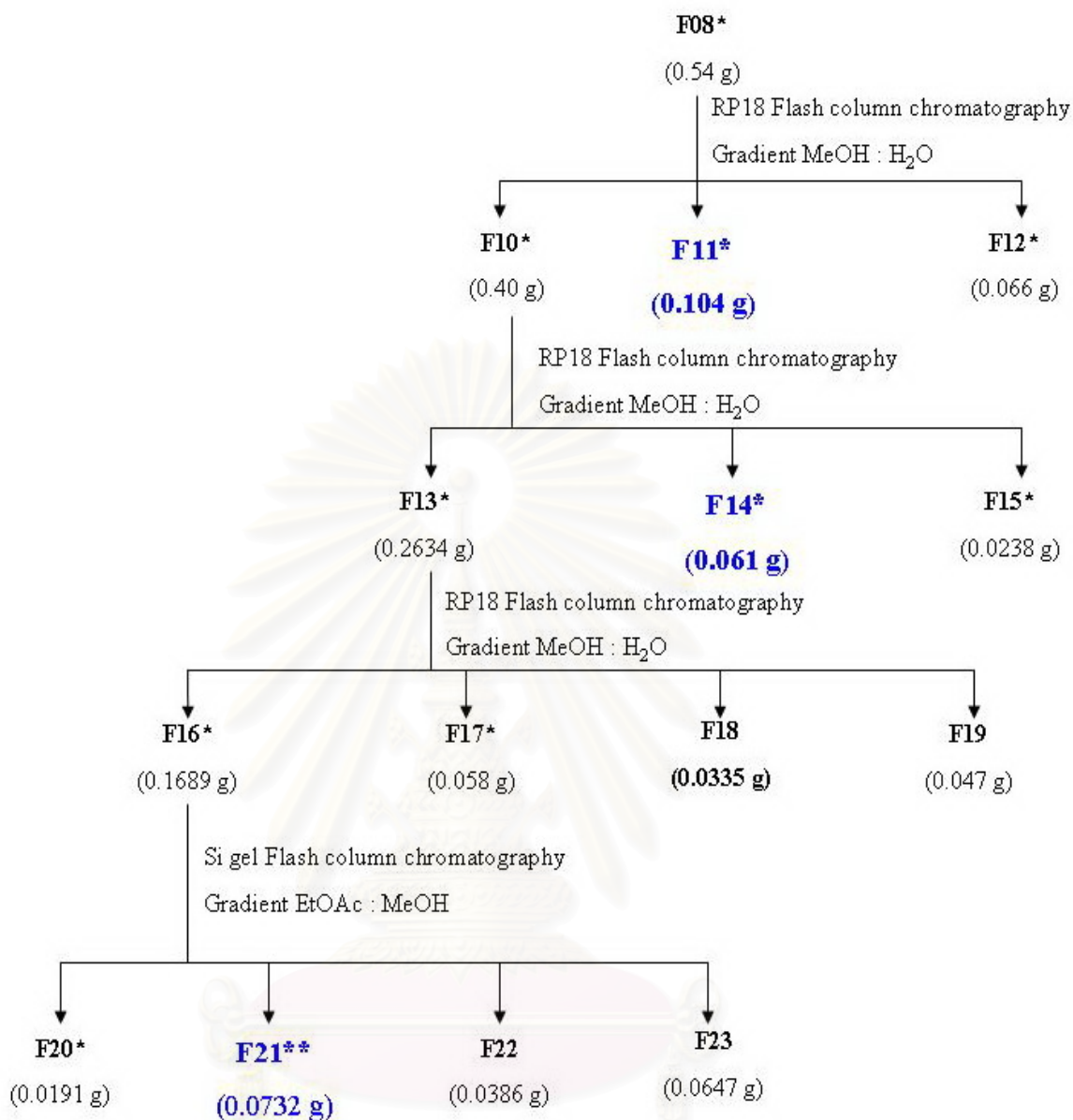
Fraction	Volume of eluate	Total weight (mg)
F16	200	169
F17	150	58
F18	150	33.5
F19	200	47

F16 was chromatographed on a silica gel column (2.5 x 16 cm.) using gradient 100%EtOAc in MeOH as the eluent. The eluates were examined by TLC (silica gel, EtOAc:MeOH = 4:1). Four fractions: F20-F23 were obtained (Table 7, Scheme 3).

Table 6 Fractions obtained from the fractionation of F16

Fraction	Volume of eluate (ml)	Total weight (mg)
F20	150	19.1
F21	250	73.2
F22	135	38
F23	200	65

Each fraction was subjected to *in vitro* α -glucosidase inhibitory assay. The percent inhibition of the isolated compounds of the aqueous extract from *G. procumbens* on α -glucosidase are shown in Table 12.



Scheme 3. Isolation of F08

* show $\geq 50\%$ inhibition on *in vitro* α -glucosidase inhibitory activity

** show highest activity

4. Acetylation of the active fractions

Several attempts to isolate the saccharides mixture from the active fractions by conventional methods have been unsuccessful. Therefore, acetylation was used for chemical transformation of the active fractions. F11, F14, and F21 were acetylated prior to separation by chromatographic techniques. The acetylated products were subjected to chemical structure determination by spectroscopic techniques.

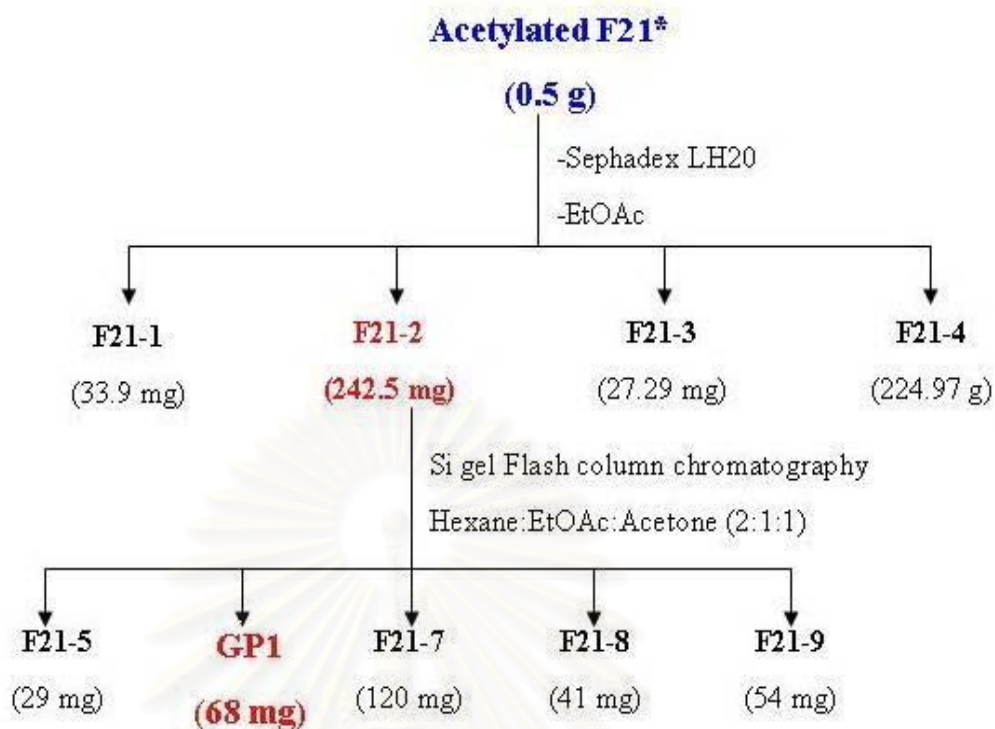
Acetylation

The sample and dimethylaminopyridine (DMAP) catalytic agent were dissolved in pyridine (0.5 ml), and then added acetic anhydride (0.5 ml). The solution was stirred at room temperature for 6 hours under argon. The reaction mixture was stopped by adding 10 ml of water into the flask. The aqueous solution was partitioned with 10 ml of EtOAc three times. The EtOAc extract was dried, and concentrated *in vacuo* to give the acetylated compound (Rho *et al.*, 1997).

4.1. Acetylation and isolation of acetylated F21

Fraction F21 (10 mg) and DMAP catalytic agent (50 mg) were dissolved with excess amount of pyridine (0.5 ml). Acetic anhydride (0.5 ml) was used as acetylating reagent. The solution was stirred at room temperature for 6 hours under argon. The reaction mixture was stopped by adding 10 ml of water into the flask. The aqueous solution was partitioned with EtOAc (10 ml x 3). The EtOAc extract was dried under reduced pressure to give a residue (1.4 g). The separation of the residue by flash column chromatography (hexane:EtOAc = 1:1) afforded a mixture of acetylated products (0.5 g).

The mixture of acetylated compounds were further separated on a sephadex LH20 column (3.5 x 50 cm.) with EtOAc as the eluent and then on a silica gel column (2.5 x 10 cm), hexane:EtOAc:acetone (2:1:1) to yield a yellow mass, acetyl derivative, GP1 (68 mg) (**Scheme 4**). The chemical structure of GP1 was determined by NMR and MS techniques.

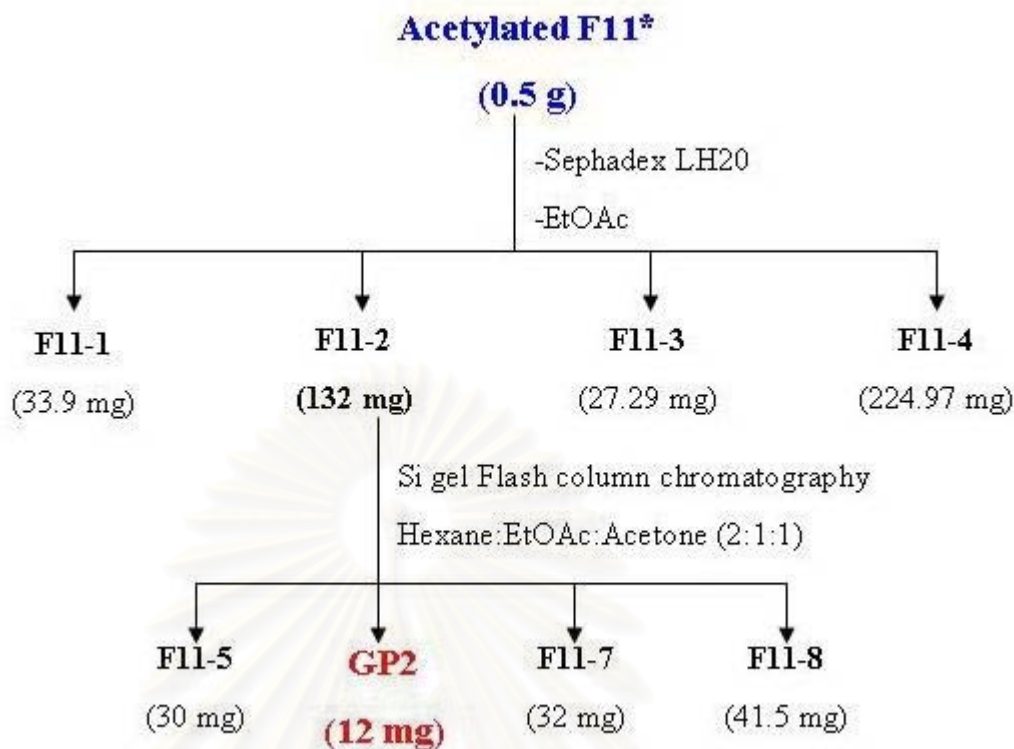


Scheme 4. Isolation of GP1

4.2 Acetylation and isolation of acetylated F11

Five mg of F11 was acetylated by using DMAP (20 mg) dissolved with 0.2 ml of pyridine and added acetic anhydride (0.5 ml) to give an acetylated residue (0.34 g). The purification of the residue by flash column chromatography and hexane:EtOAc (1:1) afforded the acetylated products (0.12 g).

Acetylated F11 was separated by sephadex LH20 column using EtOAc as the solvents to give the acetylated compounds (F11-2, 132 mg). F11-2 was further purified on a silica gel flash column (1.5 x 10 cm) using isocratic hexane:EtOAc:acetone (2:1:1) to give an acetyl derivative, GP2 (12 mg). (Scheme 5)

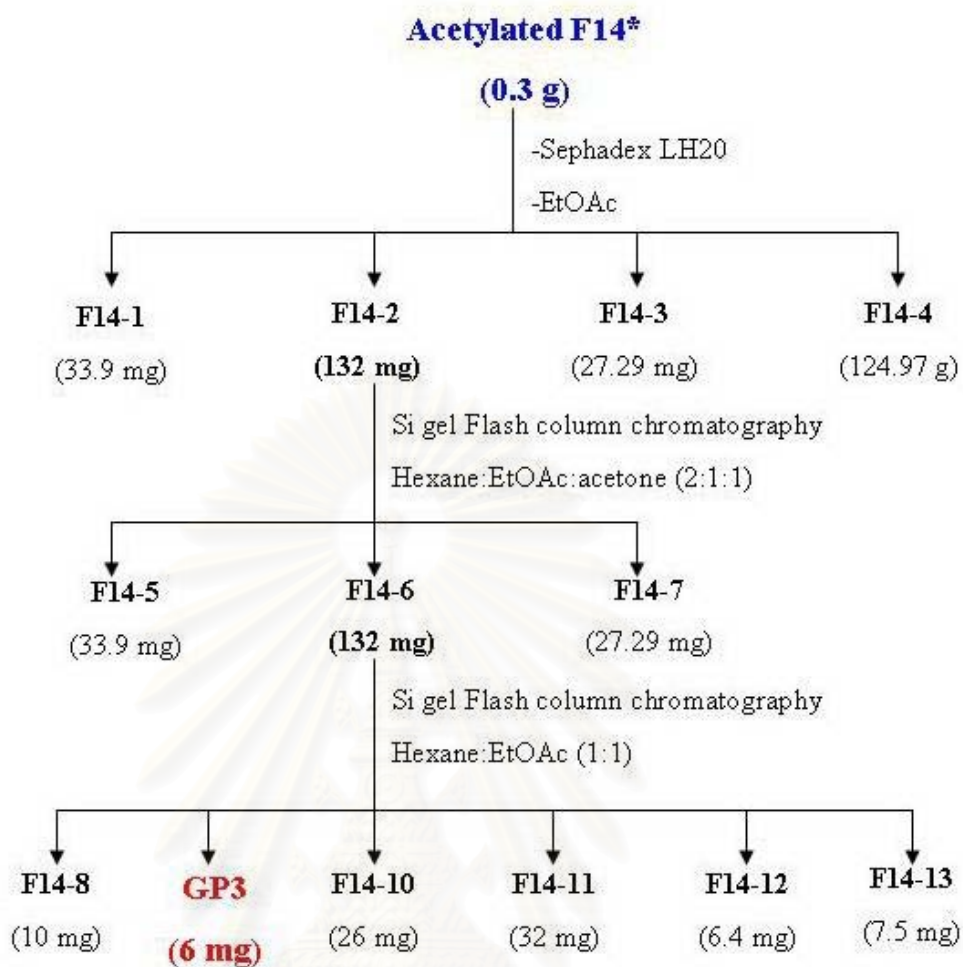


Scheme 5. Isolation of GP2

4.3 Acetylation and isolation of acetylated F14

Fraction F14 (5 mg), DMAP catalytic agent (20 mg) were dissolved with excess amount of pyridine (0.2 ml). Acetic anhydride (0.5 ml) was added, and the solution was stirred at room temperature for 6 hours under argon to give the residue (0.65 g). Purification of the residue by flash column and hexane:EtOAc (1:1) were carried out to afford the acetylated products (acetylated F14, 0.3 g).

The acetylated products of F14 were further separated by Sephadex LH20 column (3.5 x 50 cm) with EtOAc, silica gel flash column, hexane:EtOAc:acetone (2:1:1) and hexane:EtOAc (1:1) to give an acetyl derivative, GP3 (6 mg) (Scheme 6).



Scheme 6. Isolation of GP3

5. Physical and spectral data of the acetylated Compounds

5.1 Compounds GP1

Compound GP1 was obtained as yellow mass.

EIMS : $[M+H]^+$ m/z 679 Figure 24

FABMS : $[M+Na]^+$ m/z 701 (calcd for $C_{28}H_{38}O_{19}$);
Figure 25

$[\alpha]_D^{25}$: + 54.6°

IR : ν_{max} cm^{-1} , Film;
2,962, 1743, 1,092 cm^{-1} Figure 26

1H NMR : δ ppm, 500 MHz in $CDCl_3$; Table 8, Figures 27 - 29

^{13}C NMR : δ ppm, 75 MHz in $CDCl_3$; Table 8, Figures 30 - 31

5.2 Compounds GP2

Compound GP2 was obtained as yellow mass.

EIMS	: [M+H] ⁺ <i>m/z</i> 637 (calcd for C ₂₆ H ₃₆ O ₁₈); Figure 39
FABMS	: [M+Na] ⁺ <i>m/z</i> 659 Figure 40
[α] _D ²⁵	: +54.8°
IR	: ν_{\max} cm ⁻¹ , Film; 3,437, 2,854, 1,744 cm ⁻¹ Figure 41
¹ H NMR	: δ ppm, 500 MHz in CDCl ₃ ; Table 9, Figures 42 - 43
¹³ C NMR	: δ ppm, 75 MHz in CDCl ₃ ; Table 9, Figures 44 – 45

5.3 Compounds GP3

Compound GP3 was obtained as yellow mass.

EIMS	: [M+H] ⁺ <i>m/z</i> 637 (calcd for C ₂₆ H ₃₆ O ₁₈); Figure 53
FABMS	: [M+Na] ⁺ <i>m/z</i> 659 Figure 54
[α] _D ²⁵	: +55.1°
IR	: ν_{\max} cm ⁻¹ , Film; 3,437, 2,854, 1,744 cm ⁻¹ Figure 55
¹ H NMR	: δ ppm, 500 MHz in CDCl ₃ ; Table 10, Figures 56 - 58
¹³ C NMR	: δ ppm, 125 MHz in CDCl ₃ ; Table 10, Figure 59 - 62

6. α -Glucosidase inhibitory activity

6.1 Material and instruments

<i>p</i> -Nitrophenyl- α -D-glucopyranoside	Sigma Chemical Co.
α -Glucosidase (Type I)	Sigma Chemical Co.
1-Deoxynojirimycin	Sigma Chemical Co.
Sodium dihydrogen phosphate	May & Baker Ltd.
Disodium hydrogen phosphate	May & Baker Ltd.
Water	Highly purified water 18.2 m Ω
Microplate reader	Perkin Elmer – Vector ³

6.2. Preparation of the test sample

The crude extract (200 mg) or test sample (2 mg) was accurately weighed in a volumetric flask, and water was added to make a 2 ml solution. The initial concentration was obtained as 100 mg/ml for crude extract and 1 mg/ml for fractioned fraction. The final concentration of the samples was expressed as μM . For the IC_{50} determination, serial dilution was performed with water until a set of sample solutions with a suitable range of concentration was obtained. The total volume of the reaction mixture was 200 μl .

6.3 Determination of α -Glucosidase inhibitory activity

The inhibitory effect of each compound on α -glucosidase activity was measured according to the literature procedure (Matsui, T *et al.*, 1996). Briefly, α -glucosidase from baker's yeast was assayed using 0.1 M phosphate buffer at pH 6.8, and 1 mM *p*-nitrophenyl- α -D-glucopyranoside (PNP-G) was used as a substrate. The concentration of the enzyme was 1 U/mL in each experiment. α -Glucosidase (4 μL) was incubated in the absence or presence of various samples (concentration 1 mg/mL, 1 μL) at 37°C. The pre-incubation time was specified at 10 min and PNP-G solution (95 μL) was added to the mixture. The reaction was carried out at 37°C for 20 min, and then 100 μL of 1 M Na_2CO_3 stopping reagent was added to terminate the reaction. Enzymatic activity was quantified by measuring the absorbance at 405 nm. 1 mM 1-Deoxynorjorimycin was used as the positive control. One unit of α -glucosidase is defined as amount of enzyme liberating 1.0 μmol of *p*-nitrophenol (PNP) per unit. The absorbance of each well was measured at 405 nm with the microplate reader.

The concentration of inhibitors required for inhibiting 50% of glucosidase activity under the assay condition with various concentrations of test samples was defined as the IC_{50} (as described in Section 6.4, Gao *et al.*, 2007).

The kinetics evaluations of the type of inhibition by F08 and F21 on α -glucosidase, were determined. The enzyme and test samples 25 and 250 mg/ml for F08 and 2.5 and 25 mg/ml for F21, respectively were incubated with increasing concentration of PNP-G substrate. Lineweaver-Burk plot was used in this study (as described in Section 6.5, Adisakwattana *et al.*, 2004).

The reaction mixture (200 μl) were measured in 3 wells (A, B, and C). In each well, the substances was added in order of mixing, as follows;

A (control)	1 μl of water
	4 μl of enzyme
	95 μl of 0.1 mM PNP-G
	100 μl of 1 M Na_2CO_3
B (blank)	5 μl of buffer 0.1 M phosphate buffer at pH 6.8
	95 μl of 0.1 mM PNP-G
	100 μl of 1 M Na_2CO_3
C (sample)	1 μl of sample solution
	4 μl of enzyme
	95 μl of 0.1 mM PNP-G
	100 μl of 1 M Na_2CO_3

$$\% \text{ Inhibition} = 100 - \frac{\text{Absorbance (sample)} - \text{Absorbance (blank)}}{\text{Absorbance (control)}} \times 100$$

6.4 Determination of IC_{50}

The IC_{50} value is the concentration of the test sample that can cause 50% inhibition of the enzyme. An IC_{50} value was obtained by plotting % inhibitions versus concentrations of the inhibitor. This was performed on a set of sample solutions with various concentrations prepared by serial dilution method.

6.5 Determination of enzyme kinetics

Kinetics can be a great value for predicting or eliminating possible reaction mechanisms under consideration, since an observed reaction rate must satisfy the proposed mechanism. The Lineweaver-Burk plot was widely used to determine important terms in enzyme kinetics, such as K_m and V_{max} before the wide availability of powerful computers and non-linear regression software, as the Y-intercept of such a graph is equivalent to the inverse of V_{max} ; the X-intercept of the graph represents $-1/K_m$. It also gives a quick and visual impression of the different forms of enzyme inhibition. Lineweaver-Burk plot can distinguish competitive inhibitors, noncompetitive inhibitors, and uncompetitive inhibitors. **Competitive inhibitors** usually resemble the substrate and compete with it for the active site. The extent of the inhibition is a function of the relative concentrations of the substrate and the inhibitors. As the substrate concentration is increased, the extent of inhibition decreases, until at infinitely high substrate concentration the inhibitor has no effect. Therefore, in the presence of a competitive inhibitor, V_{max} remains the same; but K_m is increased. Competitive graph was shown the same Y-intercept (**Figure 5a**), but there is different slopes and X-intercept between the 2 data sets. **Noncompetitive inhibition**, in contrast to competition inhibitors, generally bind at a site other than the binding site of the substrate, and thus the inhibitor and substrate are not in direct competition. In this case, the inhibition is dependent of the substrate concentration and depends only on the inhibitor concentration. The effect of inhibitor is simply to remove some of the enzyme molecules from participation in the catalytic process. The enzyme molecules bound by inhibitor, however, still generally possess the capability of binding substrate but not of converting it to product. Noncompetition graph were produced plot with the same X-intercept (K_m is unaffected) but different slopes and Y-intercepts (**Figure 5b**). **Uncompetitive inhibition** causes different intercepts on both the Y and X axes but the same slope (**Figure 5c**).

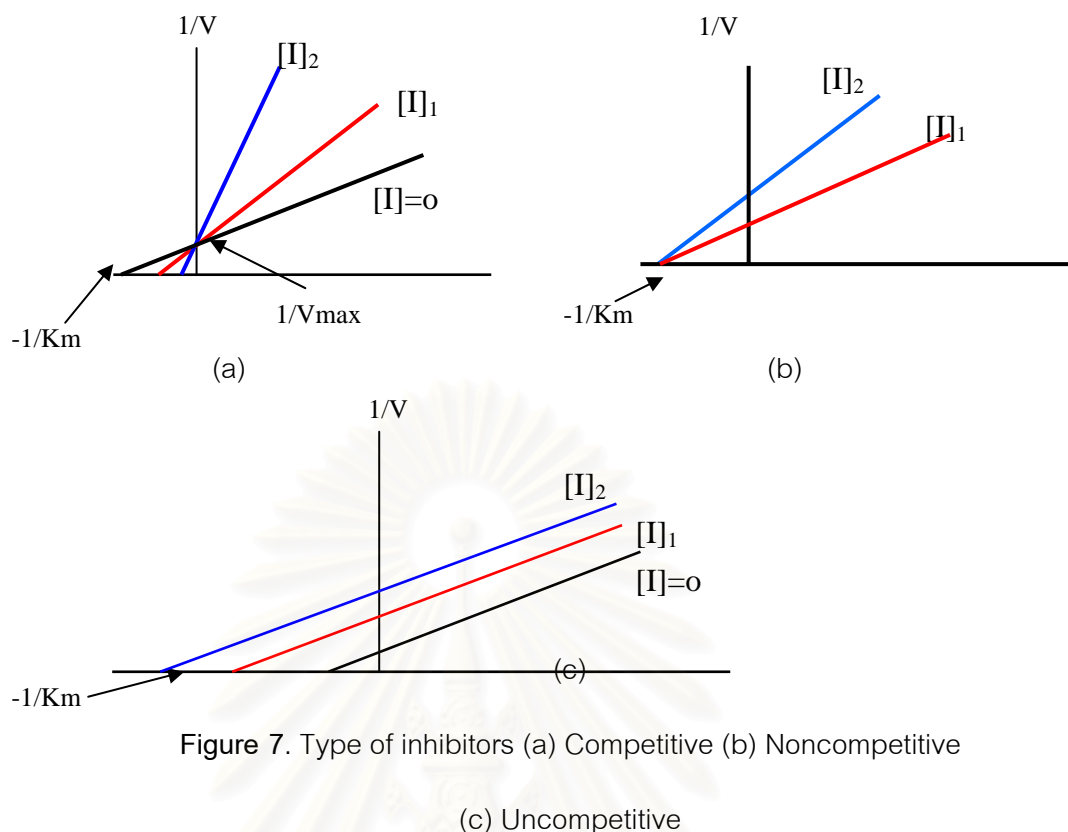


Figure 7. Type of inhibitors (a) Competitive (b) Noncompetitive
(c) Uncompetitive

The procedure for investigating the kinetics was performed using the α -glucosidase inhibitory activity. Measurement of the initial rate of *p*-nitrophenol formation of the reaction mixture was expressed as the increase of absorbance at wavelength 405 nm per min ($\Delta A_{405}/\text{min}$). The Michaelis-Menten constant (K_m) and maximal velocity (V_{max}) of α -glucosidase were determined by Lineweaver-Burk plot with various concentrations of PNP-G as the substrate.

The experiment was carried out in triplicate using a series of α -glucosidase solutions against two concentrations of the test samples in comparison with the control. First, PNP-G was accurately weighed (15.06 mg) and then dissolved in 10 ml of 0.1 mM phosphate buffer (pH 6.8) to give 5 mM PNP-G solution. This solution (5 ml) was then transferred to a volumetric flask and the final volume of the solution was adjusted to 10 ml to give 2.5 mM PNP-G solution. Further serial dilutions were carried out in a similar manner to give 1.25 mM and 0.625 mM solution of PNP-G. In addition, 1 ml of 5 mM of PNP-G solutions was diluted with buffer to give 6 ml of 0.83 mM of PNP-G solution. In the test, 95 μl of the serial of PNP-G substrate solutions was added to the reaction

mixture of each well of the microplate to give the final concentration of PNP-G as 1, 1/2, 1/4, 1/6, and 1/8 mM, respectively.

The two concentrations of the test sample selected for the kinetics study were 0.1, and 1 fold of the IC_{50} concentration. The absorbance was taken every 1 second for 1 minute, then inverse of V versus the inverse of the substrate concentration were plotted in Lineweaver-Burk plot. K_m , V_{max} , and K_i were obtained from the below equations

$$\text{X-intercept} = -1/K_m$$

$$K_m = \text{Michaelis-Menten constant}$$

$$\text{Y-intercept} = 1/V_{max}$$

$$V_{max} = \text{the velocity at maximal concentration of substrate}$$

$$K_i = [I] / \{V_{max}/V_{max'}\} - 1$$

where

$$K_i = \text{the dissociation constant for inhibitor binding}$$

$$[I] = \text{concentration of inhibitor}$$

$$V_{max} = \text{the maximum enzyme velocity}$$

$$V_{max'} = \text{the enzyme velocity with the presence of inhibitor}$$

The type of enzyme inhibition was determined by analyses of K_i , V_{max} , and K_m values. The dissociation constant for inhibitor binding, K_i , if K_i is low indicated the affinity is high. The Michaelis-Menten constant, K_m ; if K_m is low indicated the complete inhibition.

CHAPTER IV

RESULTS AND DISCUSSION

The aqueous ethanolic extract of the fresh aerial part of *G. procumbens* was evaporated and then partitioned with ethyl acetate. The ethyl acetate extract was then partitioned between hexane and methanol. The aqueous part exhibited significant α -glucosidase inhibitory activity, with the 54 % inhibition activity, and was further fractionated using several chromatographic techniques. The active fractions were acetylated and separated to give three acetyl derivatives including GP1, GP2, and GP3.

The structures of all acetylated compounds were determined by interpretation of their IR, NMR, and Mass spectral data, as well as by comparison with literature values.

1. Structure determination of the acetylated compounds from the aqueous extract of *G. procumbens*.

1.1 Structure determination of GP1

Fraction F21 from the aqueous extract showing a brown-purple spot upon spraying with anisaldehyde-sulfuric reagent, was subjected to evaluation for the α -glucosidase inhibitory activity. The ^1H NMR spectrum of fraction F21 showed the broad proton signals at δ between 2.8–5.9 ppm, suggesting the saccharide characteristics.

Several attempts to isolate the saccharide mixture from the fraction by conventional methods have been unsuccessful. Therefore, to separate the saccharides, fraction F21 was acetylated prior to separation by chromatography. Compound GP1 was isolated from the acetylated fraction, and subjected to chemical structure determination by spectroscopic techniques.

Compound GP1 was a yellow mass giving purple color with anisaldehyde-sulfuric reagent on the silica gel TLC plate ($R_f = 0.78$) using hexane: EtOAc: acetone (2:1:1) as a developing solvent. The IR spectrum displayed absorption bands at 2,962 cm^{-1} (C-H stretching), 1,743 cm^{-1} (C=O stretching), and 1,092 cm^{-1} (C-O-C stretching) (Figure 26). The molecular formula of $\text{C}_{28}\text{H}_{38}\text{O}_{19}$ (MW = 678) was proposed from the

combination of the EIMS and FABMS (Figures 24-25) showing the $[M+H]^+$ peak at m/z 679, $[M+Na]^+$ peak at m/z 701, respectively, and the 125 MHz ^{13}C -NMR spectrum of GP1 in CDCl_3 giving twenty-eight carbon signals. The carbon signals were classified by DEPT 135, and DEPT 90 spectra (Figure 31) and HMQC spectrum (Figures 34-35) as three methylene carbon signals at δ 61.55, 62.68, and 63.42 ppm; eight methyl carbons of the acetyl groups at δ 20.52 - 21.00 ppm; seven methine carbons at δ 68.02, 68.29, 69.43, 70.07, 74.80, 75.51, 78.90, one anomeric methine carbon at δ 89.73 ppm, and one anomeric quaternary carbon at δ 103.78 ppm; and eight carbonyl carbons of the acetate parts at δ 169.86, 170.02, 170.23, 170.39, 170.46, 170.46, 170.84, and 170.05 ppm. Two anomeric carbons at δ 89.73 and 103.78 suggested the presence of 2 saccharide units

Analyses of the 500 MHz ^1H -NMR and the ^1H - ^1H COSY spectrum of GP1 recorded in CDCl_3 established the first saccharide unit as follows: H1 δ 5.64 (d, $J = 3.7$) coupled to H2 δ 4.81 (dd, $J = 3.7, 10$); H2 coupled to H3 δ 5.38 (t, $J = 10$,); H3 coupled to H4 δ 5.01 (t, $J = 10$); H4 coupled to H5 δ 4.22 (td, $J = 3.1, 10$); H5 coupled to H6a δ 4.08 (d, $J = 3.1$) and H6b δ 4.18 (dd, $J = 3.1$). The connectivity of the second saccharide unit was established as follows: H3' δ 5.38 (d, $J = 5.9$) coupled to H4' δ 5.30 (t, $J = 5.9$) as shown in Figures 27-29. The chemical shifts of the overlapping signal protons at the range of 4.0-4.3 ppm were confirmed by the HMQC spectrum.

The connectivity of the first saccharide unit was confirmed by following long range H-C correlations in the HMBC ($^nJ_{\text{C-H}} = 8$ Hz) spectrum (Figures 36-37): H-1 correlated to C-4; H-2 to C-3; H-3 to C-2; and H-4 to C-5; and the second unit was confirmed by following HMBC correlations: H-1' correlated to C-2' and C-3'; H-3' to C-1', C2', and C-4'; H-4' to C-2', and C-3'. The connectivity of the first unit to the second unit via a (1 \rightarrow 2)-O-glycosidic linkage was confirmed by a long range H-C correlation in the HMBC spectrum (Figure 37). HMBC correlations of GP1 were summarized in Figure 8.

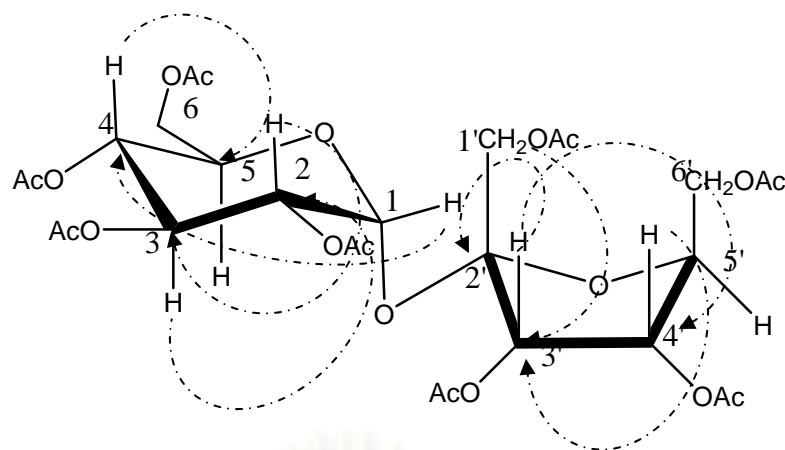


Figure 8 The ^1H - ^{13}C long-range correlations in HMBC ($^nJ_{\text{C-H}} = 8 \text{ Hz}$) spectra of GP1

The relative configuration of the first saccharide was established based on NOESY spectral data (Figure 38). H-1 showed NOE correlation with H-2; H-2 to H-4; and H-4 to H-6a, indicating that these three protons were arranged on the same face of the molecule. The relative configuration of the second saccharide was also established by NOESY spectral data. H-1' of the second saccharide showed NOE correlation to H-3'; H-3' to H-4'; and H-4' to H-6'a, indicating that these four protons were arranged on the same face of the molecule. NOE correlations of GP1 were summarized in Figure 9.

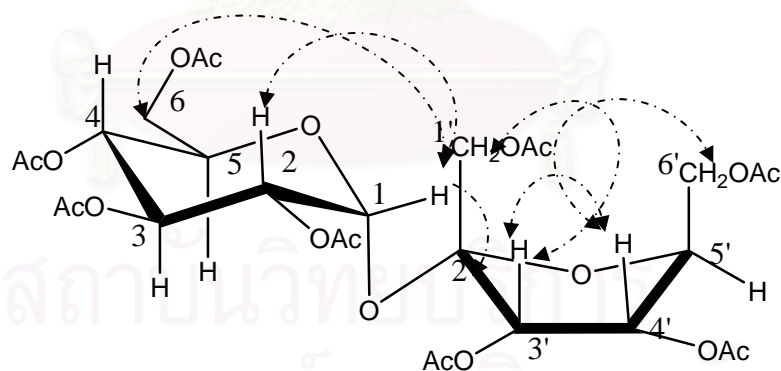


Figure 9 NOESY correlations of GP1

The configuration of H-1 was established in β -equatorial by coupling constant of H-1 to H-2 (3.7 Hz), indicating β -equatorial H-1 and β -axial H-2. Based on the above evidence, the basic skeleton of the first unit of saccharide was determined as glucose. The upfield signal of H-5' (δ 4.14) compared to the downfield signals of H-3' (δ 5.38)

and H-4' (δ 5.30) indicated that C-5' connected to C-2' by an ether linkage. Therefore, the second saccharide unit was determined as furanopsicose. Based on the above evidence, the basic skeleton of GP1 was determined as 2-[3,4-diacetate-2,5-bis(acetatemethyl)oxolan-2-yl]ate-6-(acetatemethyl)oxane-3,4,5-triacetate. Finally, the parent compound of GP1 was determined as a new α -D-glucopyranosyl-(1 \rightarrow 2)-O-psicofuranoside as shown in Figure 10.

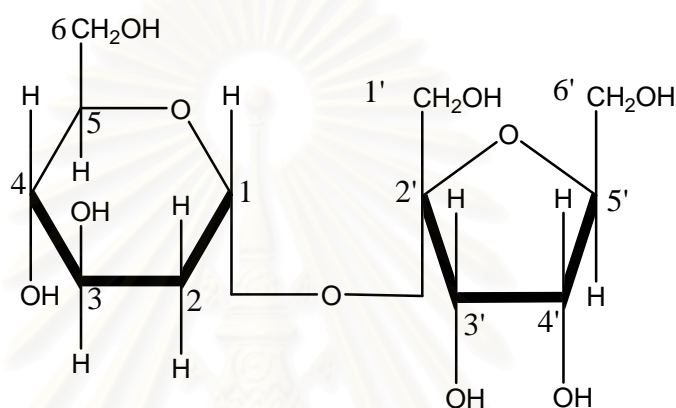


Figure 10 The structure of α -D-glucopyranosyl-(1 \rightarrow 2)-O-psicofuranoside.

Glucosylpsicose has been reported as a novel compound obtained from transglycosylation of arabinoxylan of *Aspergillus sojae*. It constituted of a glucose unit linked to D-psicose (a rare sugar with pyranoside skeleton, Figure 11) by an β -(1 \rightarrow 4) ether linkage (Oshima *et al.*, 2006). In 2007, Oshima *et al* synthesized an α -(1 \rightarrow 4) glucosylpsicose from transglycosylation of α -cyclodextrin. Moreover, D-psicose has been reported as a plant growth regulation inducing gene transcription.

D-Psicose is a C-3 epimer of D-fructose and is presented at a very small concentration in nature. D-Psicose was realized to be an inhibitor of some of the intestinal disaccharidases such as α -amylase in Male Wistar rats and intestinal α -glucosidase (*in vitro*) (Tatsuhiko *et al*, 2006). Moreover, D-psicose significantly inhibited the increase of plasma glucose concentration induced by sucrose and maltose with uncompetitive inhibitory activities and suppressed glycemic responded after carbohydrate ingestion (Matsuo *et al.*, 2006).

Table 7. The ^1H and ^{13}C NMR assignments, ^1H - ^1H COSY, HMBC, and NOESY correlations of GP1 (acetylated part)

Position	$\delta^{13}\text{C}$ (ppm)	$\delta^1\text{H}$ (multiplicity, J in Hz)	^1H - ^1H COSY	HMBC	NOESY
1	89.73	5.64 (1H, d, 3.7)	H2	C4,C2'	H2,H1',H4'
2	70.07	4.81 (1H, dd, 3.7,10)	H3	C1,C3	H4,H6
3	69.43	5.38 (1H, t, 10)	H4	C2	H1'a,b,H6'b
4	68.02	5.01 (1H, t, 10)	H5	C5	H2
5	62.29	4.21 (1H, dt, 3.1,10)	H6	C3	H3
6a	61.55	a 4.08 (1H, d, 12)			H2
6b		b 4.18 (1H, dd, 3.1,12)			
1a',b'	62.68	4.10 (2H, s)		C2',C3'	
2'	103.78	-		C4'	
3'	75.51	5.38 (1H, d, 5.9)	H4'	C1',C4'	H4',H6'b
4'	74.50	5.30 (1H, t, 5.9)	H4'	C3'	H2'
5'	78.90	4.14 (m)	H5'		
6a'	63.42	a 4.24 (1H, dd, 7,18)	H7'		
6b'		b 4.28 (1H, d, 18)			
-CO- <u>CH₂</u>	21.00-20.52	~2.5-2.9			
- <u>C=O</u>	170.05,170.84, 170.46,170.46, 170.39, 170.23.170.20, 169.86				

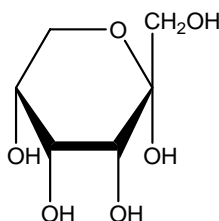


Figure 11 The structure of α -D-psicopyranoside

1.2 Structure determination of GP2

Compound GP2 from fraction 11 was a light yellow mass giving a purple spot with anisaldehyde-sulfuric reagent on the silica gel TLC plate (hexane:EtOAc:acetone = 2:1:1, R_f = 0.6). The IR spectrum displayed absorption bands at $3,400\text{ cm}^{-1}$ (O-H stretching, broad), $2,962\text{ cm}^{-1}$ (C-H stretching), $1,743\text{ cm}^{-1}$ (C=O stretching), and $1,092\text{ cm}^{-1}$ (C-O-C stretching) (Figure 41). The molecular formula of $\text{C}_{26}\text{H}_{36}\text{O}_{18}$ was proposed from the combination of the EIMS and FABMS (Figures 39-40) showing the $[\text{M}+\text{H}]^+$ peak at m/z 637 and $[\text{M}+\text{Na}]^+$ peak at m/z 659 (calcd for $\text{C}_{26}\text{H}_{36}\text{O}_{18}$) and 75 MHz ^{13}C -NMR spectrum of GP2 in CDCl_3 giving twenty-six carbon signals. Moreover, from the combination of EI and IR spectral data of GP2, the IR displayed O-H stretching at $3,400\text{ cm}^{-1}$ and the molecular formula of GP2 from MS was $\text{C}_{26}\text{H}_{36}\text{O}_{18}$ indicated one unacetylated hydroxyl group. The carbon signals were classified by DEPT 135, and DEPT 90 spectra (Figure 45) and the HMQC spectrum (Figure 49) as three methylene carbon signals at δ 62.07, 63.15, and 63.97 ppm; seven methyl carbons of the acetyl groups at δ 20.52 - 21.00 ppm; seven methine carbons at δ 68.65, 69.87, 70.76, 72.81, 74.74, 75.83, 78.64, an anomeric methine at δ 90.12 ppm, and one quaternary anomeric carbon at δ 103.66 ppm; and eight carbonyl carbons of the acetate parts at δ 169.86, 170.02, 170.23, 170.39, 170.46, 170.46, 170.84, and 170.05 ppm. Two anomeric carbons at δ 89.73 and 103.66 suggested the presence of 2 saccharide units.

Analyses of the 500 MHz ^1H -NMR and the ^1H - ^1H COSY spectrum of GP2 recorded in CDCl_3 established the first saccharide unit as follows: H1 δ 5.61 (d, J = 3.8) coupled to H2 δ 4.76 (dd, J = 3.8, 10); H2 coupled to H3 δ 3.98 (t, J = 10); H3 coupled

to H4 δ 4.90 (t, $J = 10$); H4 coupled to H5 δ 4.2 (td, $J = 1.8, 10$); H5 coupled to H6 δ 4.26 (d, $J = 1.8$). Since the H3 signal was shifted to up field and the HMQC spectral data indicated the proton at this position was unacetylated. The connectivity of the second saccharide unit was established as follows: H3' δ 5.37 (d, $J = 6.5$) coupled to H4' δ 5.46 (t, $J = 6.5$) as shown in **Figures 42-43**. The chemical shifts of the overlapping signal protons at the range of 3.8-4.3 ppm were confirmed by HMQC spectrum.

The connectivity of the first saccharide unit was confirmed by the following long range H-C correlations in the HMBC (${}^nJ_{C-H} = 8$ Hz) spectrum (**Figures 50-51**). H-1 correlated to C-4; H-2 to C-3; H-4 to C-2; H-4 to C-5 and the second unit was confirmed by following H-1' correlated to C-2' and C-3'; H-3' to C-1', C2', and C-4'; H-4' to C-2', and C-3'. The connectivity of the first unit to the second unit via a (1 \rightarrow 2)-O-glycosidic linkage was confirmed by a long range H-C correlation in the HMBC spectrum (**Figure 51**). HMBC correlations of GP2 were summarized in **Figure 12**.

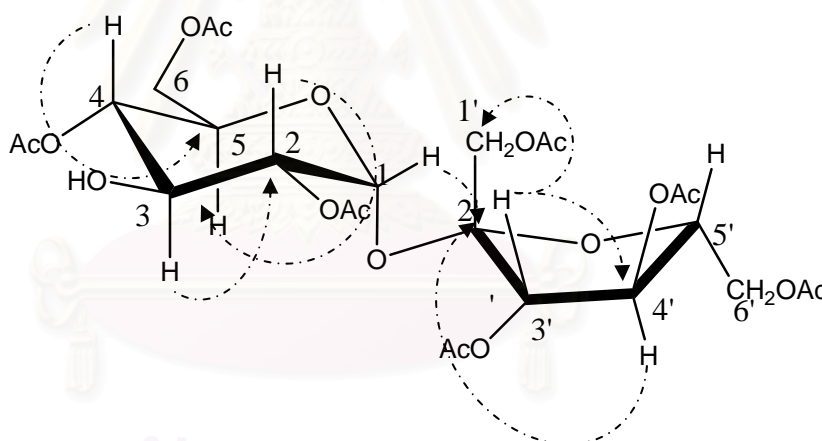


Figure 12 The ${}^1\text{H}$ - ${}^{13}\text{C}$ long-range correlations in HMBC (${}^nJ_{C-H} = 8$ Hz) spectra of GP2

The relative configuration of the first saccharide was established using NOESY spectral data (**Figure 52**). H-1 showed NOE correlation with the H-2; H-2 to H-4; and H-4 to H-6a, indicating that three protons were arranged on the same face of the molecule. The relative configuration of the second saccharide was determined based on NOESY spectral data. H-1' of the second saccharide showed NOE correlation to H-3'; H-3' to

H-5', and H-4' to H6'a, no correlation between H3' and H4'. NOE correlations of GP2 were summarized in Figure 13.

The configuration of H-1 was established in β -equatorial by analyses of the 500 MHz $^1\text{H-NMR}$, which showed that the coupling constant of H-1 to H-2 was 3.8 Hz, indicating β -equatorial to β -axial position. Based on the above evidence, the basic skeleton of the first unit of saccharide was determined as glucose. The upfield signal of H-5' (δ 4.16) compared to the downfield signals of H-3' (δ 5.46) and H-4' (δ 5.37) indicated that C-5' connected to C-2' by an ether linkage. Therefore, the second saccharide unit was determined as furanofructose.

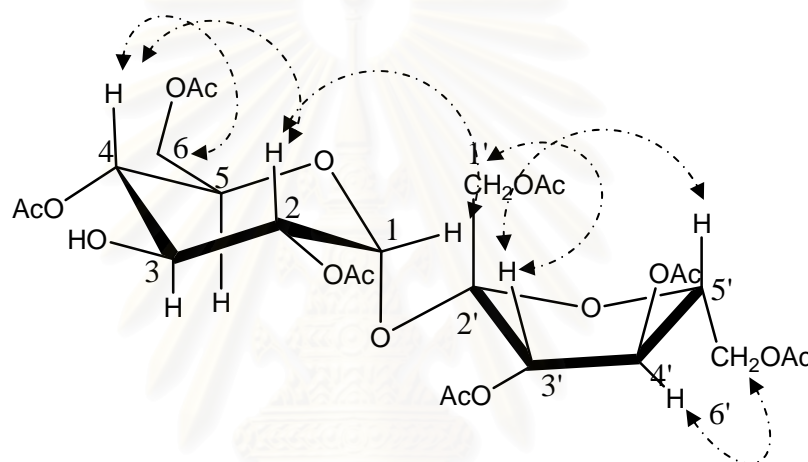


Figure 13 NOESY correlations of GP2

Based on the above evidence, the basic skeleton of GP2 was determined as 2,4-diacetate-3-hydroxy-2,5-bis(acetatemethyl)oxolan-2-yl]ate-6-(acetatemethyl)oxane-3,4,5-triacetate. Finally, the parent compound of GP1 was determined as a α -D glucopyranosyl-(1 \rightarrow 2)-O-fructofuranoside as shown in Figure 14.

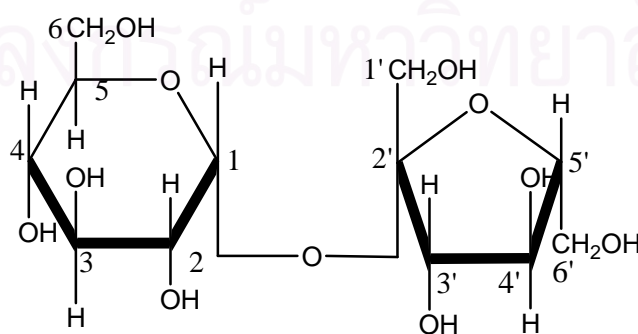


Figure 14 The structure of α -D-glucopyranosyl-(1 \rightarrow 2)-O-fructofuranoside

Table 8. The ^1H and ^{13}C NMR assignments, ^1H - ^1H COSY, and HMBC correlations of GP2 (acetylated part)

Position	$\delta^{13}\text{C}$ (ppm)	$\delta^1\text{H}$ (multiplicity, J in Hz)	^1H - ^1H COSY	HMBC	NOESY
1	90.12	5.61 (1H, d, 3.8)	H2	C2',C3	H2,H4', H4'
2	72.81	4.77 (1H,dd, 3.7, 10)	H3	C1,C4	H4
3	69.87	3.98 (1H,t, 10)	H4	C2, C4	H5
4	70.76	4.90 (1H, t, 10)	H5	C3	H1
5	78.64	4.20 (1H, td, 1.8,10)	H6		H3
6	62.07	4.26 (1H, d, 1.8)		C5	
1'	63.97	a 4.30 (m)			
		b 4.28 (m)			
2'	103.66	-			
3'	75.83	5.46 (1H, d ,6.7)	H4'	C4'	H5'
4'	74.74	5.37 (1H, t, 6.7)	H5'	C3'	
5'	68.65	4.16 (m)	H6'		H3'
6'	63.15	4.14 (1H, dd, 6.7,5.1)			
-COCH ₃	21.00-20.52				
-C=O	170.77,170, 170.65, 170.5,170.0, 169.93, 169.55				

1.3 Structure determination of compounds GP3

Compound GP3 from fraction F14 was a light yellow mass giving a purple spot with anisaldehyde-sulfuric reagent on the silica gel TLC plate (hexane:EtOAc:acetone =2:1:1, $R_f = 0.45$). GP3 was a mixture of saccharides, however, the main structure was established as a disaccharide by 1D and 2D-NMR spectral data. The IR spectrum of the main compound displayed absorption band at $3,400\text{ cm}^{-1}$ (O-H stretching, broad), $2,960\text{ cm}^{-1}$ (C-H stretching), $1,742\text{ cm}^{-1}$ (C=O stretching), and $1,092\text{ cm}^{-1}$ (C-O-C stretching) (Figure 55). The molecular formula of $\text{C}_{26}\text{H}_{36}\text{O}_{18}$ was proposed from the combination of the EIMS and FABMS (Figures 53-54) showing the $[\text{M}+\text{H}]^+$ peak at m/z 637 and $[\text{M}+\text{Na}]^+$ peak at m/z 659 (calcd for $\text{C}_{26}\text{H}_{36}\text{O}_{18}$). The 125 MHz ^{13}C -NMR spectrum of GP3 in CDCl_3 giving twenty-six carbon signals. Moreover, from the combination of EI and IR spectral data of GP3, the IR displayed O-H stretching at $3,400\text{ cm}^{-1}$ and the molecular formula of GP3 from MS was $\text{C}_{26}\text{H}_{36}\text{O}_{18}$ indicated one unacetylated hydroxyl group. The carbon signals were classified by DEPT 135, and DEPT 90 spectra (Figure 62) and the HMQC spectrum (Figures 65-68) as three methylene carbon signals at δ 62.06, 62.44, and 63.59 ppm; seven methyl carbons of the acetyl groups at δ 20.52 - 21.00 ppm; seven methine carbons at δ 68.48, 69.85, 70.94, 72.67, 73.11, 78.54, 80.39, an anomeric methine carbon at δ 89.04 ppm, and one quaternary anomeric carbon at δ 102.5 ppm; and eight carbonyl carbons of the acetate parts at δ 170.15, 170.60, 170.60, 170.60, 170.73, 171.18, and 171.29 ppm. Two anomeric carbons at δ 89.04 and 102.5 suggested the presence of 2 saccharide units.

Analyses of the 500 MHz ^1H -NMR and the ^1H - ^1H COSY spectrum of GP3 recorded in CDCl_3 established the first saccharide unit as follows: H1 δ 5.61 (d, $J = 3.8$) coupled to H2 δ 4.77 (dd, $J = 3.8, 10$); H2 coupled to H3 δ 3.98 (t, $J = 10$); H3 coupled to H4 δ 4.90 (t, $J = 10$); H4 coupled to H5 δ 4.2. Since the H3 signal was shifted to upfield and the HMQC spectral data indicated the proton at this position was unacetylated. The connectivity of second saccharide unit was as follows: H3' δ 5.46 (d, $J = 6.3$) coupled to H4' δ 4.16 as shown in Figures 56-58. The chemical shifts of the overlapping signal protons at the range of 3.8-4.3 ppm were confirmed by HMBC spectrum.

The connectivity of the first saccharide unit was confirmed by following long range H-C correlations in the HMBC (${}^nJ_{C-H} = 8$ Hz) spectrum (Figures 69-70). H-1 correlated to C-2 and C-3; H-2 to C-3; H-3 to C-2 and C-5; H-4 to C-2 and C-5; and H-6 to C-5; and the second unit was confirmed by following H-1 correlated to C-2'; H-3' to C-4'; H-4' to C-3', and C-6'; H-5' to C-4'. The connectivity of the first unit to the second unit via a (1 \rightarrow 2)-O-glycosidic linkage was confirmed by a long range H-C correlation in the HMBC spectrum (Figure 70). HMBC correlations of GP3 were summarized in Figure 15.

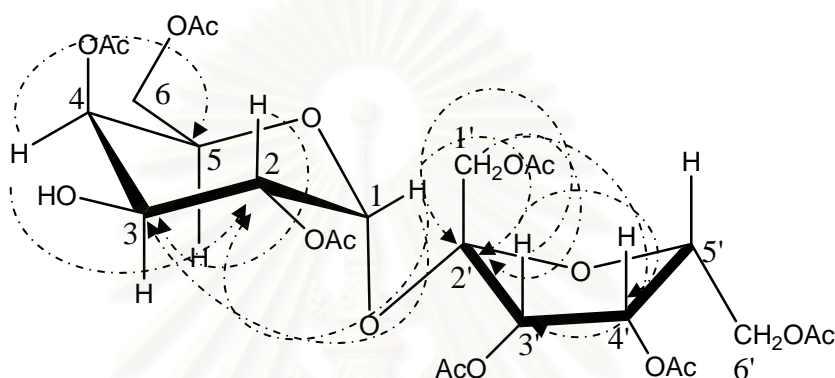


Figure 15 The ${}^1\text{H}$ - ${}^{13}\text{C}$ long-range correlation in HMBC (${}^nJ_{C-H} = 8$ Hz) spectra of GP3

The relative stereochemistry of GP3 was established based on NOESY spectral data (Figures 71). H-1 showed NOE correlation with the H-2 and H-6; H-3 to H-4; H-4 to H-5; and H-1' of the second saccharide showed NOE correlation to H-3'; H-3' to H-4'; and H-4' to H-5', indicating that these protons were arranged on the same face of the molecule. Moreover, H-3 showed NOE correlation with the H-4 and H-5. NOE correlations of GP2 were summarized in Figure 16.

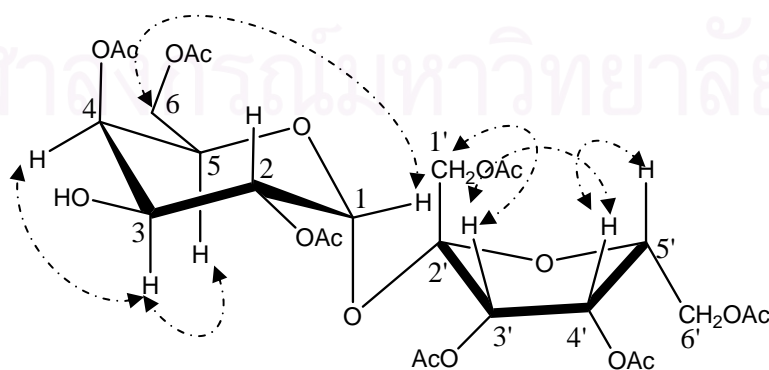


Figure 16 NOESY correlations of GP3

The configurations of H-1 were established as β -equatorial by analyses of the 500 MHz $^1\text{H-NMR}$, the coupling constant of H-1 to H-2 was 3.8 Hz, indicating β -equatorial to β -axial position. Based on the above evidence, the basic skeleton of first unit of saccharide was determined as galactose. The upfield signal of H-5' (δ 4.27) compared to the downfield signals of H-3' (δ 4.16) and H-4' (δ 4.27) indicated that C-5' connected to C-2' by an ether linkage. Therefore, the second saccharide unit was determined as furanotagatose.

Based on the above evidence, the tentative structure of GP3 was established as disaccharide, the basic skeleton of GP3 was determined as 2,4-diacetate-3-hydroxy-2,5-bis(acetatemethyl)oxolan-2-yl]ate-6-(acetatemethyl)oxane-3,4,5-triace. Finally, the parent compound of GP3 was determined as a new α -D-galactosyl-(1 \rightarrow 2)-O-tagatoside.

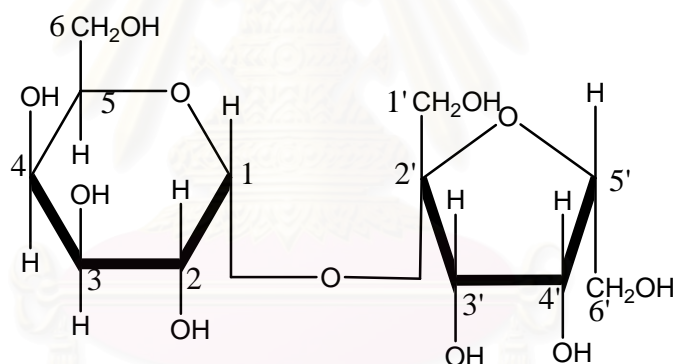


Figure 17 The structure of α -D-galactosyl-(1 \rightarrow 2)-O-tagatoside.

Table 9. The ^1H and ^{13}C NMR assignments, ^1H - ^1H COSY, and HMBC correlations of GP3 (acetylated part)

Position	$\delta^{13}\text{C}$ (ppm)	$\delta^1\text{H}$ (multiplicity, J in Hz)	^1H - ^1H COSY	HMBC	NOESY
1	89.04	5.61 (1H,d,3.8)	H2	C2,C4,C 5,C2',C5'	H2,H 6,H2'
2	72.67	4.77 (1H,dd,3.8,10)	H3	C3,C4	H1
3	69.85	3.98 (1H,t,10,10)	H4	C2, C5	H5, H1', H6'
4	80.39	4.057 (1H,m)	H5	C2	H1
5	70.94	4.28 (1H,m)	H6		H3
6	62.44	4.26 (1H,t,2.8, 6.5)		C5	
		4.29 (1H,d,2.8)			
1'	63.59	4.16 (2H,s)		C4'	C3
2'	102.50	-			
3'	78.54	5.46 (1H,d,6.3)	H4'	C4'	H5'
4'	68.48	4.16 (1H,dd,2.8,8.6)	H5'	C1'	H4'
5'	73.11	4.27 (1H,dt,2.3,8.6)	H6'	C6'	
6'	62.06	4.33 (1H,dd,5.6,4.7)		C3'	
-CO-CH ₃	21.00-20.52				
-C=O	170.15,170, 170.73, 171.18, 171.29				

α -D-Tagatose is a C-4 epimer of D-fructose, it was established as a new sweetener with low energy content. This low energy content may be due to either low absorption of the D-tagatose or decreased absorption of other nutrients. In 2001, Donner *et al.* investigated the ability of D-tagatose on a patients with type 2 diabetic, it was found that D-tagatose was enhanced insulin sensitivity and increased insulin secretion in a gastrointestinal tract. D-Tagatose may also suppressed the absorption of other carbohydrates, either by inhibited the intestinal enzymes connected to the brush border membranes or by increasing transit time. Tagatose is generally recognized as safe by the FAO/WHO and has been since 2001 (Norme'n *et al.*, 2001).

Because of its excellent taste, bulk properties, and very low energy value, D-tagatose has potential for using as a sweetener. Moreover, glucosyltagatose has been reported as a functional sweetener. It is a naturally occurring monosaccharide, specifically a hexose and was founded in dairy products. It is very similar in texture to sucrose with a 92% as sweet, but with only 38% of the calories. At present there is no report on α -glucosidase inhibitory activity of the galactosyltagatose.

2. α - Glucosidase inhibitory activity

2.1 Screening for α - glucosidase inhibitory activity

Mammalian α - glucosidase are located in the brush border surface membrane of intestinal cells, it is the key enzyme which catalyzes the final step in the digestive process of carbohydrates. Hence, α - glucosidase inhibitors can retard the liberation of D-glucose from complex and reduce postprandial hyperglycemia by suppressing the absorption of glucose, being effective for the treatment of type II diabetes and obesity.

All of the crude extracts including F02 (hexane extract), F03 (methanolic extract), and F04 (aqueous extract) were evaluated for α -glucosidase inhibitory assay at the concentration 100 mg/ml, using 1 mM of 1-deoxynojirimycin as the positive control. In preliminary examination, the aqueous extract of *G. procumbens* showed 55% inhibitory effect on α -glucosidase. The aqueous extract was further separated using several chromatographic techniques and them evaluated for their bioactivity using α -

glucosidase inhibitory assay (Adisakwatana, 2004). The most active fraction was F21. The results are shown in Table 10, and Figure 18.

Table 10: The percent inhibition of the isolated fractions from the aqueous extract of *G. procumbens* on α -glucosidase at concentration 1 mg/ml

Sample	% Inhibition			Mean % inhibition	IC ₅₀ (mg/ml)
F02	-14.05	-14.88	-20.11	-16.34	NT
F03	-6.45	-3.77	-2.16	-4.126	NT
F04	54.11	53.45	55.09	54.21	NT
F05	-3.61	-4.69	-3.89	-4.03	NT
F06	49.39	48.94	50.12	49.33	NT
F07	50.12	51.11	48.64	49.95	NT
F08	58.13	61.61	59.02	59.58	4.23
F09	54.11	56.47	55.24	55.27	NT
F10	68.09	69.11	67.25	68.15	NT
F11	59.13	60.1	59.02	59.41	NT
F12	58.13	61.11	59.2	59.48	NT
F13	71.11	68.94	70.01	70.02	NT
F14	64.11	63.45	65.09	64.21	2.08
F15	69.13	69.31	68.33	68.92	NT
F16	71.91	69.94	68.01	69.95	NT
F17	75.09	76.33	74.25	75.22	NT
F18	39.39	38.94	40.12	39.48	NT
F19	35.39	40.94	40.33	38.88	NT
F20	64.33	63.65	63.09	63.69	NT
F21	82.44	83.14	81.33	82.30	0.25
1-DNJ	85.09	84.42	82.44	83.98	5.1 μ M

1DNJ = 1 mM 1-Deoxynojirimycin

NI^a = No inhibition, less than 30% at the concentration 1 mg/ml

NT = Not test

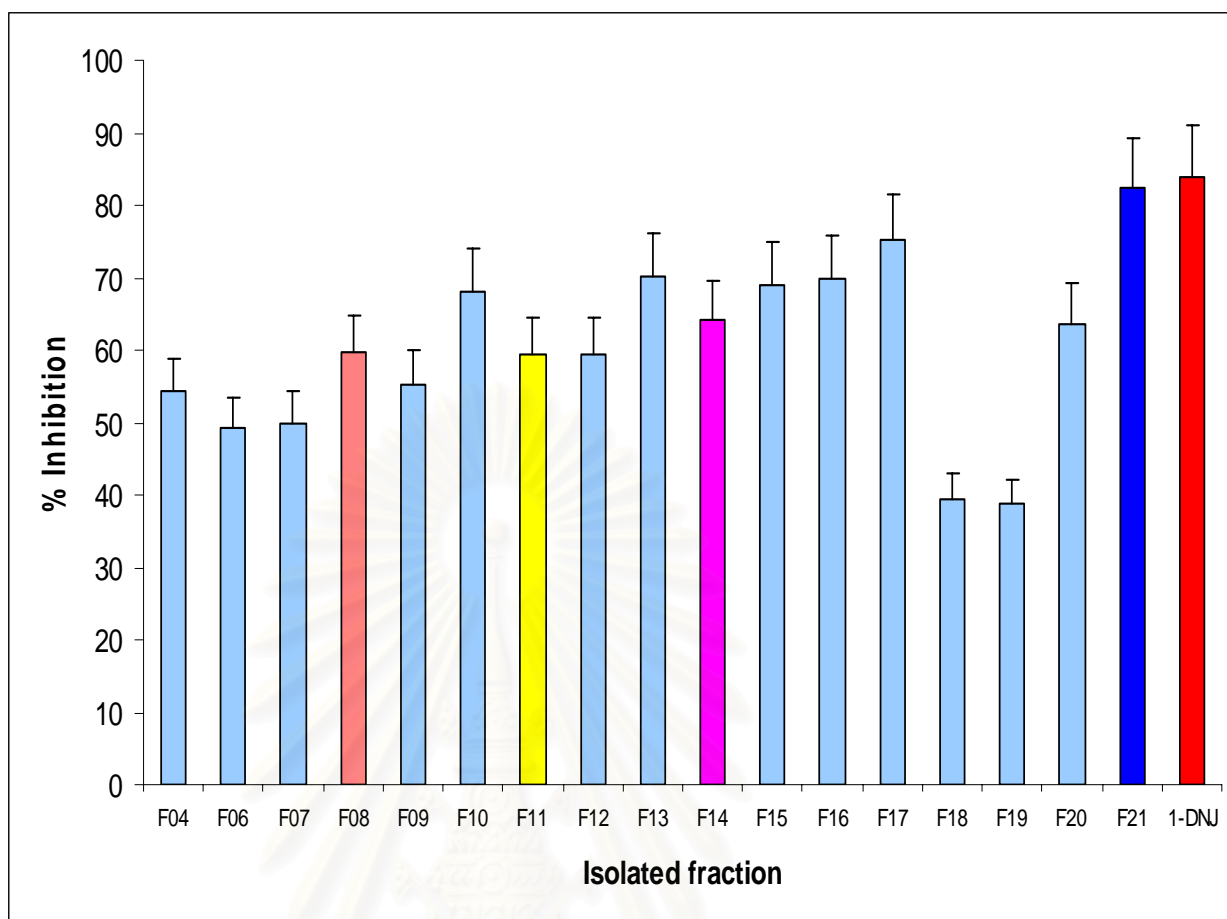


Figure 18: The percenti inhibition of the isolated fractions from the aqueous extract of *G. procumbens* on α -glucosidase at concentration 1 mg/ml

Therefore the IC_{50} values of F08, F14, and F21 showed 4.23, 2.08, and 0.25 mg/ml while reference 1-deoxynojirimycin showed an IC_{50} of 5.1 μ M. Each sample showed dose dependent enzyme inhibitory effect (Figure 19).

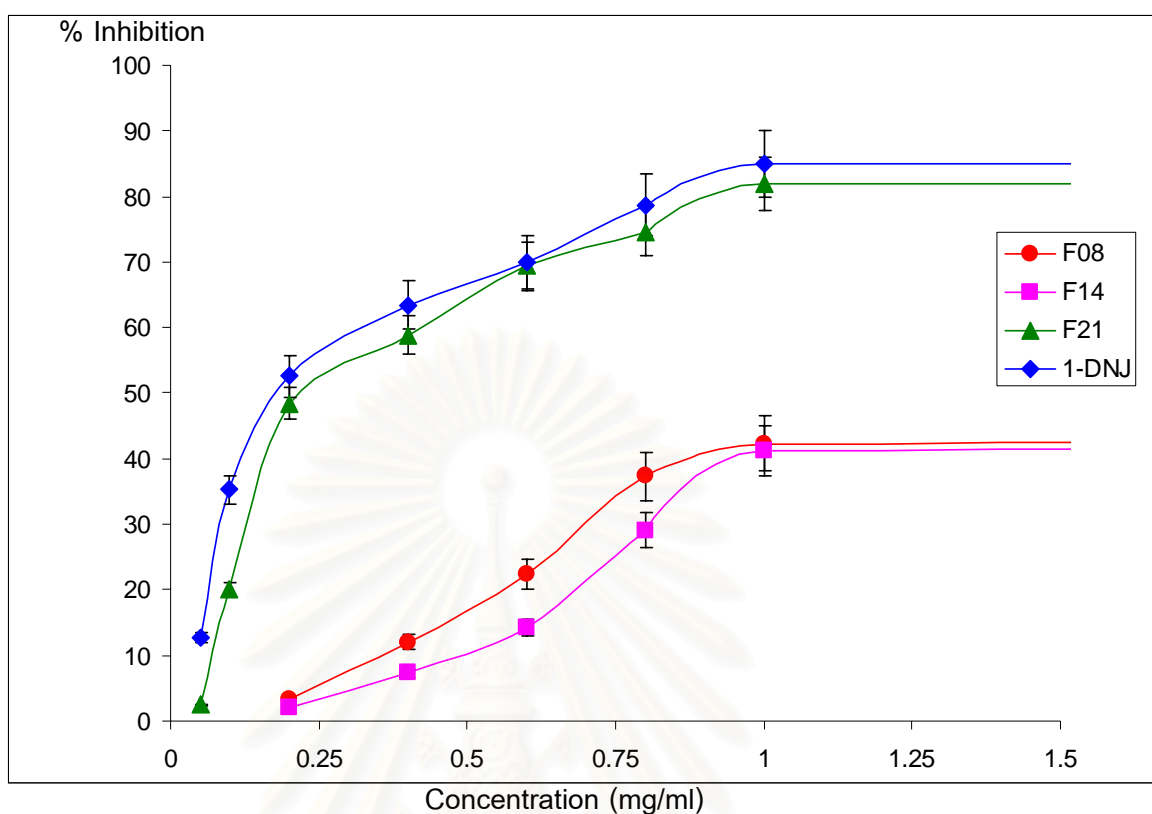


Figure 19: Dose-dependent inhibitory effect on α -glucosidase by F08 (circle, ●), F14 (square, ■), F21 (triangle, ▲), 1-deoxynojirimycin (diamond, ◆).

2.2 Enzyme kinetics

To determine the mechanism of α -glucosidase inhibition by F08 and F21, a kinetic study of the enzyme in the presence of the fraction conducted and analyzed in comparison with 1-deoxynojirimycin. The results of this study are shown in Tables 12, 13, and 14, and Figures 20, 21, and 22. From Table 12 and Figure 20, it can be seen that 1-deoxynojirimycin did not affect K_m , but decreased V_{max} of the enzyme, and therefore was a non-competitive of α -glucosidase. This is consistent with earlier reports (Kimura, *et al.*, 2003 and Gao *et al.*, 2007). However, the kinetic results of F08 and F21 were competitive inhibitors.

Table 11: The 1/V value of 1-deoxynojirimycin with variety of substrate concentrations

1/[S]	Control	S.D.	1-DNJ 50 mM	S.D.	1-DNJ 5 mM	S.D.
8.00	31.18	12.14	80.11	6.12	69.33	14.15
6.00	24.09	8.76	65.21	11.8	54.12	2.44
4.00	16.09	2.34	47.12	7.3	38.32	11.98
2.00	9.8	1.87	28.14	13.58	21.14	16.98
1.00	2.54	12.09	9.21	3.11	6.11	4.12

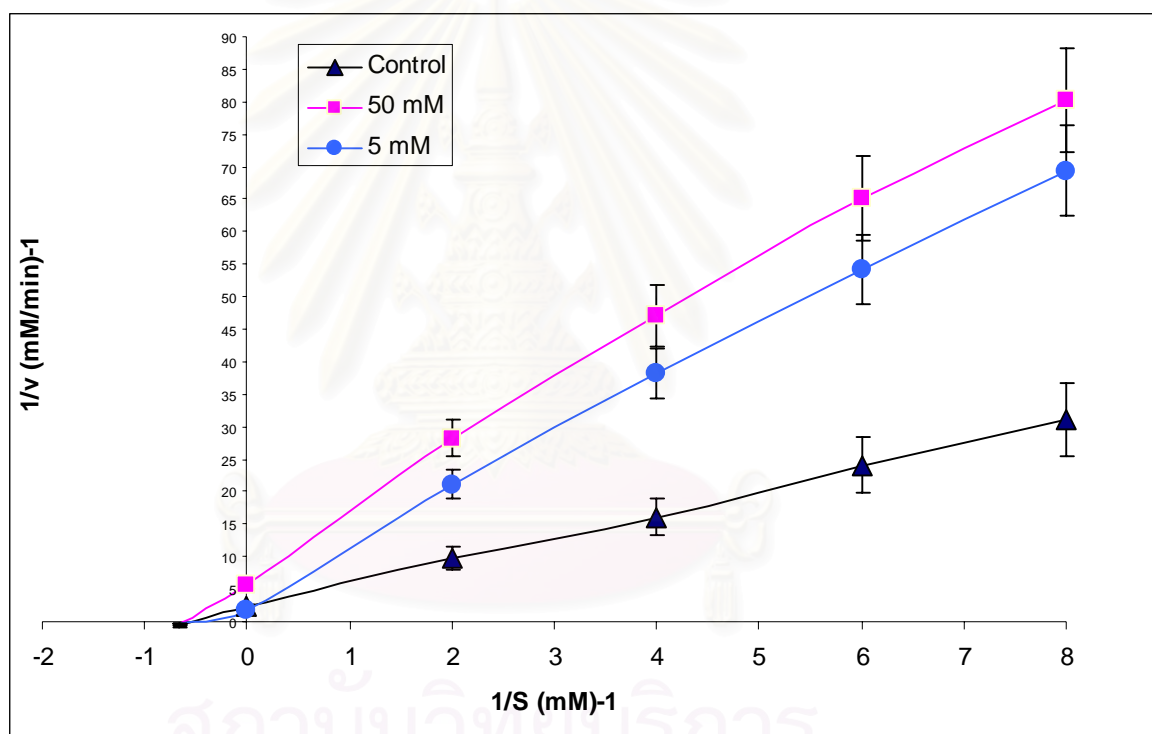


Figure 20 Lineweaver-Burk plot of α -glucosidase in presence of 1-Deoxynojirimycin. Data were obtained as mean values of $1/V$, inverse of increase of absorbance at the wavelength 405 nm per minute ($\Delta A_{405}/\text{min}$), with different concentrations of PNP-G as a substrate. Inhibitors of enzyme were 50 mM (circle, \blacksquare) and 5 mM (circle, \bullet) and no 1-deoxynojirimycin (triangle, \blacktriangle).

Table 12: Kinetics parameters of α -glucosidase in the presence of 1-deoxynojirimycin

Inhibitor	Dose (mM)	K_m (M)	V_{max} ($\Delta A_{405}/\text{min}$)	K_i
None	-	1.49	0.44	-
1-DNJ	5	2.85	0.61	1.79×10^{-2}
1-DNJ	50	3.19	0.18	3.46×10^{-2}

From **Table 13**, 5 mM 1-DNJ and 50 mM 1-DNJ showed K_i value at 8.09×10^{-3} and 49.0×10^{-3} , respectively. The results suggesting that 5 mM 1-DNJ showed high affinity of enzyme – inhibitor complex than 50 mM 1-DNJ, with lower in K_i value

Table 13: The $1/V$ value of F08 with variety of substrate concentrations

$1/[S]$	Control	S.D.	F08 (25 mg/ml)	S.D.	F08 (250 mg/ml)	S.D.
8.00	42.14	4.12	46.11	6.12	56.33	14.12
6.00	22.25	3.11	37.12	4.18	46.92	12.44
4.00	16.18	2.34	26.22	7.34	32.32	11.13
2.00	10.10	1.54	12.14	3.58	14.14	6.98
1.00	5	1.45	5.21	3.11	6.21	4.12

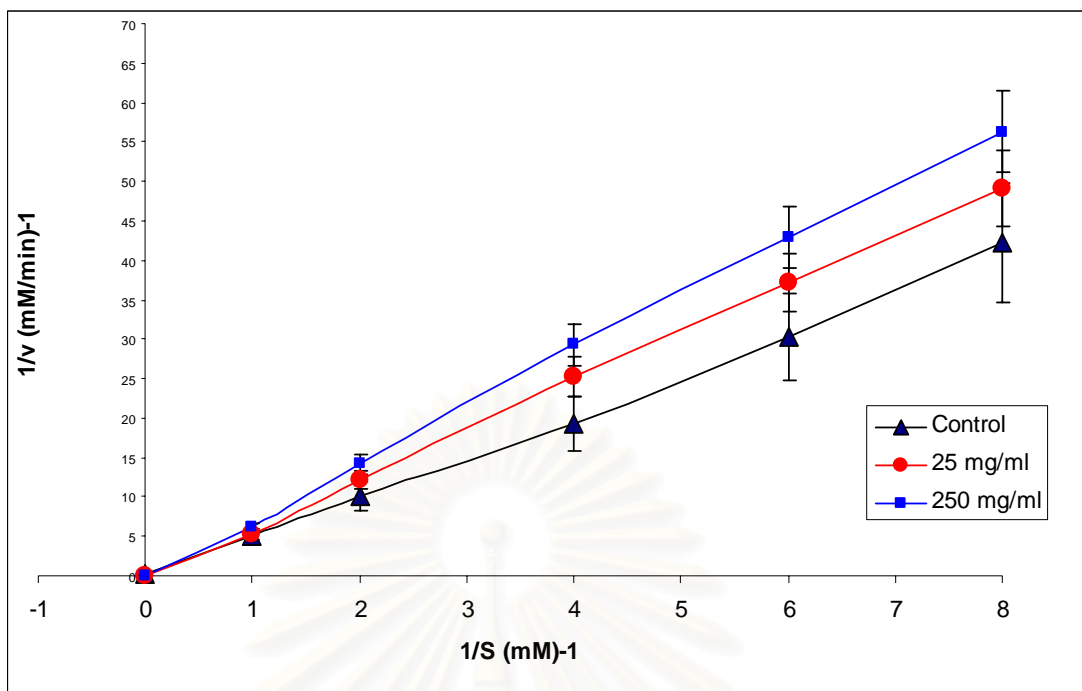


Figure 21 Lineweaver-Burk plot of α -glucosidase in presence of F08. Data were obtained as mean values of $1/V$, inverse of increase of absorbance at the wavelength 405 nm per minute ($\Delta A_{405}/\text{min}$), with different concentrations of PNP-G as a substrate. Inhibitors of enzyme were 25 mg/ml (circle, ■) and 250 mg/ml (circle, ●) and no F08 (triangle, ▲).

Table 14: Kinetics parameters of α -glucosidase in the presence of F08

Inhibitor	Dose (mg/ml)	K_m (mg/ml)	V_{max} ($\Delta A_{405}/min$)	K_i
None	-	0.83	4.06	-
F08	25	1.683	10.04	0.419
F08	250	2.0	23.27	0.302

Table 15: The $1/V$ value of F21 with variety of substrate concentrations

$1/[S]$	Control	S.D.	F21 (2.5 mg/ml)	S.D.	F21 (25 mg/ml)	S.D.
8.00	42.14	4.12	46.11	6.90	66.33	11.33
6.00	32.25	3.11	37.12	7.18	47.2	10.65
4.00	19.18	2.34	27.22	6.98	32.32	5.09
2.00	9.87	1.54	15.14	3.58	17.34	6.98
1.00	N/A	N/A	9.21	3.67	10.1	3.09

สถาบันวิทยบริการ
จุฬาลงกรณ์มหาวิทยาลัย

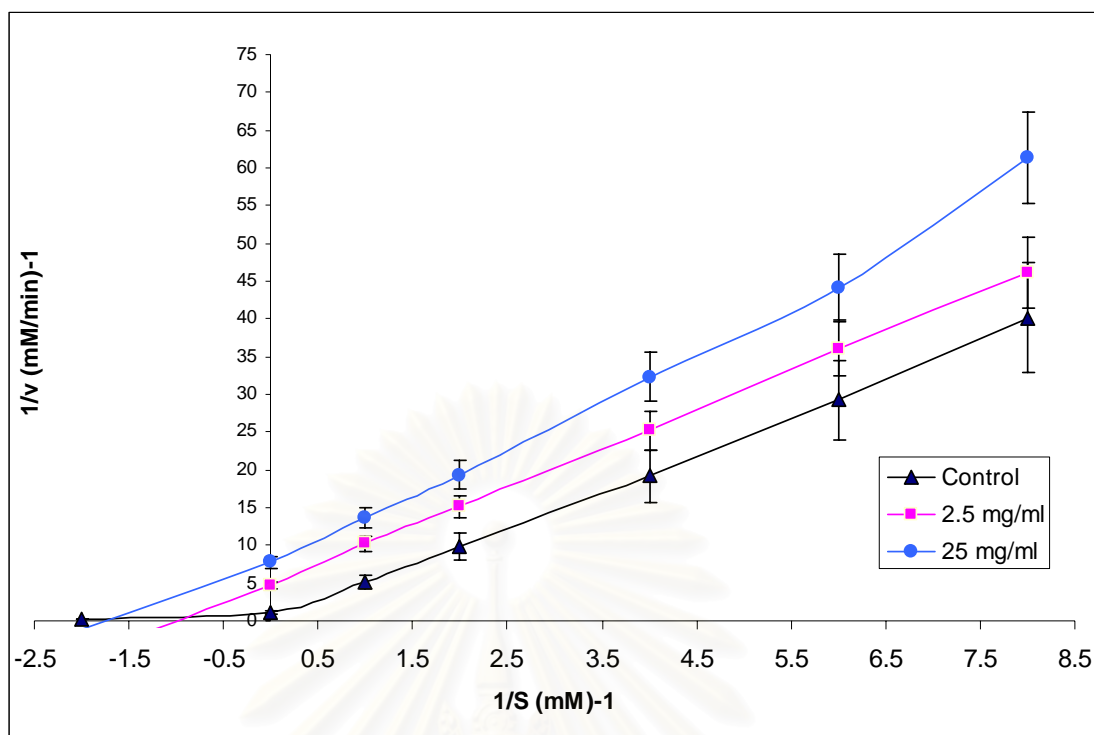
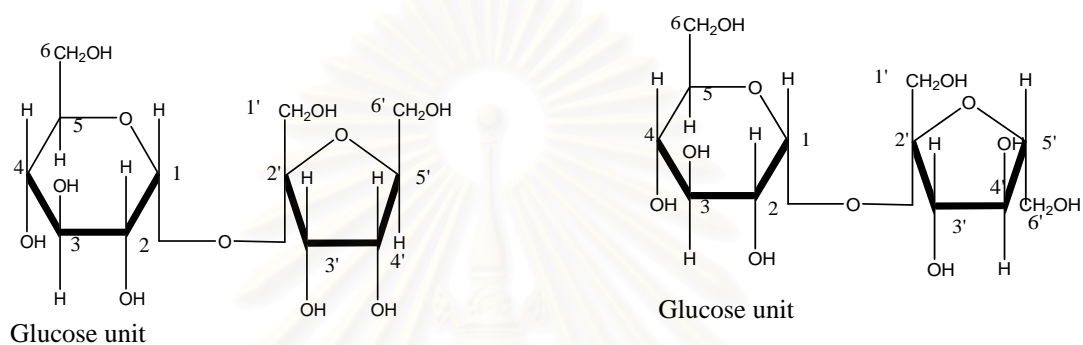


Figure 22 Lineweaver-Burk plot of α -glucosidase in presence of F21. Data were obtained as mean values of $1/V$, inverse of increase of absorbance at the wavelength 405 nm per minute ($\Delta A_{405}/\text{min}$), with different concentrations of PNP-G as a substrate. Inhibitors of enzyme were 2.5 mg/ml (circle, \blacksquare) and 25 mg/ml (circle, \bullet) and no F21 (triangle, \blacktriangle).

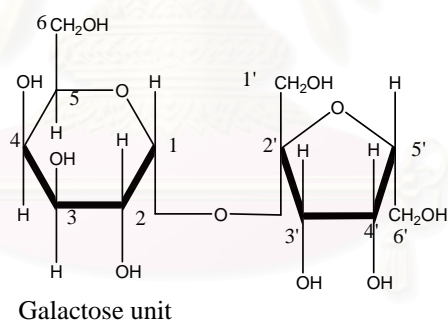
Table 16: Kinetics parameters of α -glucosidase in the presence of F21

Inhibitor	Dose (mg/ml)	K_m (mg/ml)	V_{\max} ($\Delta A_{405}/\text{min}$)	K_i
None	-	67.1	0.227	-
F21	2.5	0.212	0.227	1.73
F21	25	0.74	0.227	0.422

In this investigation the most active fractions of the aqueous extract were acetylated and separated to afford three acetyl derivatives including GP1, GP2, and GP3. The structures of all acetylated compounds were determined by interpretation of their UV, IR, NMR, and Mass spectral data, by comparison with literature reviews as acetyl derivatives of α -D-glucopyranosyl-(1 \rightarrow 2)-O-psicofuranoside, α -D-glucopyranosyl-(1 \rightarrow 2)-O-fructofuranoside, and α -D-galactopyranosyl-2-O - tagatofuranoside, respectively.



α -D-glucopyranosyl-(1 \rightarrow 2)-O-psicofuranoside α -D-glucopyranosyl-(1 \rightarrow 2)-O-fructofuranoside



α -D-galactopyranosyl-2-O -tagatofuranoside

Figure 23. Parent compounds of GP1, GP2, and GP3, respectively

Parent compounds of GP1, GP2, and GP3 which was the main component of the active fractions, F21, F11, and F14 showed 82.30, 59.41, and 64.21% α -glucosidase inhibitory activity, respectively.

From the structure of the parent compounds, GP1 and GP2 contained glucose as a first saccharide unit and the second unit was psicofuranose and fructofuranose,

respectively. Since the inhibitory activity of F21 (parent compound of GP1) was more potent than F11 (parent compound of GP2), psicofuranose should be more potent than fructofuranose. F21 (parent compound of GP1) was more potent than F14 (parent compound of GP3). From these relationships, it could be draftly concluded that the disaccharide containing glucose and psicofuranose has the highest α -glucosidase inhibitory activity, whilst galactose and tagatofuranose showed lower activity.

From kinetics studies of F08 and F21 were competitive inhibitor for F08 and uncompetitive inhibitor for F21. 1-DNJ (1mM) and F21 (1mg/ml) were showed 83.98 and 82.3 percent inhibitory activity, respectively on α -glucosidase. The IC_{50} of F21 was 0.25 mg/ml while the positive control 1-deoxynojirimycin was 5.1 μ M.

Lineweaver-Burk plot of α -glucosidase kinetics were shown in **Figures 21-22**, the kinetics results demonstrated that the mechanism of α -glucosidase inhibition of F08 and F21 were uncompetition with K_i value 0.42 and 0.32 mg/ml, respectively. At this point, K_i value was calculated using the values of V_{max} obtained at 250 and 25 mg/ml, respectively. However, 1-deoxynojirimycin exhibited non-competition with K_i value 3.4×10^{-2} .

CHAPTER V

CONCLUSION AND RECOMMENDATION

In a preliminary evaluation of the extracts of *Gynura procumbens* for α -glucosidase inhibitory activity, the aqueous extract showed highest inhibitory activity. Further bioactivity-guided fractionation of the active aqueous gave fractions showing 82.93, 59.41, and 64.21% inhibition on α -glucosidase at concentration 1mg/ml, respectively. Moreover, the kinetic study of the most active fractions was performed as uncompetition on α -glucosidase

The active fractions were acetylated with acetic anhydride to give 3 acetyl derivatives, GP1, GP2, and GP3, respectively. The structures were determined by analyses of ^1H , ^{13}C and 2D-NMR, IR and mass spectrometry as acetyl derivatives of a new α -D glucopyranosyl-(1 \rightarrow 2)-O -psicofuranoside, α -D glucopyranosyl-(1 \rightarrow 2)-O -fructofuranoside, and a new α -D galactopyranosyl-(1 \rightarrow 2)-O -tagatofuranoside.

The most active fraction F21 is a disaccharide contained a new α -D glucopyranosyl-(1 \rightarrow 2)-O -psicofuranoside as a main component. The second saccharide unit is α -D-psicofuranose, it is a C-3 epimer of D-fructose, it has been reported as a novel a novel compound obtained from transglycosylation of arabinoxylan of *Aspergillus sojae*. D-psicose is a rare sugar with pyranoside skeleton by an β -(1 \rightarrow 4) ether linkage. Moreover, D-psicose has been reported as a plant growth regulation inducing gene transcription.

α -D-Psicose was realized to be an inhibitor of all or some of the intestinal disaccharidases in Male Wistar rats and *in vitro* α -glucosidase. (Tatsuhiro *et al*, 2006). Moreover, D-psicose significantly inhibited the increased of plasma glucose concentration induced by sucrose and maltose with uncompetitive inhibitory activities and suppressed glycemic responded after carbohydrate ingestion (Matsuo *et al.*, 2006).

The active fraction F14 is a disaccharide, it containing α -D galactopyranosyl-(1 \rightarrow 2)-O -tagatofuranoside. α -D-tagatose is a C-4 epimer of D-fructose, it was established as a new sweetener with low energy content. This low energy content may

be due to either low absorption of the D-tagatose or decreased absorption of other nutrients (Donner *et al.*, 2001). Moreover, D-tagatose have been reported as a dietary supplement for a patients with type 2 diabetic, which was enhanced insulin sensitivity and increased insulin secretion in a gastrointestinal tract.

From the research of Tatsuhiro *et al.*, in α -glucosidase inhibitory activity of D-psicose, it was confirmed the results in this studied, the structure of the most active fractions, F21 contained α -D glucopyranosyl-(1 \rightarrow 2)-O -psicofuranoside as a main component, indicated the inhibitory activity of F21 may related with psicose moiety.

At present there is no report on α -glucosidase inhibitory activity of α -D-glucopyranosyl-(1 \rightarrow 2)-O-psicofuranoside, only the reported of α -D-glucosyl-(1 \rightarrow 4)-O-psicoside isolated from microbacteria. Moreover, no report on α -glucosidase inhibitory activity of α -D-galactopyranosyl-(1 \rightarrow 2)-O tagatofuranoside and no report in the structure of α -D-galactopyranosyl-(1 \rightarrow 2)-O tagatofuranoside, only the reported of glucopyranosyl-(1 \rightarrow 4)-O-tagatoside as a sweetening agent.

Furthermore, the evaluation of the inhibitory activity of the aqueous extract of *G. procumbens* on α -glucosidase was done by using the beaker's yeast α -glucosidase. It is known to be structurally different to those of mammalian origins. The microbial α -glucosidase inhibitors may or may not inhibit the mammalian α -glucosidase. For example, (+)-catechin, a natural inhibitor of yeast α -glucosidase does not show any inhibitory activity on mammalian α -glucosidase. On the other hand, acarbose and voglibose show very high inhibitory activity on porcine small intestine α -glucosidase, but both of them show very low inhibitory activity on microbial α -glucosidase (Oki *et al.*, 1999). These suggest that ongoing experiments should be focused on the inhibitory activity of these compounds against mammalian intestinal α -glucosidase. Moreover, the anti-hyperglycemic activity should be done on the other models such as insulin secretion, glucose uptake in human cell lines such as L6, L8, and adipocyte cell, and *in vivo*-test such as alloxan-induced diabetes.

References

- สวนพฤกษศาสตร์ป่าไม้. 2542. พรรณไม้ต้นของประเทศไทย. กรุงเทพมหานคร: ไดมอนด์พรีนติ้ง.
- สำนักนายกรัฐมนตรี องค์การสวนพฤกษศาสตร์. 2542. ไม้ต้นไม้สวน. พิมพ์ครั้งที่ 1.
กรุงเทพมหานคร : อักษรสยามการพิมพ์.
- เสงี่ยม พงษ์บุญรอด. 2522. ไม้เทศเมืองไทย สวนพฤกษศาสตร์และยาไทย. กรุงเทพมหานคร :
เกษมบรรณกิจ.
- Adisakwattana S., Roengsumran S., Sookkongwaree K., Petsom A.,
Ngamrojnavanich S., Deesamer S., and Yibchok-anan S. 2004. Structure-activity
relationships of trans-cinnamic acid derivatives on α -glucosidase inhibition.
Bioorg. and Med. Chem. Lett. 14:2893-2896.
- Akowuah A.G., Amirin S., Mariam A., and Amanish I. 2001. Blood glucose
lowering activity of *Gynura procumbens* extract. J. Trop. Med. Plants 1: 1-5.
- Alembert T., Shamsun N., Fuendjiep V., Francois N., Annie N., and Muhammad I. 2007.
 α -glucosidase inhibitors from *Millettia conraui*. Chem Phar. Bull. 55(9); 1402-
1403.
- Atsuo K., Jin H., Lee I.S., Park K., Chiba D., and Kim D. 2004. Two potent competitive
inhibitors discriminating α -glucosidase family I and family II. J. Carbo. Res.
339: 1035-1040.
- Atsuo T., Mitsuyoshi U., Toshiuki M., Naomi K., and Masako A. 2003. Molecular
Breeding of Polysaccharide-Utilizing Yeast Cells by Cell Surface Engineering.
Enzyme Engineering XIV: 528-537.
- Bohlmann F., and Aero C. 1977. Gynuron, ein neues Terpen-cumtoarin-derivat
A aus *Gynura crepioides*. Phychemistry 16: 494-5.
- Bailey C.J. 1989. Traditional treatments for diabetes. Diabetic care 12: 553-564.
- Bischoff, H., 1994. Pharmacology of α - glucosidase inhibition. Eur. J. Clin.
Invest. 24, 3-10.
- Boonclarm D. and Svasti J. 2002. Screening of Thai plants for natural α -
glucosidases and β -glucosidase enzyme. J. of Cell Biol. 156(18): 1003-1013.

- Chatterjee B. P., Sarker N., and Rao A. 1982. Serological and chemical investigations of the anomeric configuration of the sugar units in the D-galacto-D-mannan of fenugreek (*Trigonella teonum-graecum*) seed. Carbohydr. Res. 104: 348-353. (CA. 97:69258k).
- Chattopadhyay RR. 1999. Possible mechanism of anti-hyperglycemic effect of *Azadiractha indica* leaf extract: Part V. J. Ethnopharmacol. 67: 373-376.
- Chen D., Ying-C.Y., Tian H.R., Jia W., Yuan J., Lai-Gen S., and Jing Z. 2007. *Gynura* root induces hepatic veno-occlusive disease: A case report and review of the literature. J. of Gastro. 13: 1628-1631.
- Ceriello, A., 2000. The postprandial state and cardiovascular disease: relevance to diabetes mellitus. Diabetes-Metabolism Research and reviews. 16, 125-132.
- Chitcharoenthum M, Picheansoonthon C, Khunkitti W. 1992. Pharmacological effects of *Gynura integrifolia*. In: Tongroach P, Watanabe H, Ponglux T, et al., editors. Advance in research on pharmacologically active substances from natural sources. Proceeding of the first JSPS-NRCT joint seminar on pharmaceutical sciences; 1992 Dec 3-5; Chiangmai, Thailand: 44-58.
- Cornish WR. 1997. Acarbose an alpha glucosidase inhibitor for the management of non insulin-dependent diabetes mellitus. Can. J. Clin. Pharmacol. 4:15-23.
- Davie A.S., Wilson J.C., Kiefel M.J., Raudies E., 1996. Isolation and characterisation of several components from the aerial part of *Gynura procumbens*. (Unpublished)
- Donckier, J., Williams, G. 1994. The roles of α -glucosidase inhibitors in diabetes. Eur. J. of Clin. Invest. 522-536.
- Eduardo Borges de M., Adriane da Silveira G., and Ivone C. 2006. α - and β -Glucosidase inhibitors: Chemical structure and biological activity. Tetrahedron 62: 10277-302.
- Ebraika S., Asmawi Z., Marium A., Ismail Z., Akwauah A., and Sadikan A. 2002. Pharmacognosical, Phytochemical, and Pharmacological studies of *Sambung Nyawa*. (*Gynura procumbens*). J. of Pharmacol Asi Pac. Vol.12: 23-24.
- Esen A. 1993. α -Glucosidase overview in α -Glucosidase. Mol. Biol. 43:1-14.

- Fischer, P. B., Kaelsson, G. B., Butters, T.D., and Platt, F. 1996. Glycosidation of envelop glycoprotein. J. of Viro. 70:7143-7152.
- Forbes S. and Hemley H. 1980. Enumeration of Plants of China 9:446-448.
- George G. and Ludvik A. 2006. Antidiabetic agents. Goodman and Gillman: the pharmacological basis of therapeutics: 11st New York. Mc Hill: 1212-1248.
- Guney E., Kisakol G., Aysin O., Yilmaz C., and Kabalak T. 2002. Effects of insulin and sulphonylureas on insulin-like growth factor-I levels in streptozotocin-induced diabetic rats. J. Neur endo. Lett. 23:37-39.
- Heightman J., Moore P., and Streitz T. 2003. The structure basis of large lysosomal subunit function. Annual rev. biochem. 72: 813-850.
- Herout V., Horub M., and Taman J. 1971. Influence of Sesquiterpene Lactones of Vernonia (Compositae) on Oviposition Preferences of Lepidoptera. Biochem and Eco. 29: 1115-1137.
- Herscovics A. 1999. Importance of glycosidases in mammalian glycoprotein biosynthesis. Bioch. Bioph. 1473: 96-107.
- Heywood VH., Harborne JB, and Turner BL. 1977. The biology and chemistry of the Compositae Vol.2. London: Academic Press.
- Hong Gao, Huang Y.N., Xu P.Y., and Kawabata J. 2007. Inhibitory effect on α -glucosidase by the fruit of *Terminalia chebula* Retz. Food Chem. 105: 628-634.
- Jarikasem S. 2000. A phytochemical study of anti-herpes simplex components from *Gynura procumbens* Merr. Philosophy's Thesis, Faculty of Pharmacy, Mahidol University.
- Jirachariyakul W., Jarikasem S., Siritantikom S., Somanabandhu A., and Frah W. 2000. Antiherpes simplex viral compounds from *Gynura procumbens* Merr. Natural medicine. Proceeding of the fifth JSPS-NRCT joint seminar on pharmaceutical sciences; 2000 Dec 15-17; Bangkok, Thailand: 70-73.
- Jong-Anunrakkun N., Bhandari M., and Kawabata J. 2006., α -Glucosidase inhibitors from Devil tree. Food chem. *In press*.
- Jong TT, and Chou-Hwang JY. 1997. An optically active chromanone from *Gynura formosana*. Phytochemistry 44 (3):853-4.

- Kasipan C., Tamra Bhesajasad Suksa. 1979. Bangkok Prachaturon Press
- Khan T., Zahid M., Asim M., Shahzad ul-Hussan, Iqbal Z., Choudhary I., M., and Uddin Ahmad, V. 2002. Pharmacological activities of crude acetone extract and purified constituents of *Salvia macrocraftiana* Wall. Phytomed. 9(8):749-752.
- Koyama H., Chayamarit K., and Lersen K. 2007. Flora of Thailand. 67: 12-30
- Kyoko I., Megumi T., Makato N., Miwa M., Haruhira K., Yukihiko K., Munehira A., Allison A., Watson R., George W., and Naoki A. 2000. Homonojirimycin analogues and their glucosides from *Lobelia sessilifolia* and *Adenophora* spp. J. Car. Res. 323: 73-80.
- Lam S.K., Idris A., Bakar Z., Ismail R., 2002. *Gynura procumbens* and blood pressure in rats: preliminary study. J. of Pharmacol Asi Pac. Vol.13: 14-15.
- Liang XT, and Roeder E. 1984. Senecionine from *Gynura segetum*. Planta Med. 51(4):362.
- Matheson JR, and Robins DJ. 1992. Pyrrolizidine alkaloids from *Gynura sarmentosa*. Fitoterapia 63(6):557.
- Matsuura, H., Asakawa, C. Masanori., Kurimoto, M, and Miutani, J. 2002. α -Glucosidase Inhibitor from the Seeds of Balsam Pear (*Momordica charantia*) and the Fruit Bodies of *Grifola frondosa*. Biosci. Biotech. and Biochem. 66(7): 1552-1554.
- Masayuki Y., Toshiyuki M, Shimada, M., Matsuda H., Yamahara J., Tanabe Y., and Muraoka O. 1998. Salacinol, potent antidiabetic principle with unique thiosugar sulfonium sulfate structure from the Ayurvedic traditional medicine *Salacia reticulata* in Sri Lanka and India. Tetrahedr. lett. 38(48): 8367-8370.
- Matsui T., Ueda T., Oki, T., Sukita K., Terahera N., and Matsumoto K. 2001. α -Glucosidase inhibitory action of natural acylated anthocyanins. 1. Survey of natural pigment with potent inhibitory activity. J. Agri and Food Chem. 49: 1948-1951.
- Melo E.B., Gomes A.S.,and Carvalho I. 2006. α and β -glucosidase Inhibitors :chemical structure and biological activity. Tetrahedron. 62: 10277-10302.
- Mitsuya H., Shirasaka T., Broder S. 1990. Design of anti-AIDS drugs. Elsevier: Amterdan. 257-318.

- Mitsuyoshi Y., Jia D.M., Fukumitsu K., Imato I., Kahma Y., Hirohata Y., and Osuki M. 1999. Metabolic Abnormalities in the Genetically Obese and Diabetic Otsuka Long-Evans and Tokushima Fatty rat can be prevented and reversed by α -glucosidase inhibitor. Metabol. 48: 347-354.
- Naoki A. 2003. Glycosidase inhibitors: update and perspectives on practical use review. Glycobiol. 13: 93-104.
- Okima T., Kimura I., and Izumuri K. 2006. Synthesis and structure analysis of novel disaccharide containing D-psicose producing by endo (1,4)- β -D-Xylanose from *Aspergillus sojae*. J.Bisci Bioeng. 101: 280-283.
- Okima T., Kimura I., Izumuri K, and Morimoto K. 2008. Synthesis and structure analysis of glucosylpsicose producing by cyclomatodextrin glucanotransferase. J. Appli Glysci. 55: 1-3.
- Perry L.M., Metger J. 1980. Medicinal Plants of East and South East Asia: Attributed Properties and Uses. London: MIT Press. Cambridge. 94-95.
- Rahihan A.U., Zaman K. 1989. Medicinal plants with hypoglycaemic activity. J. of Ethnopharmacol. 26: 1-55.
- Ren Y., Himmeldirk K., and Chen X. 2006. Synthesis and structure activity relationship study of antidiabetic penta-O-galloyl -D-glucopyranose and its analogues. J. of Med Chem. 49: 2829-2837.
- Rho, M.C., Yasuda, K., Matsunaga, K., and Ohizumi, Y. 1997. A monogalactopyranosyl acylglycerol from *Oltmannsiellopsis unicellularis* (NIES-359). Phytochem. 44(8): 1507-1509.
- Roeder E, Eckert A, Wiedenfeld H. 1996. Pyrrolizidine alkaloids from *Gynura divaricata* Planta Med. 62:386.
- Sadikun A, Idus A, and Ismail N. 1996. Sterol and sterol glycosides from leaves of *Gynura procumbens*. Nat. Prod. Sci. 19-23.
- Saleem A., Husheem M., Harkonen P., and Pihlaja K. 2002. Inhibition of cancer cell growth by crude extract and phenolics of *Terminalia chebula* Rezt. fruit. J. of Ethnopharmacol. 81: 327-336.
- Schweden J., Borgmann C., Legler G., Bause E., and Harper V. 1986. N-linkaged of oligosaccharide. Biochem. Biophys. 248: 335-340.

- Shiu Y, H. 1994. The Compositae of China. Quaternary J. Of Taiwan. 19: 279-284.
- Smitinand T. 2001. Thai Plant names (Botanical names-Vernacular names).
Bangkok: Funny Publishing Limited Partnership.
- Smitinand T. 2001. Thai Plant names (Botanical names-Vernacular names)
revised edition. Bangkok: The Forest Herbarium, Royal Forest Department.
- Sonei S., Satoshi M., Hiroyasu T., Ryu Y., Shizuo K., Makiko S., and Yuishi Hashimoto.
2000. Novel α -glucosidase inhibitors with a tetrachlorophthalimide skeleton. J. Bioor and Med. 10: 1081-1084.
- Stewart G., Patricia, C., Poindexter, J. L., Monica, M. P. and Somerville C. 2004. α -glucosidase I is required for cellulose biosynthesis and morphogenesis in *Arabidopsis*. Cell Biol. 156: 1003-1013.
- Takahira M, Kondo Y, and Kusano G. 1997. Four new 3α -hydroxyspirost-5-ene derivatives from *Gynura japonica* Makino. Tetrahedr. Lett. 41: 3647-50.
- Toda M., Kawabata J., and Kasai T. 2001. Inhibitory effects of ellagi and gallotannins and rat intestinal α - glucosidase complexes. Biosci. 65: 542-547.
- Wiedenfeid H. 1982. Two pyrrolizidine alkaloids from *Gynura scandens*.
Phytochemistry 21(11):2767-8.
- Xueshao C, and Xizhi L. 1987. Pharmacological studies of *Gynura segretum* I. Effects of Local Anesthesia. Chin. Trad. Herb. Dr. 18 (6) 261-6.
- Yoshikawa M., Morikawa T., Matsuda H., Tanabe G., and Muraoka O. 2002. Absolute stereostructure of potent α -glucosidase inhibitor, salacinol, with unique thiosugar sulfate inner salt structure from *Salacia reticulate*. Bio and Med Chem. 10: 1547-1554.
- Yoshitama K, Kaneshige M, Ishikura N, Akati F, Yahara S, and Abe K. 1994. A stable reddish purple anthocyanin in the leaf of *Gynura aurantiaca* CV. Purple passion. J. Plant Res. 10:209-14.
- Yoshimitsu Y., Katakami N., Matsuhisa M., Hayaishi O., M., Kajimoto Y., Kosugi K., Hatano and Hori M. 2005. α -Glucosidase inhibitor reduces the progression of carotid intima-media thickness. Diab. Res. Clin. Pr. 67: 204-210.
- Yihao L., Suping W., Bhavani P., Gang P., George Q., Johji Y., and Basil R. 2005.

Punica granatum flower tract, a potent α -glucosidase inhibitors, improves postprandial hyperglycemia in zucker diabetic fatty rats. J. Ethn Phar. 99: 239-244.

Zimmet, P., Alberti, K., and Shaw, J., 2001. Global and societal implications of the diabetes epidemic. Nature 414, 782-787.

Zhang XF., Tan BK. 2002. Effect of an ethanolic extract of *Gynura procumbens* on serum glucose, chlorestero and triglyceride levels in normal and streptozotocin-induced diabetic rats. J. Singapore Med vol.41(1): 45-48.

The Flora of China web pages are copyrighted by the Flora of China Project; the Flora of China manuscripts by Missouri Botanical Garden Press, St. Louis, and Science Press, Beijing; the Flora of China Illustrations by the Editorial Committee of Flora Reipublicae Popularis Sinicae, Science Press, and Missouri Botanical Garden Press; and journal publications by their respective publishers. Photographs are the property of the respective photographer Vol. 21: 169-175.



สถาบันวิทยบริการ
จุฬาลงกรณ์มหาวิทยาลัย



APPENDIX

สถาบันวิทยบริการ
จุฬาลงกรณ์มหาวิทยาลัย

1. α -Glucosidase inhibitory activity

1.1 Preparation of the reaction mixture

1.1.1 Preparation of 0.1 mM Phosphate buffer (pH 6.8)

Solution A $\text{NaH}_2\text{PO}_4 \cdot 2\text{H}_2\text{O}$ (1.56 mg) was dissolved in 100 ml of water

Solution B Na_2HPO_4 (1.42 mg) was dissolved in 100 ml of water. Then, portions of solutions A and B were slowly mixed until pH 6.8 was reached.

1.1.2 Preparation of 1 mM *p*-nitrophenyl- α -D-glucopyranoside

p-Nitrophenyl- α -D-glucopyranoside (MW. = 301.25, 3.01 mg) was dissolved in 10 ml of 0.1 mM phosphate buffer pH (6.8).

1.1.3 Preparation of 1U/ml of α -glucosidase solution

Accurately weighed α -glucosidase enzyme (1000 unit/23 mg 0.115 mg) was dissolved in 5 ml of 0.1 mM phosphate buffer (pH 6.8).

1.1.4 Preparation of 1 M Na_2CO_3 (Mw = 106)

Na_2CO_3 (Mw = 106, 10.60 g) was dissolved in 100 ml of water.

1.1.5 Preparation of 1 mM 1-deoxynojirimycin

Accurately weighed 1-deoxynojirimycin (MW = 199, 1.99 mg) was dissolved in 1 ml of 0.1 mM phosphate buffer (pH 6.8).

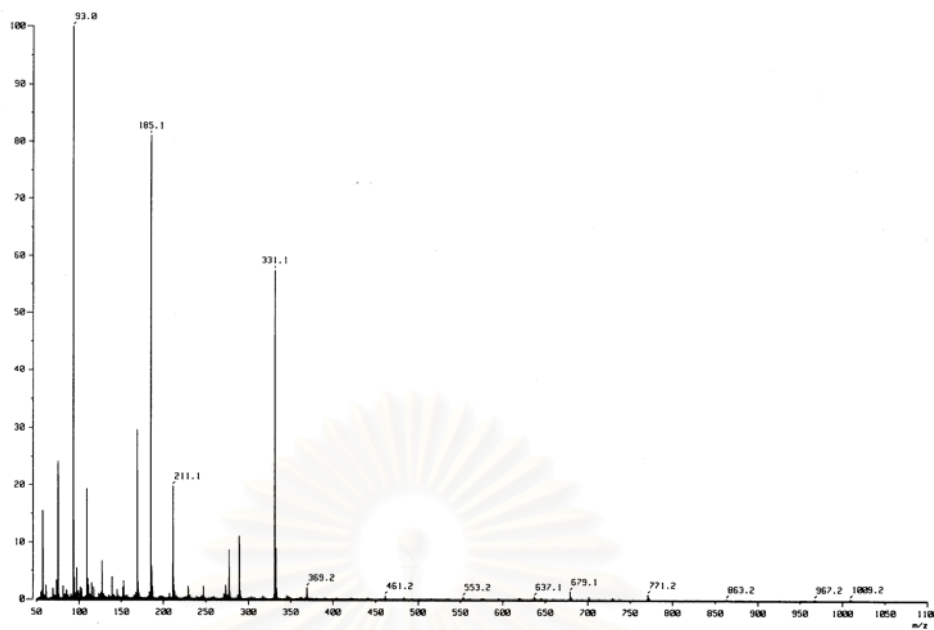


Figure 24 EIMS Spectrum of GP1

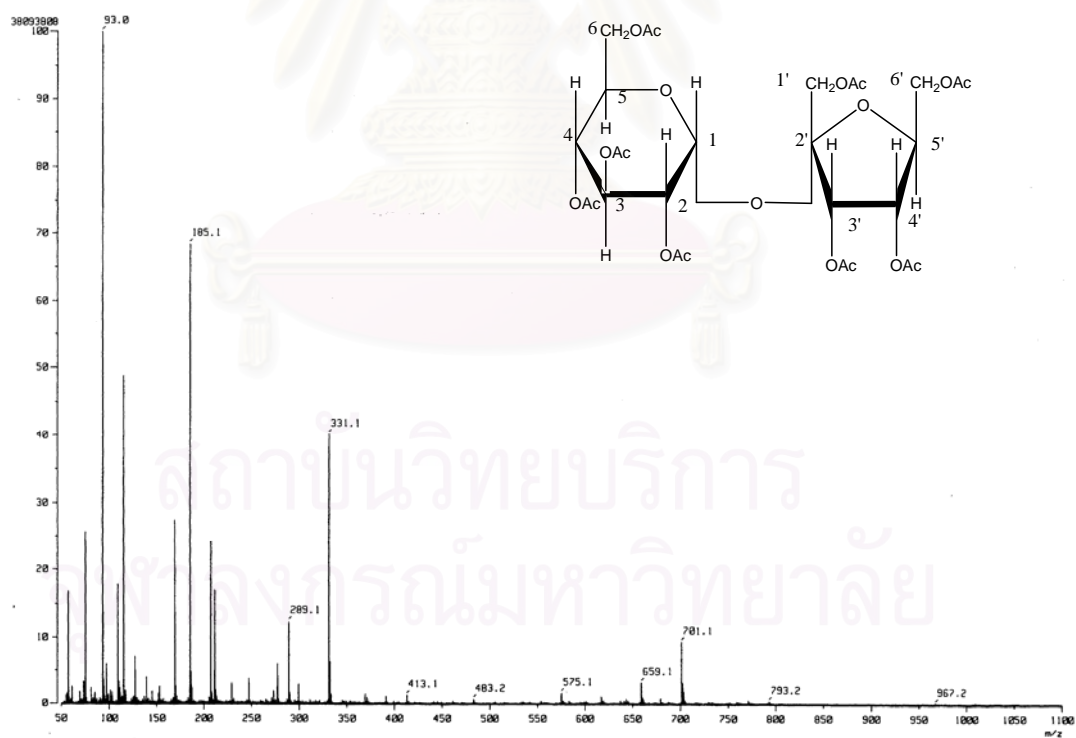


Figure 25 FABMS Spectrum of GP1

Figure 26 IR Spectrum (Film) of GP1

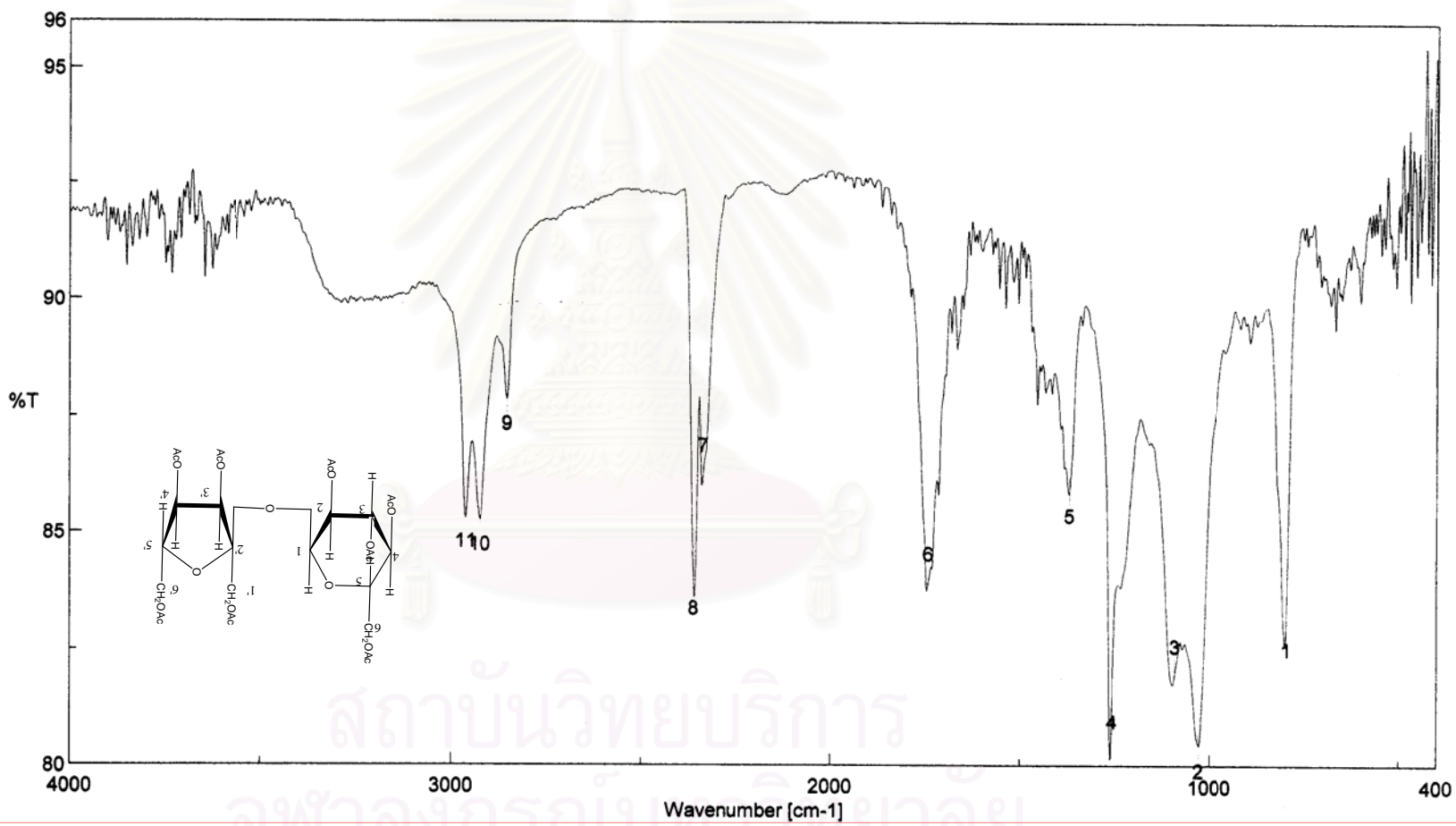
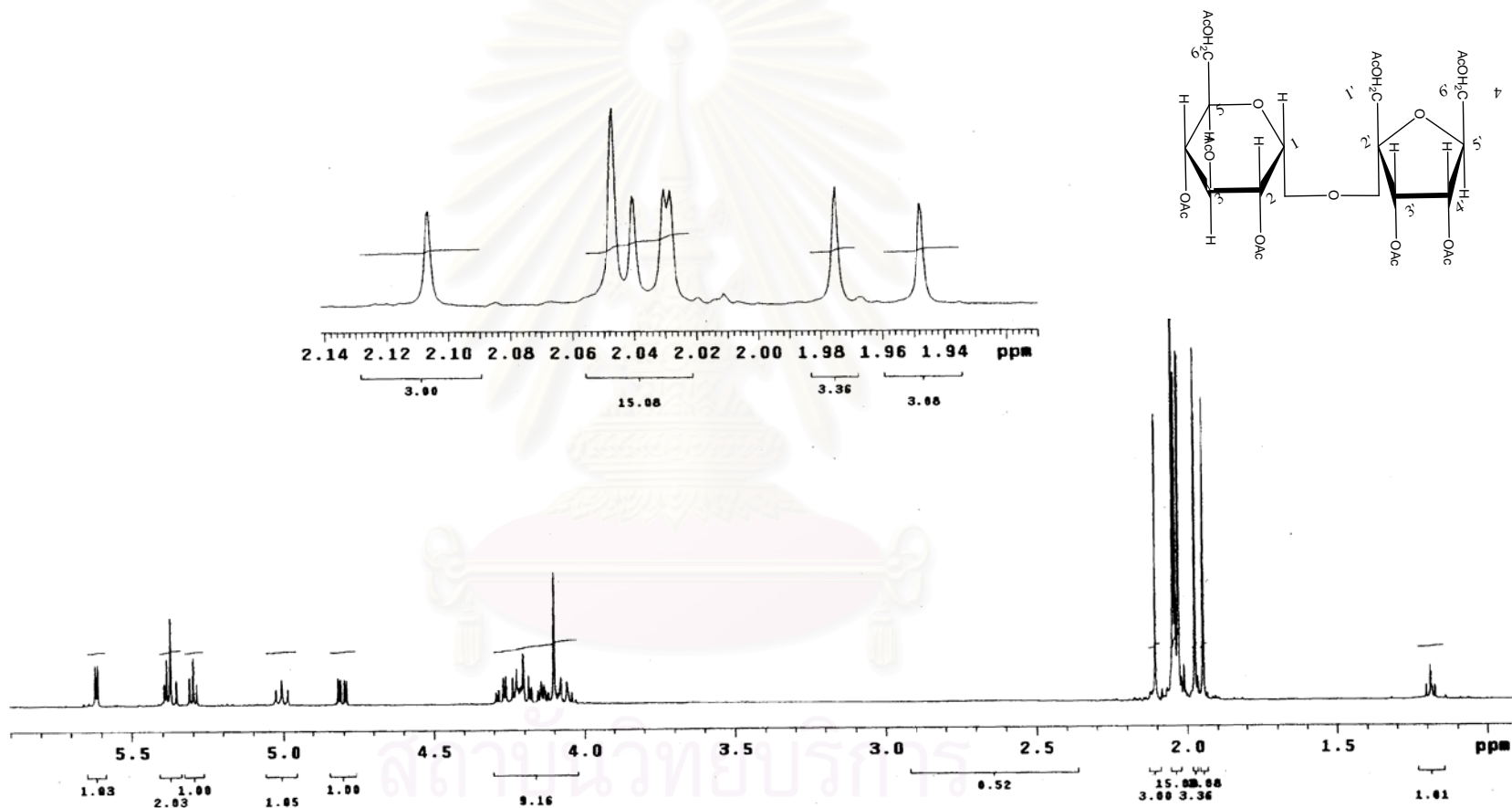


Figure 27 ^1H NMR (500 MHz) Spectrum of GP1 in CDCl_3



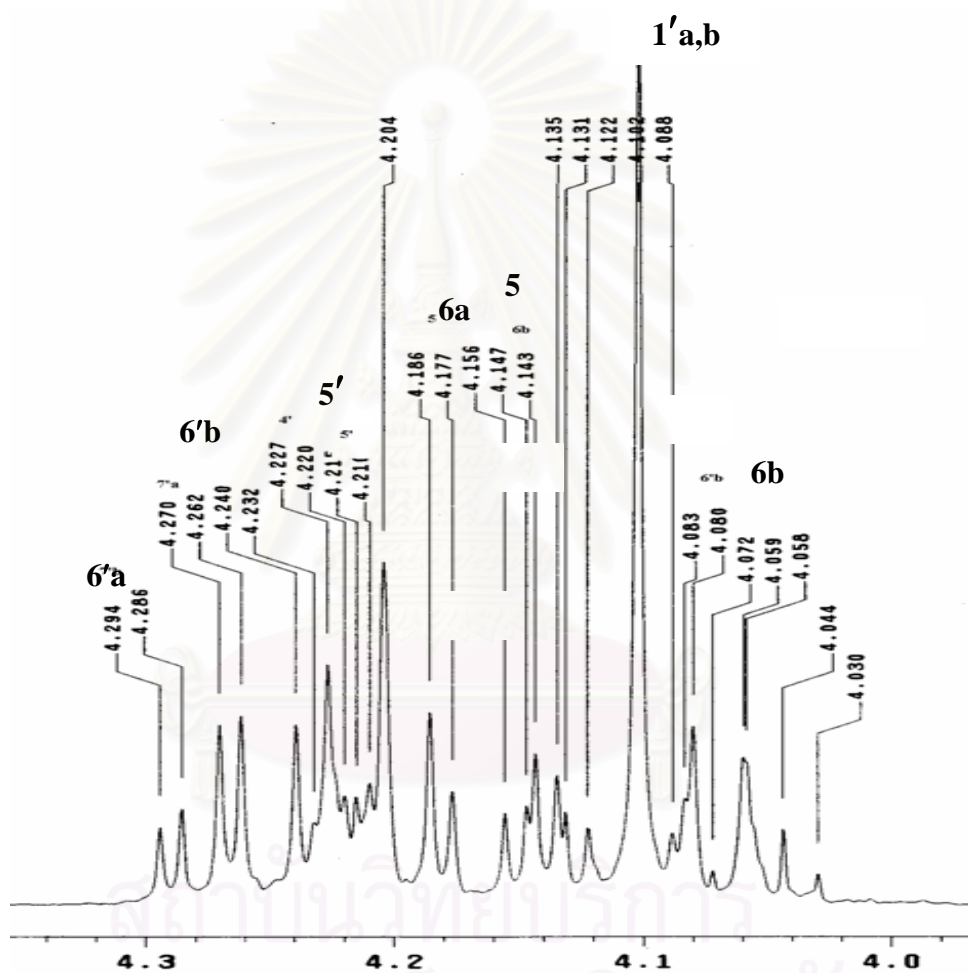
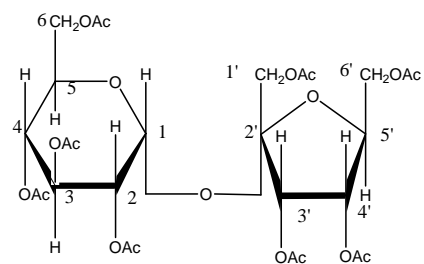


Figure 28 ¹H NMR (500 MHz) Spectrum of GP1 in CDCl₃

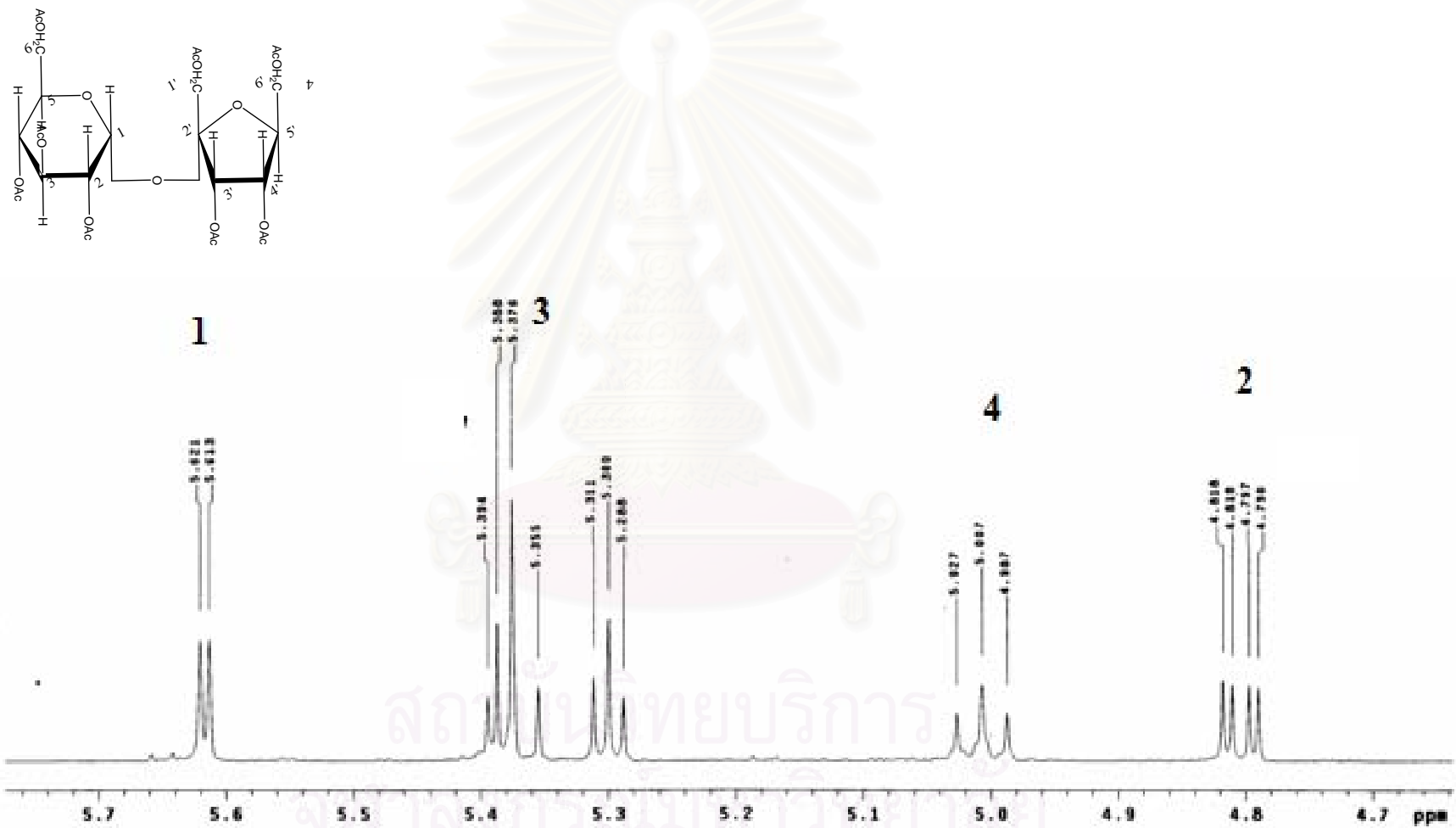


Figure 29 ¹H NMR (500 MHz) Spectrum of GP1 in CDCl₃

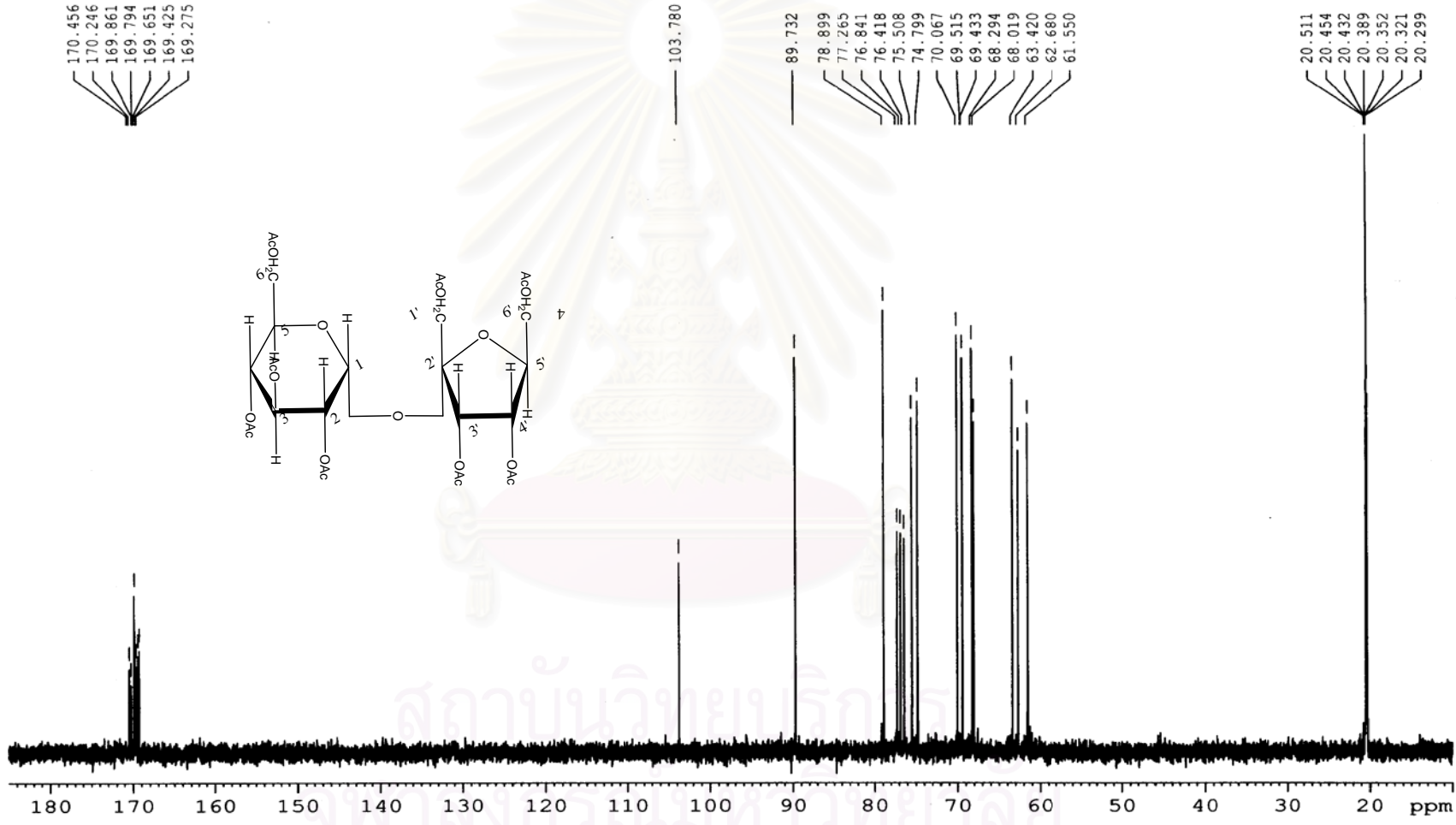
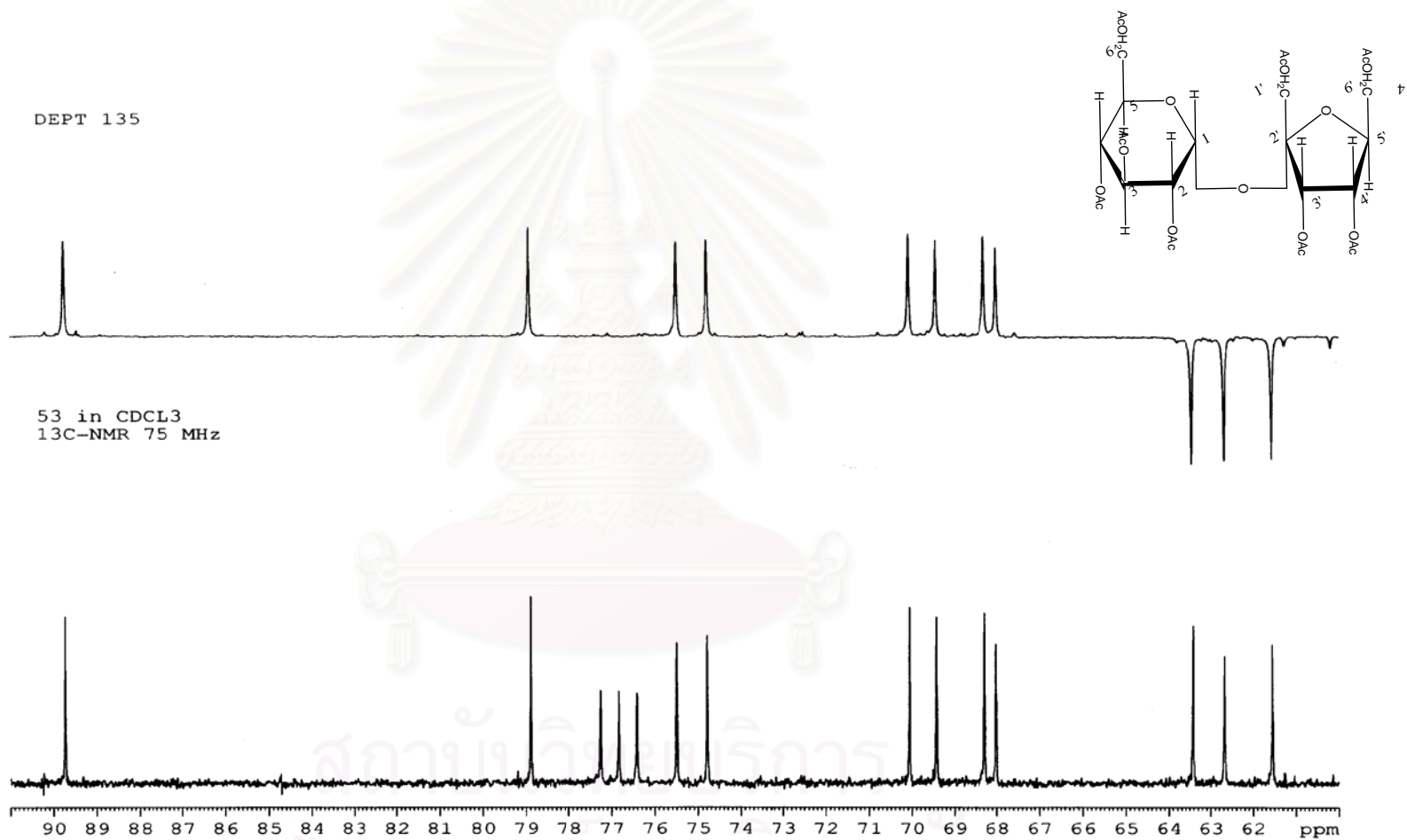


Figure 30 ¹³C NMR (75 MHz) Spectrum of GP1 in CDCl₃

Figure 31 ^{13}C NMR (75 MHz) Spectrum of GP1 in CDCl_3



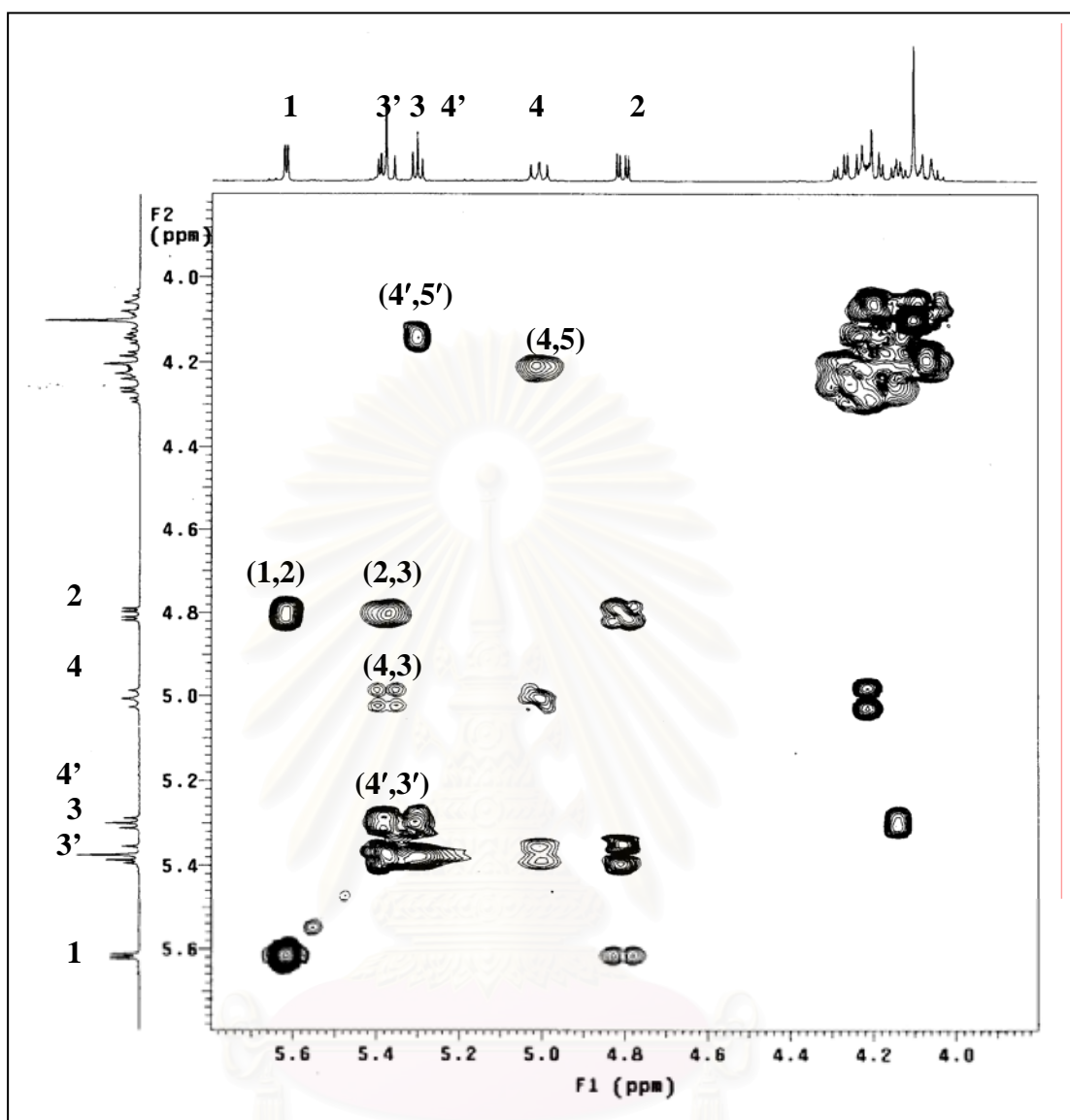
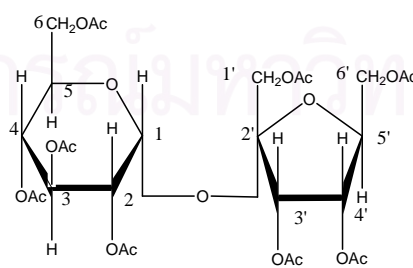


Figure 32 ^1H - ^1H COSY Spectrum of GP1 in CDCl_3



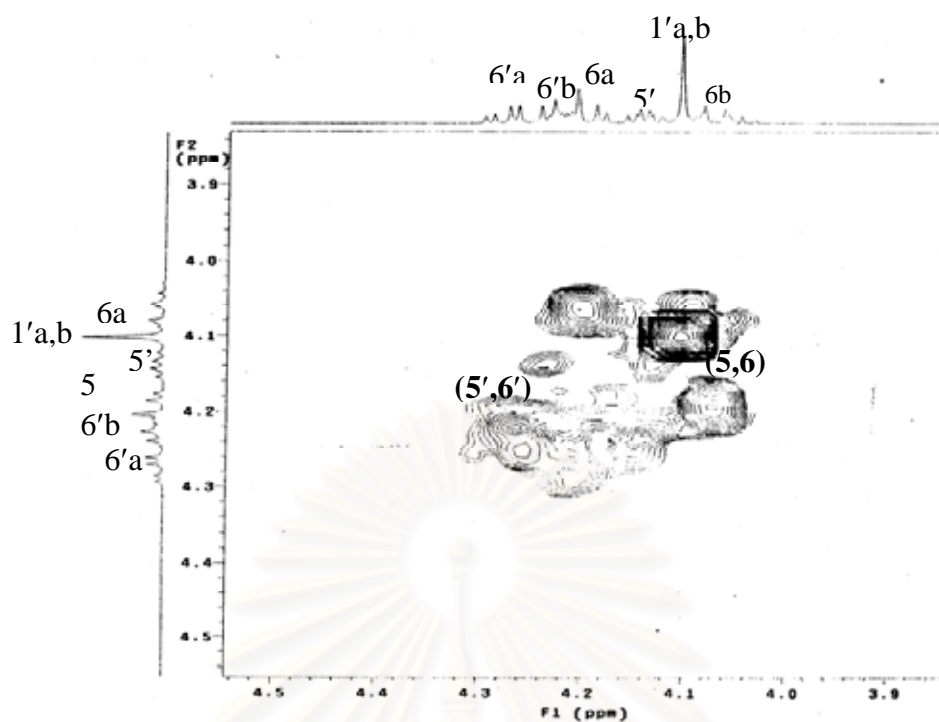


Figure 33 ^1H - ^1H COSY Spectrum of GP1 in CDCl_3

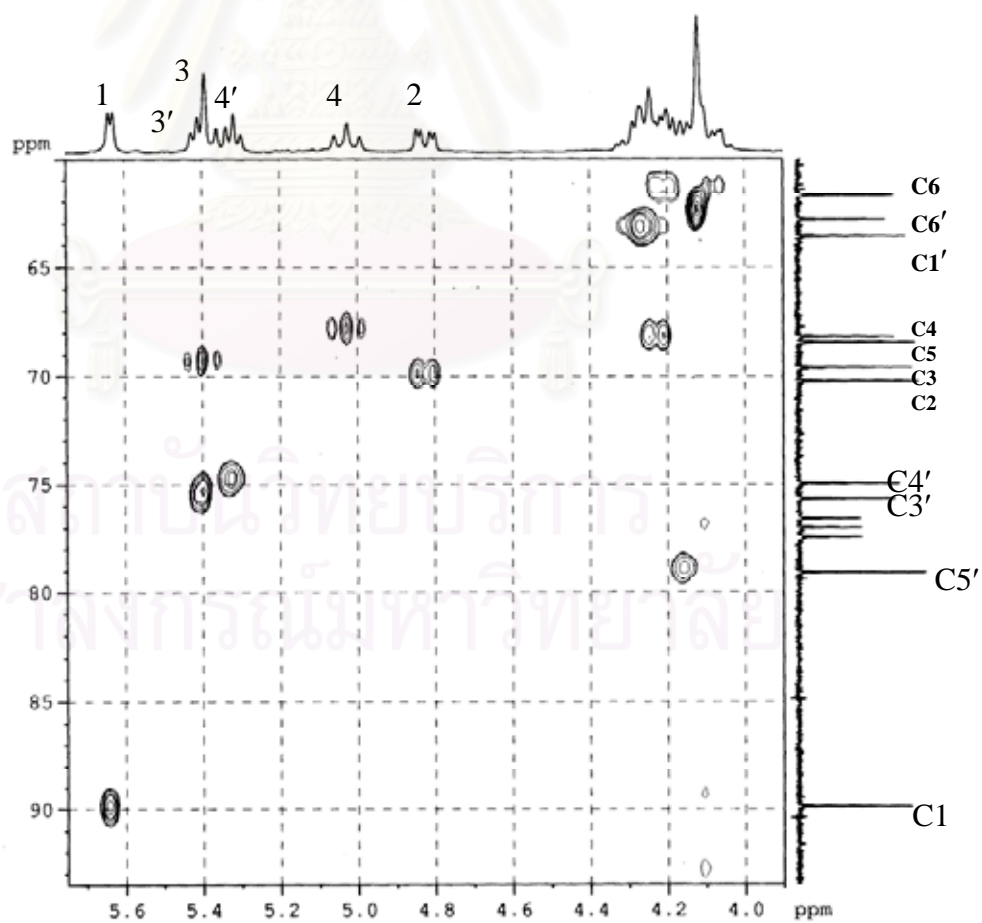


Figure 34 HMQC Spectrum of GP1 in CDCl_3

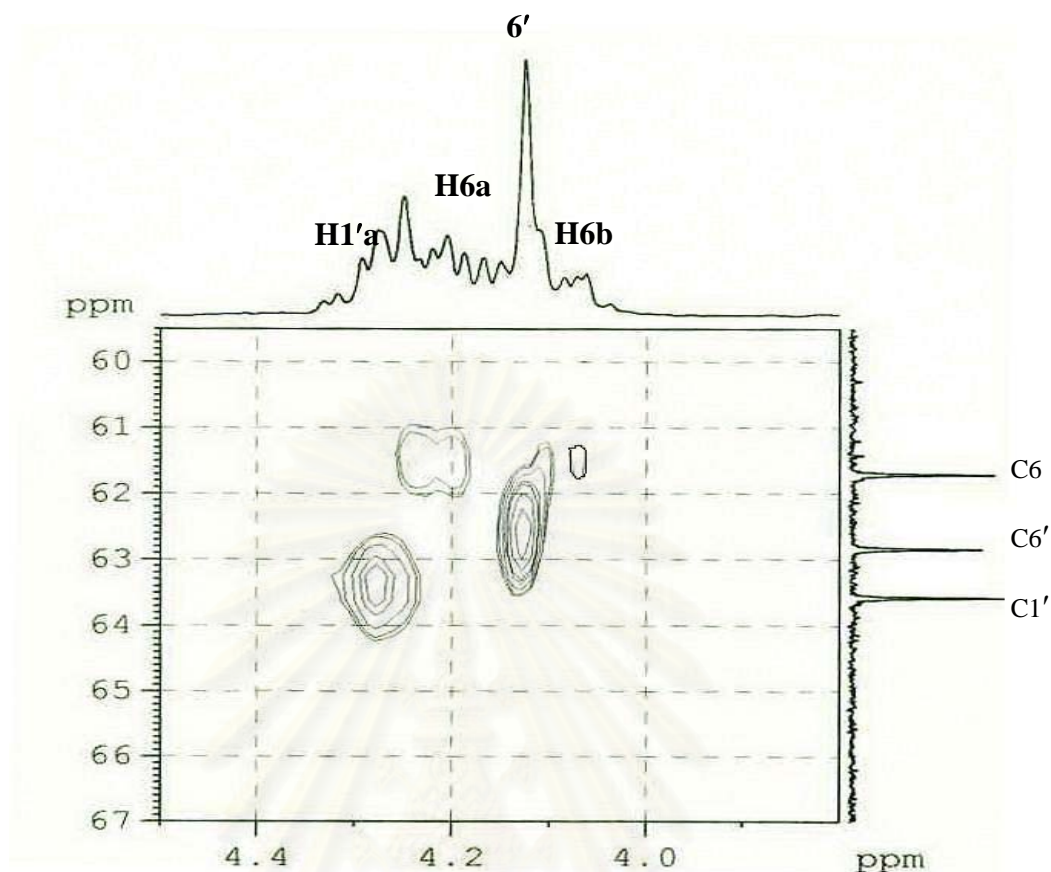


Figure 35 HMQC Spectrum of GP1 in CDCl₃

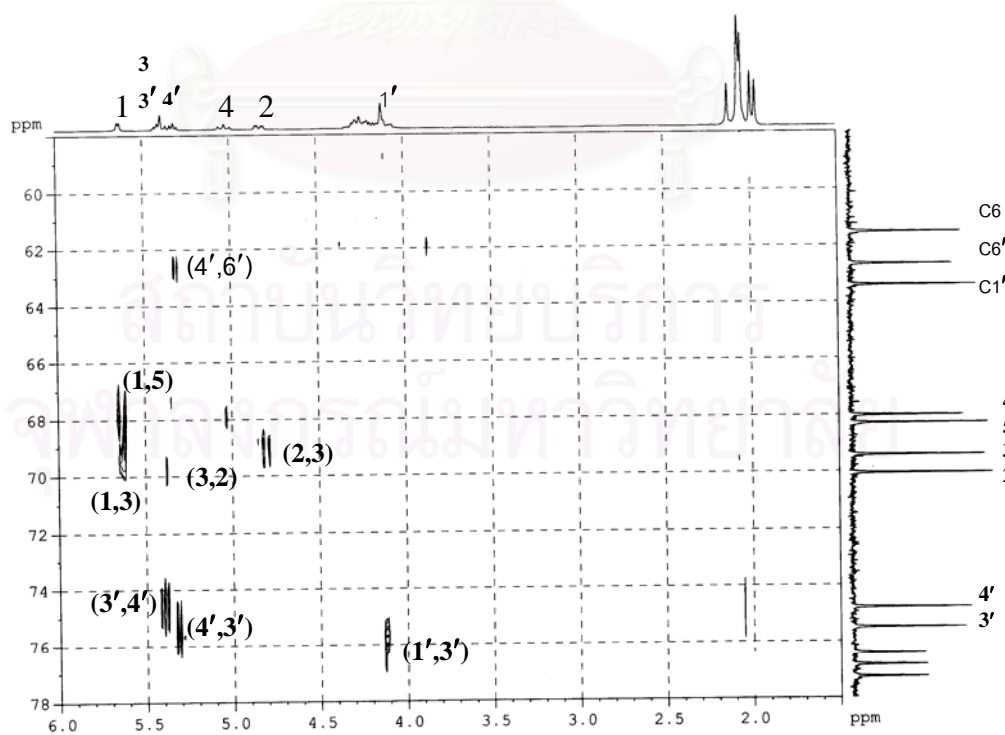


Figure 36 HMBC ($^nJ_{\text{H-C}} = 8 \text{ Hz}$) Spectrum of GP1 in CDCl₃

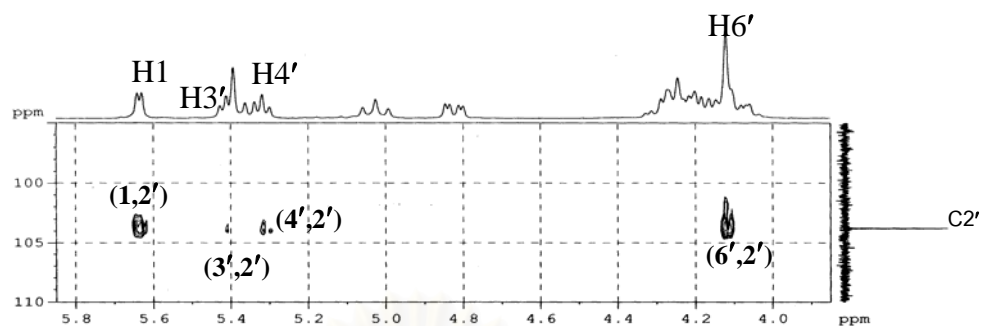


Figure 37 HMBC ($^nJ_{\text{H-C}} = 8 \text{ Hz}$) Spectrum of GP1 in CDCl_3

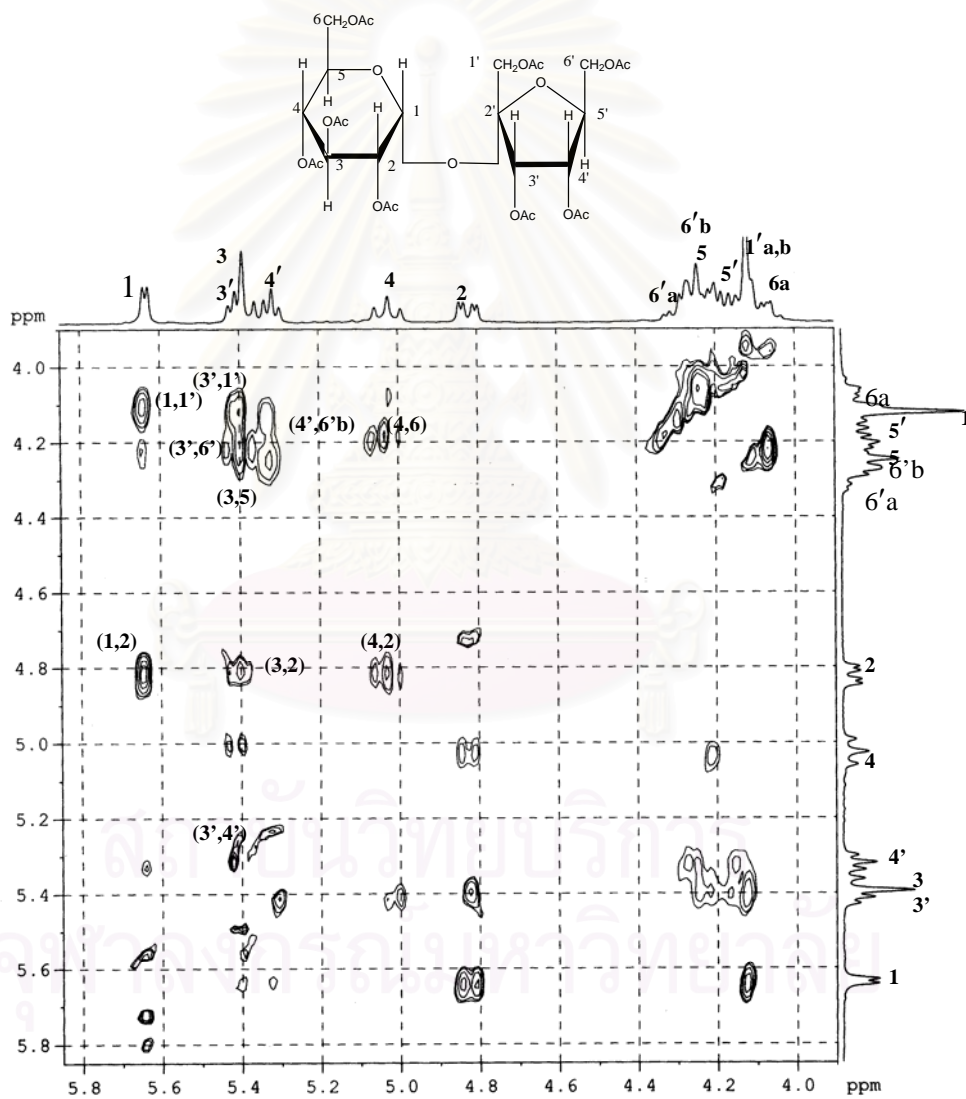


Figure 38 NOESY Spectrum of GP1 in CDCl_3

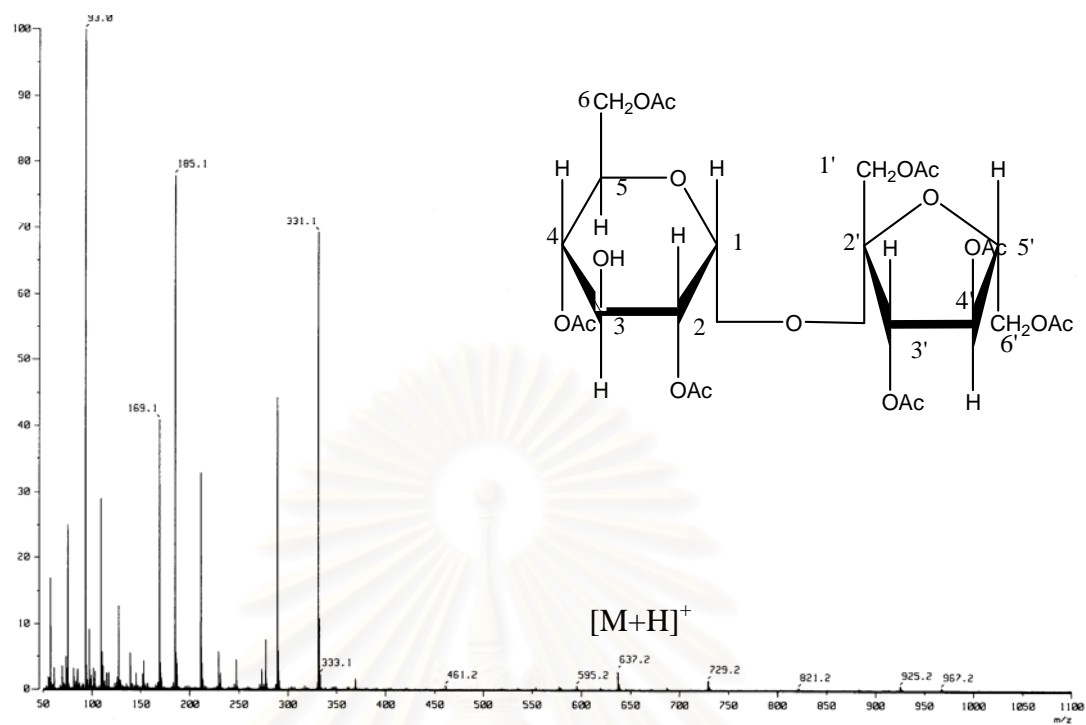


Figure 39 EIMS Spectrum of GP2

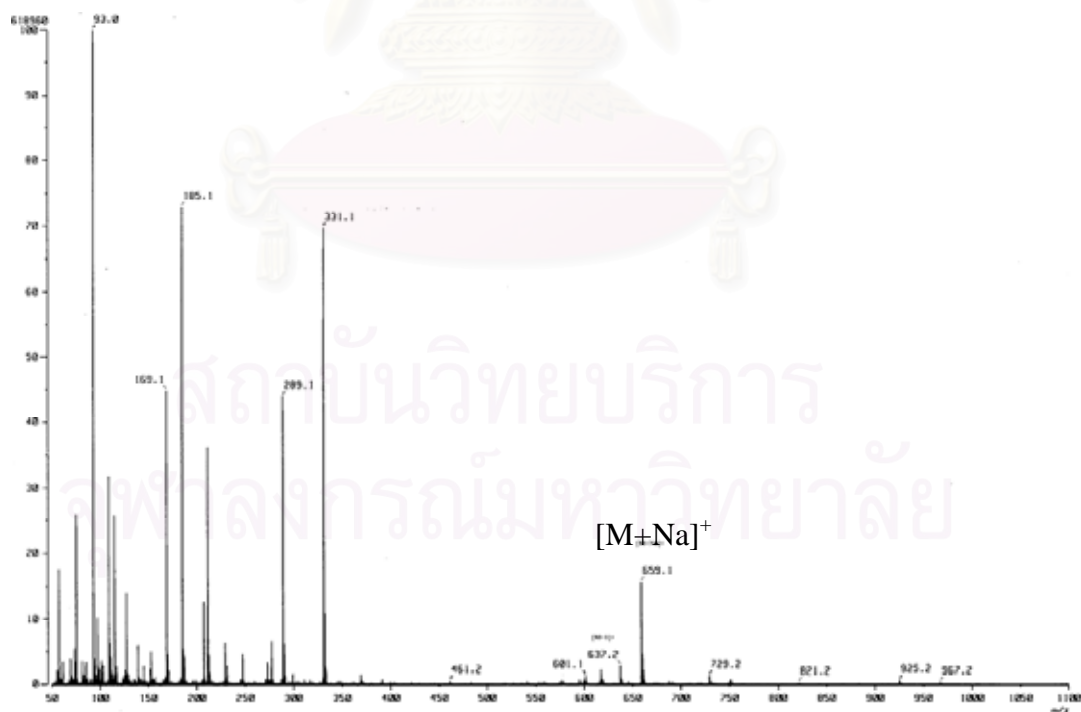
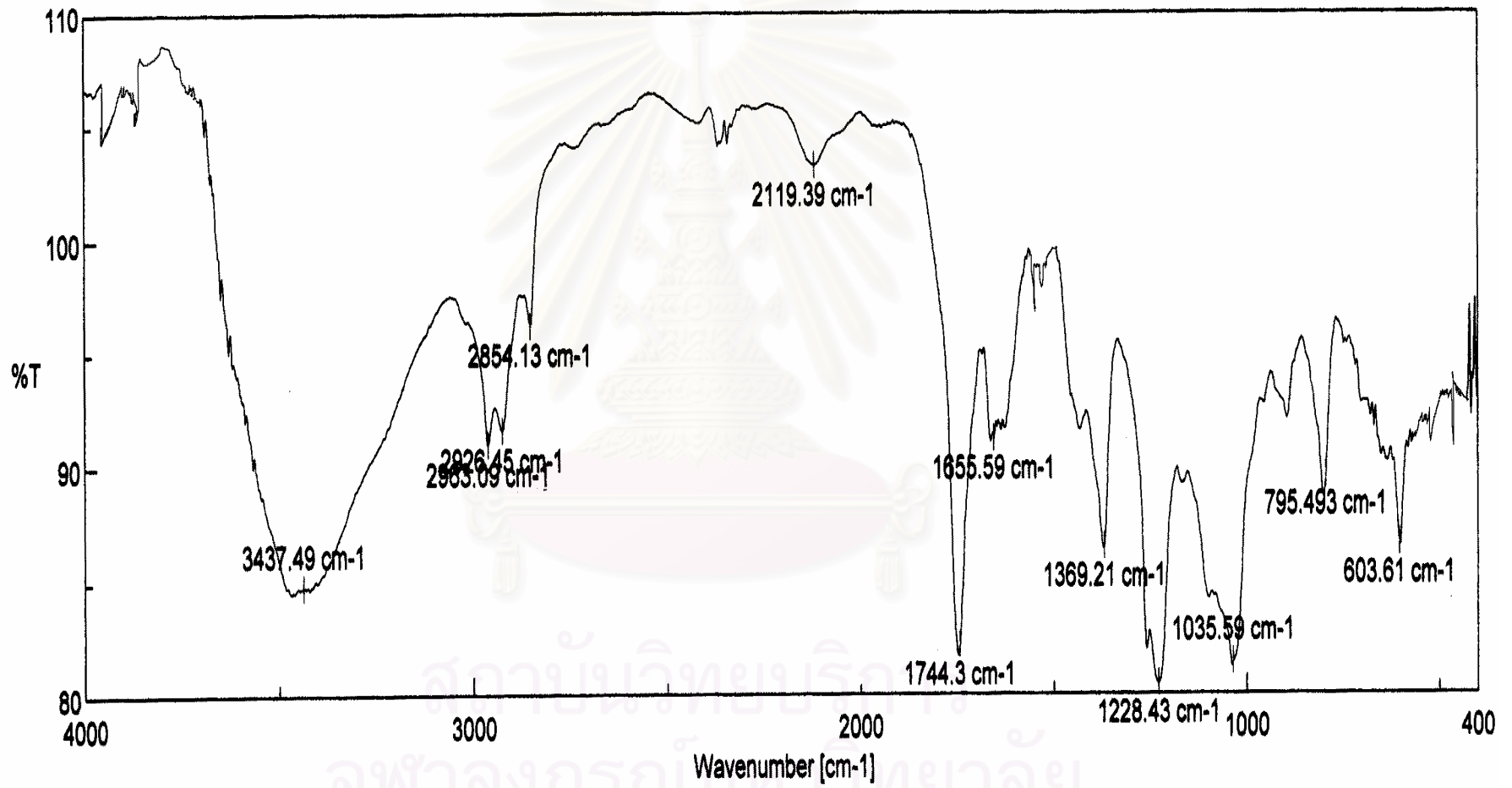


Figure 40 FABMS Spectrum of GP2

Figure 41 IR Spectrum (film) of GP2



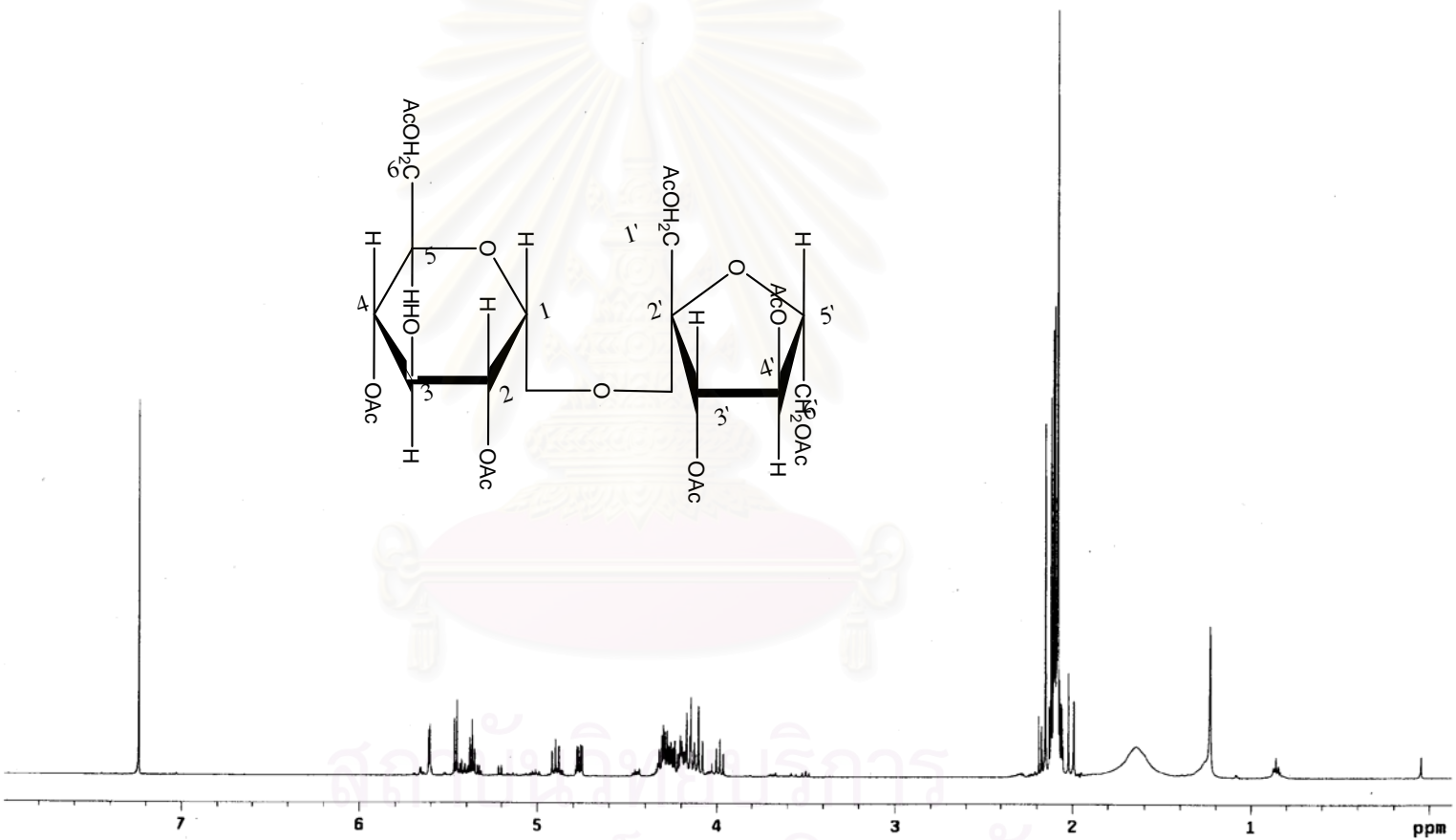


Figure 42 ¹H NMR (500 MHz) Spectrum of GP2 in CDCl₃

จุฬาลงกรณ์มหาวิทยาลัย

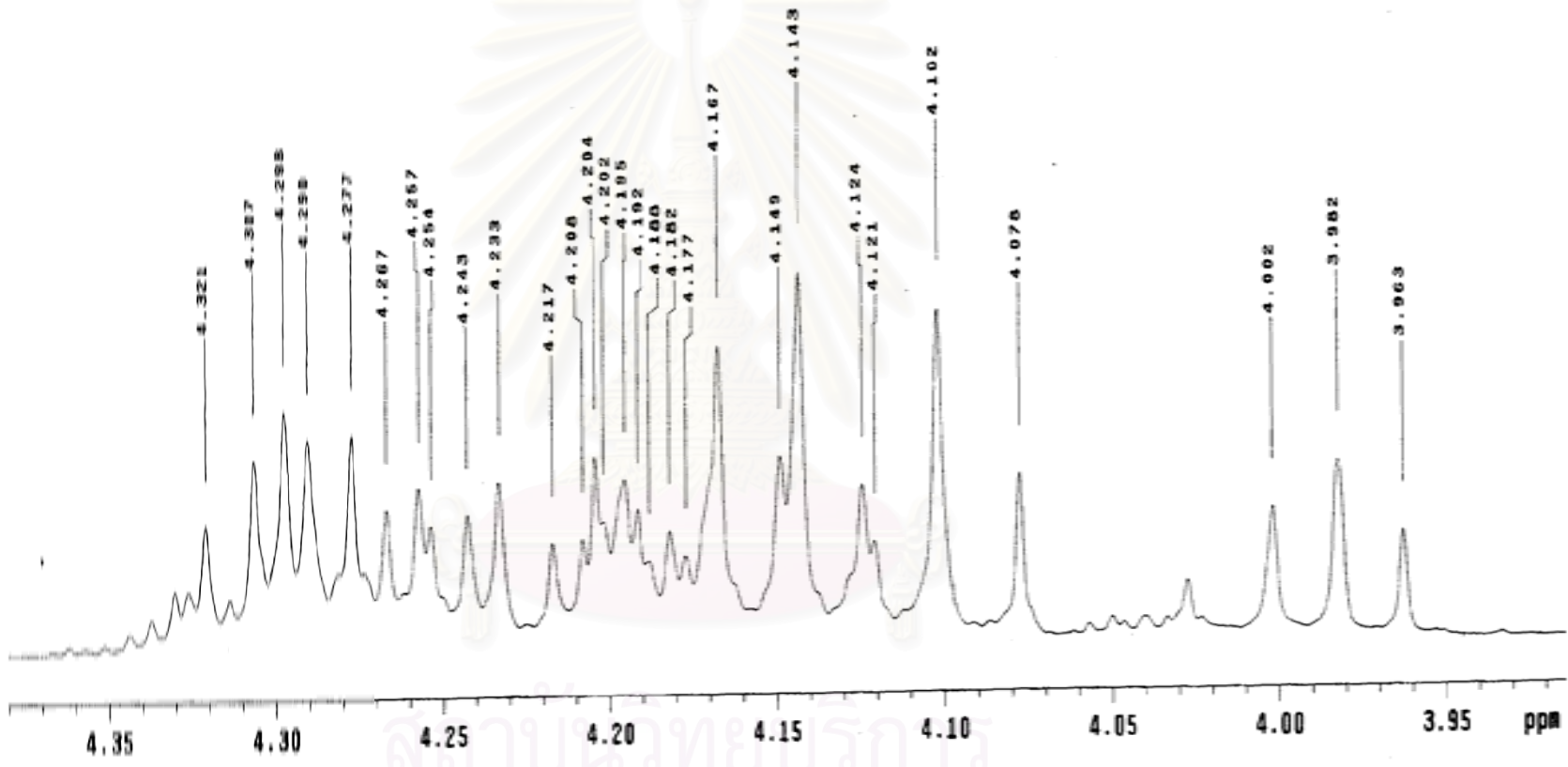


Figure 4.3 ^1H NMR (500 MHz) Spectrum of GP2 in CDCl_3 .

สถาบันวิทยบริการ
จุฬาลงกรณ์มหาวิทยาลัย

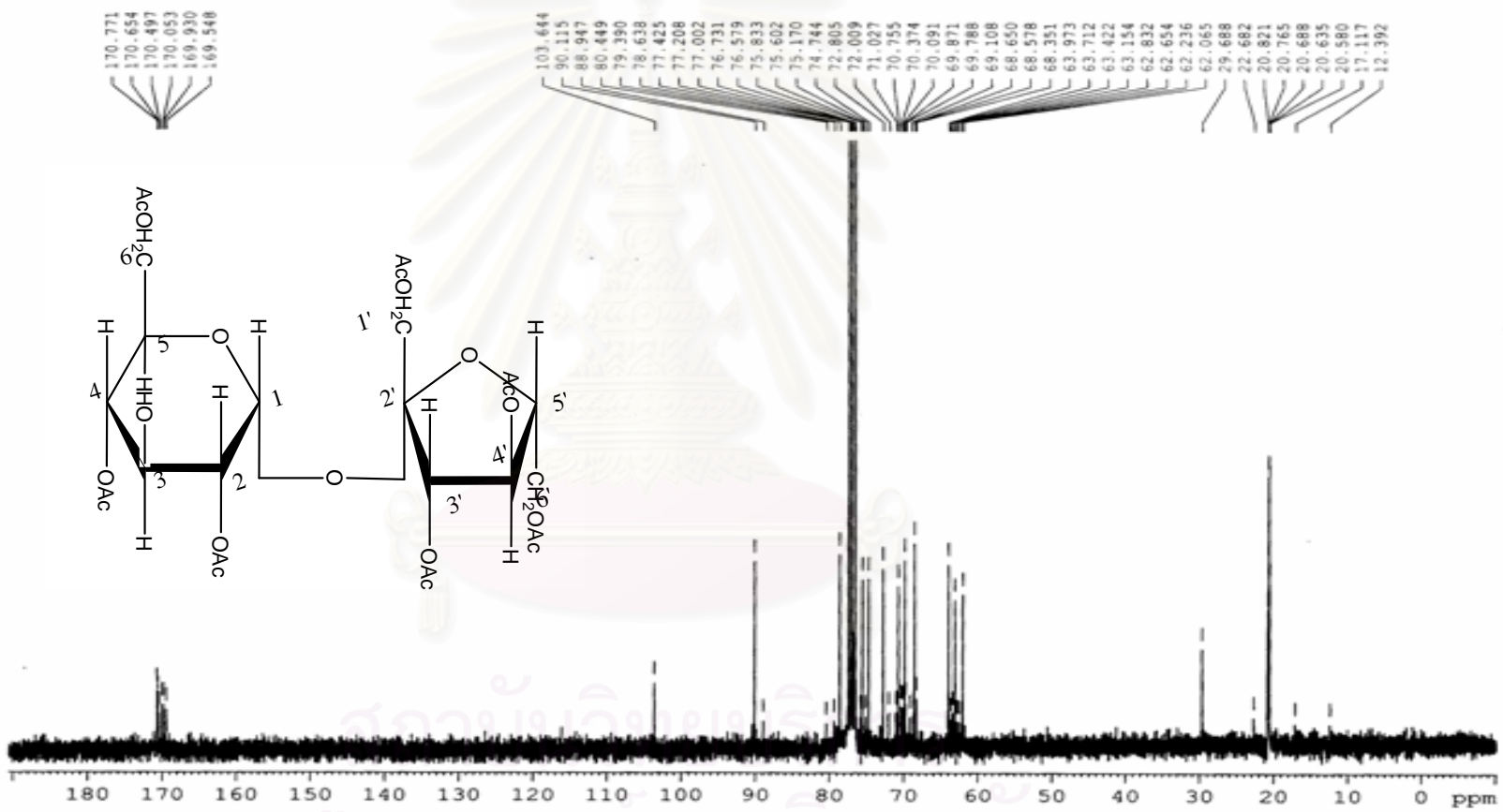
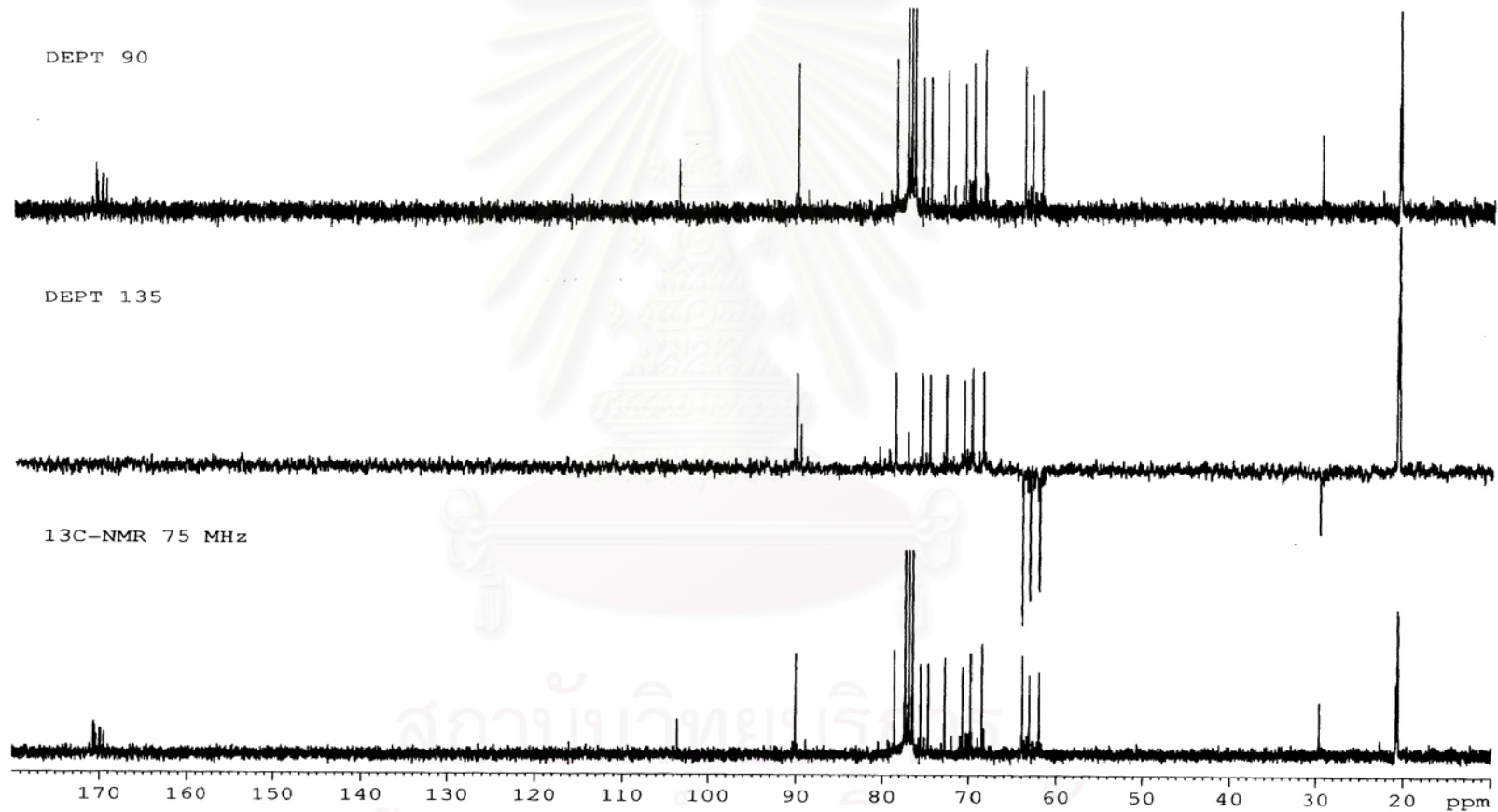
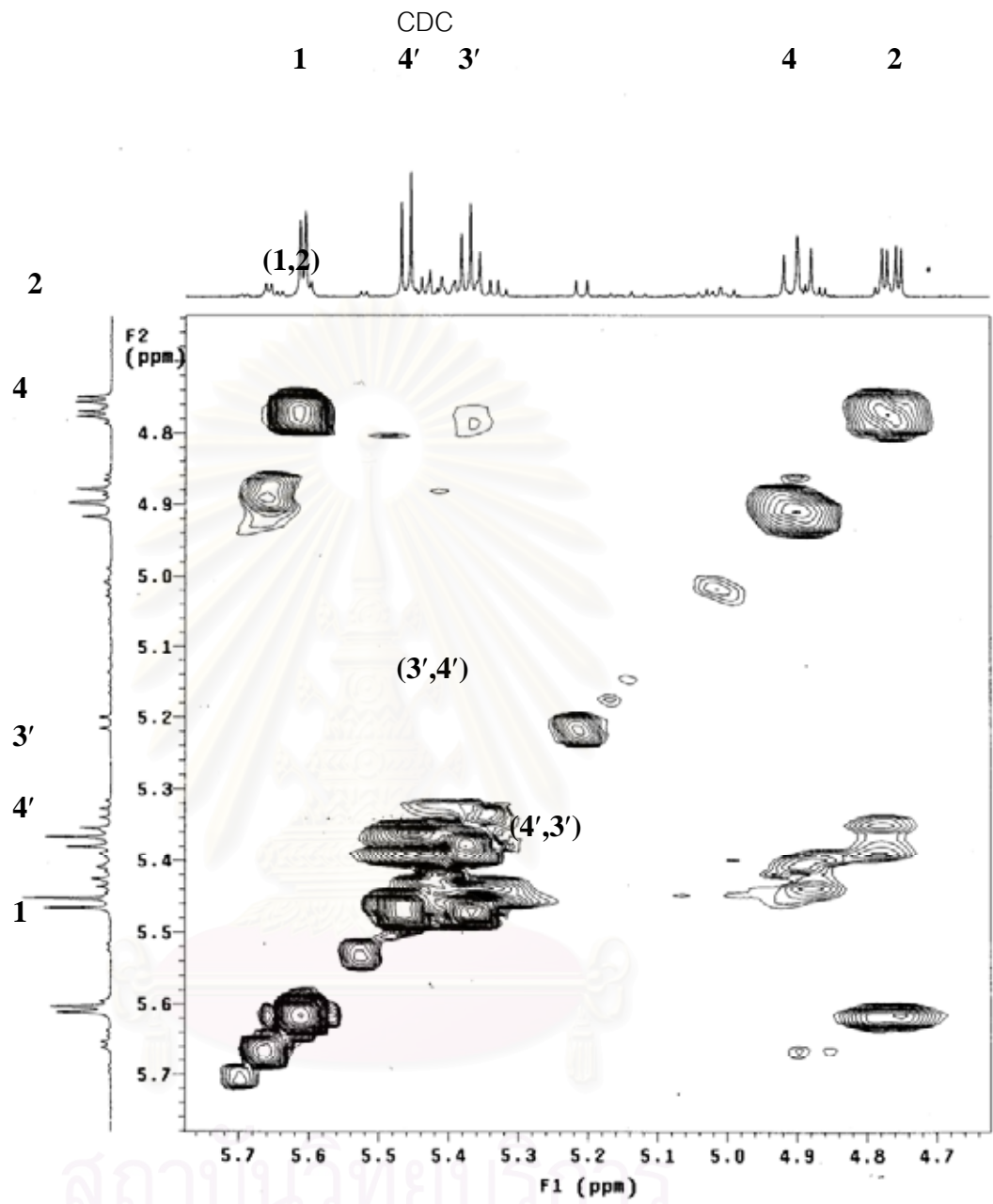
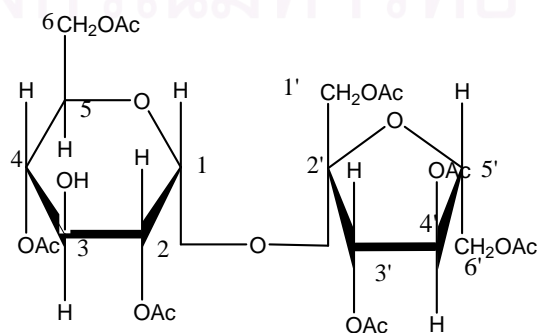


Figure 44 ^{13}C NMR (75 MHz) Spectrum of GP2 in CDCl_3



สภามหาวิทยาลัย
จุฬาลงกรณ์มหาวิทยาลัย

Figure 45 DEPT Spectra of GP2 in

Figure 46 ^1H - ^1H COSY Spectrum of GP2 in CDCl_3 

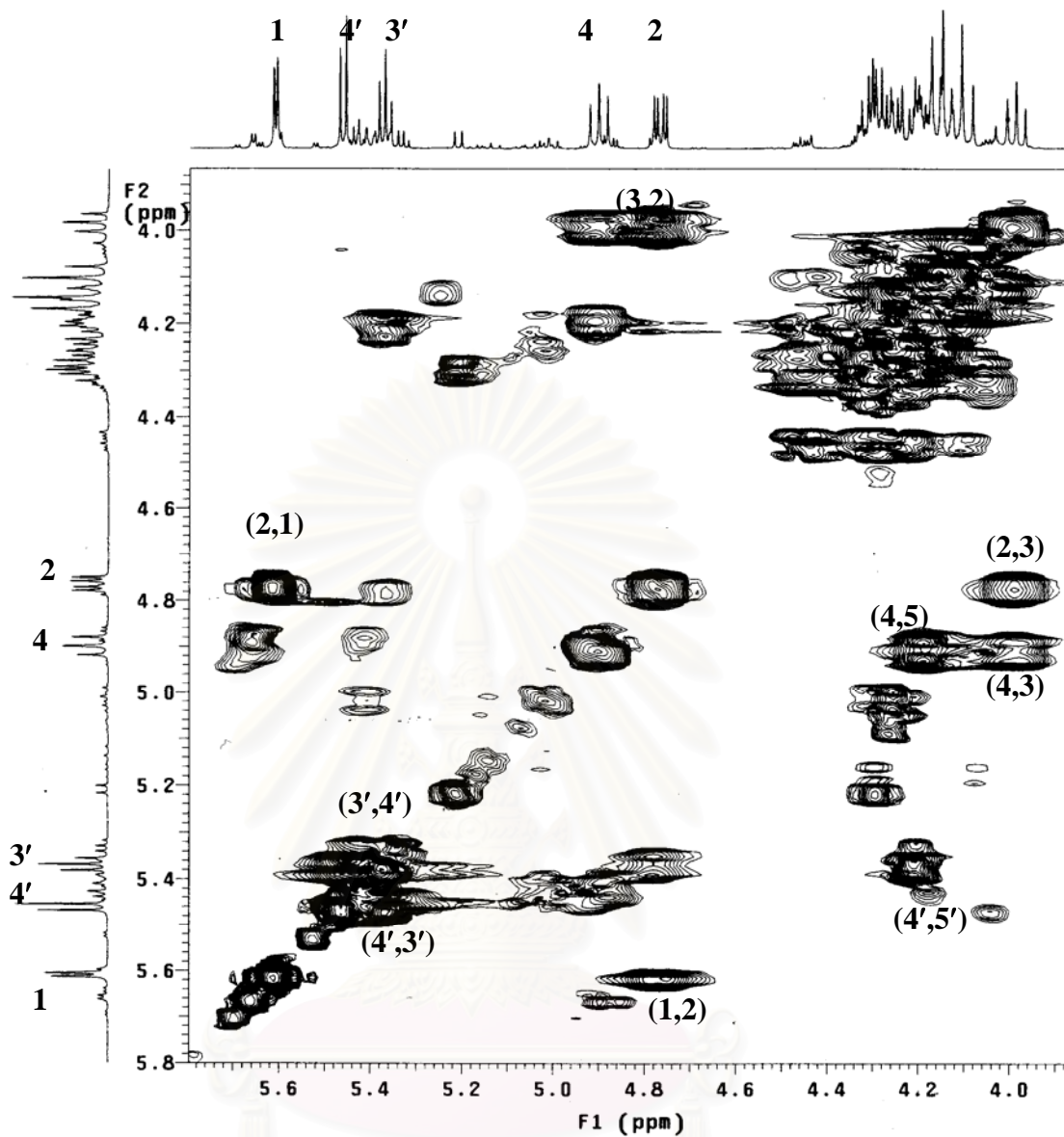
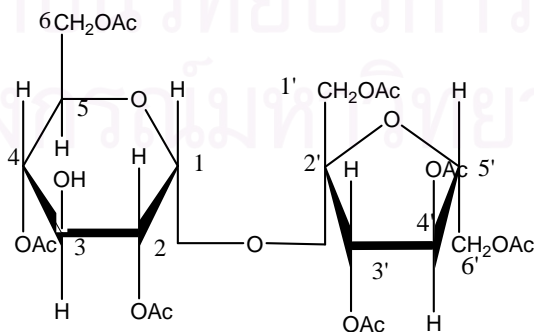


Figure 47 ^1H - ^1H COSY Spectrum of GP2 in CDCl_3



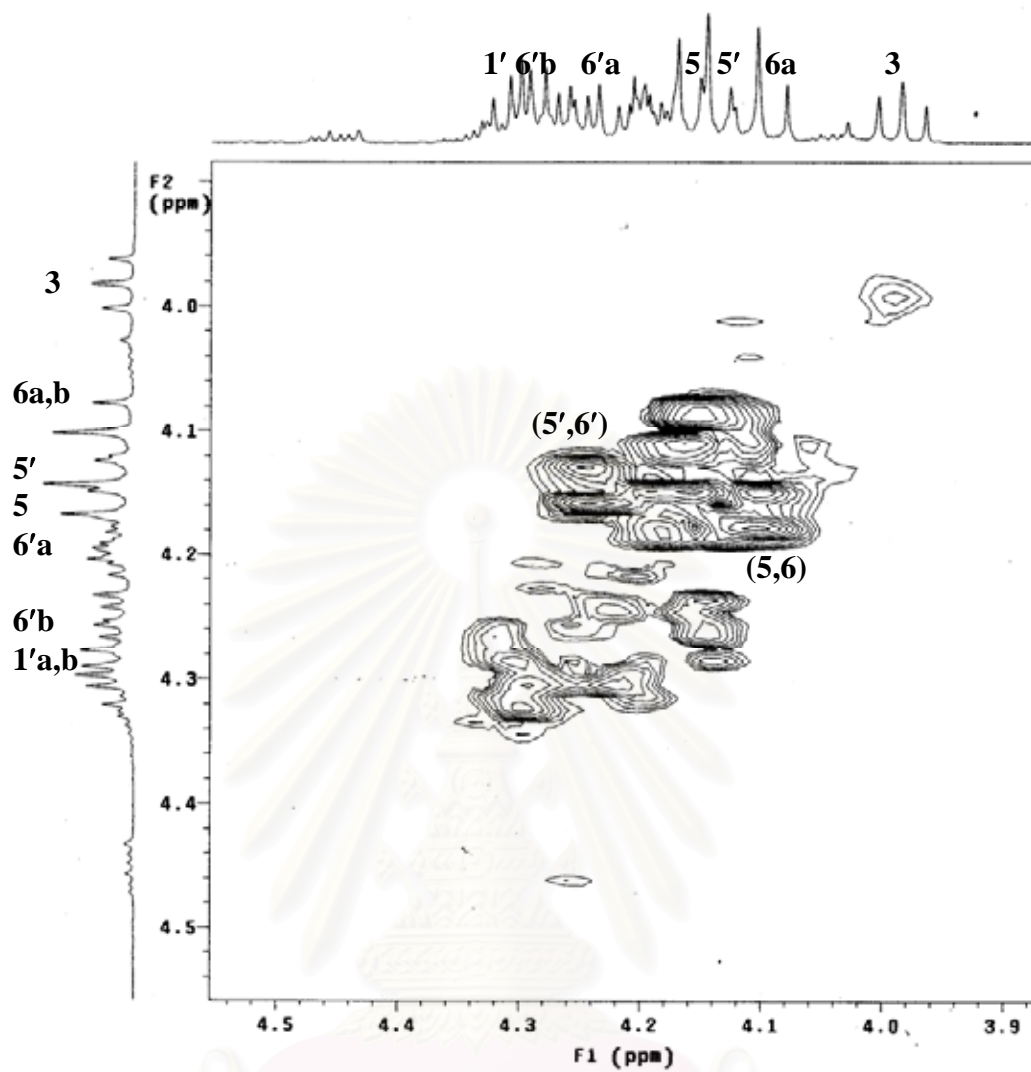


Figure 48 ^1H - ^1H COSY Spectrum of GP2 in CDCl_3

สถาบันวิทยบริการ
จุฬาลงกรณ์มหาวิทยาลัย

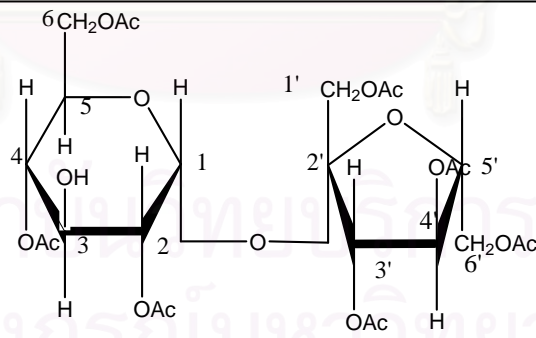
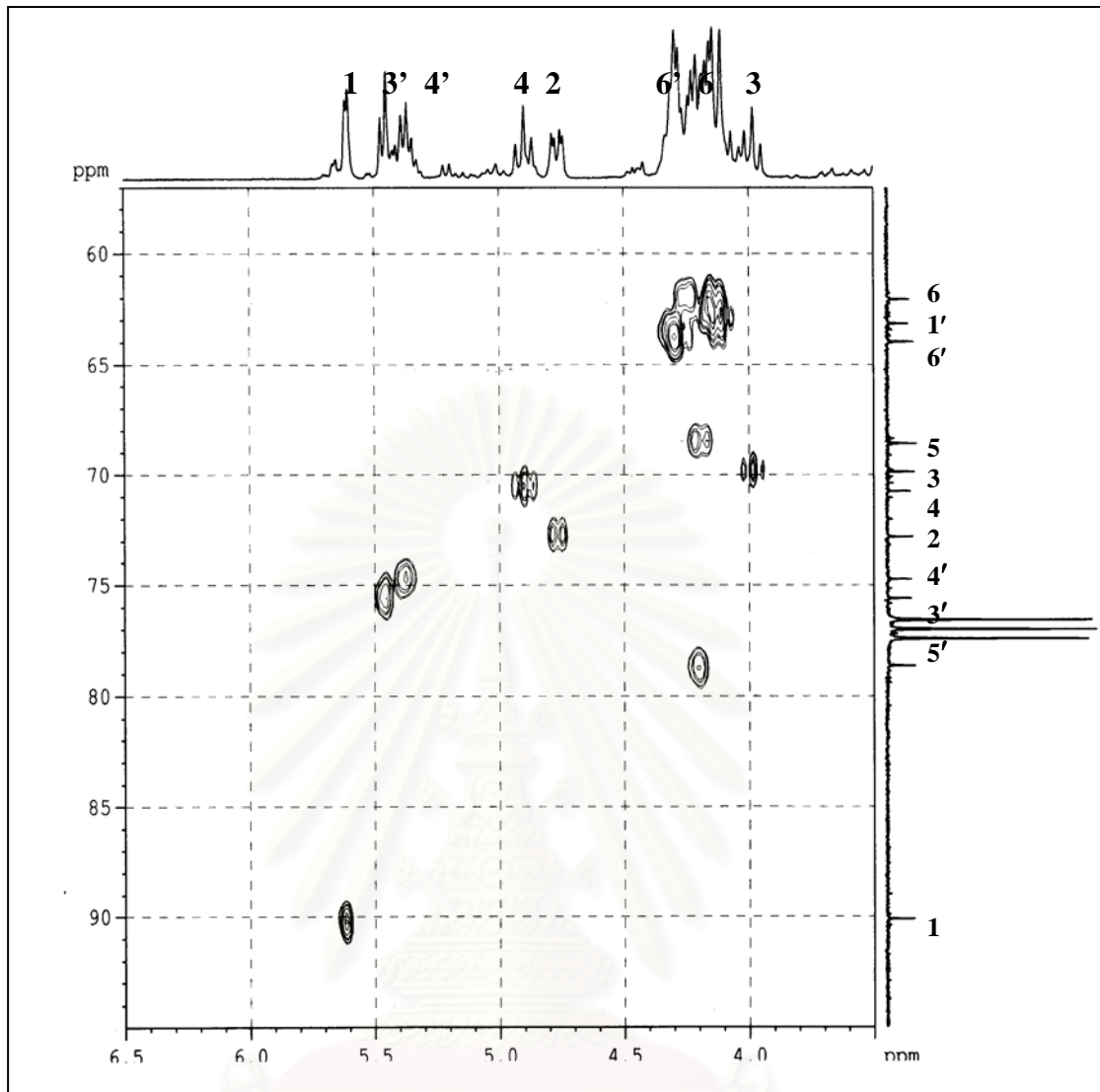


Figure 49 HMBC Spectrum of GP2 in CDCl_3

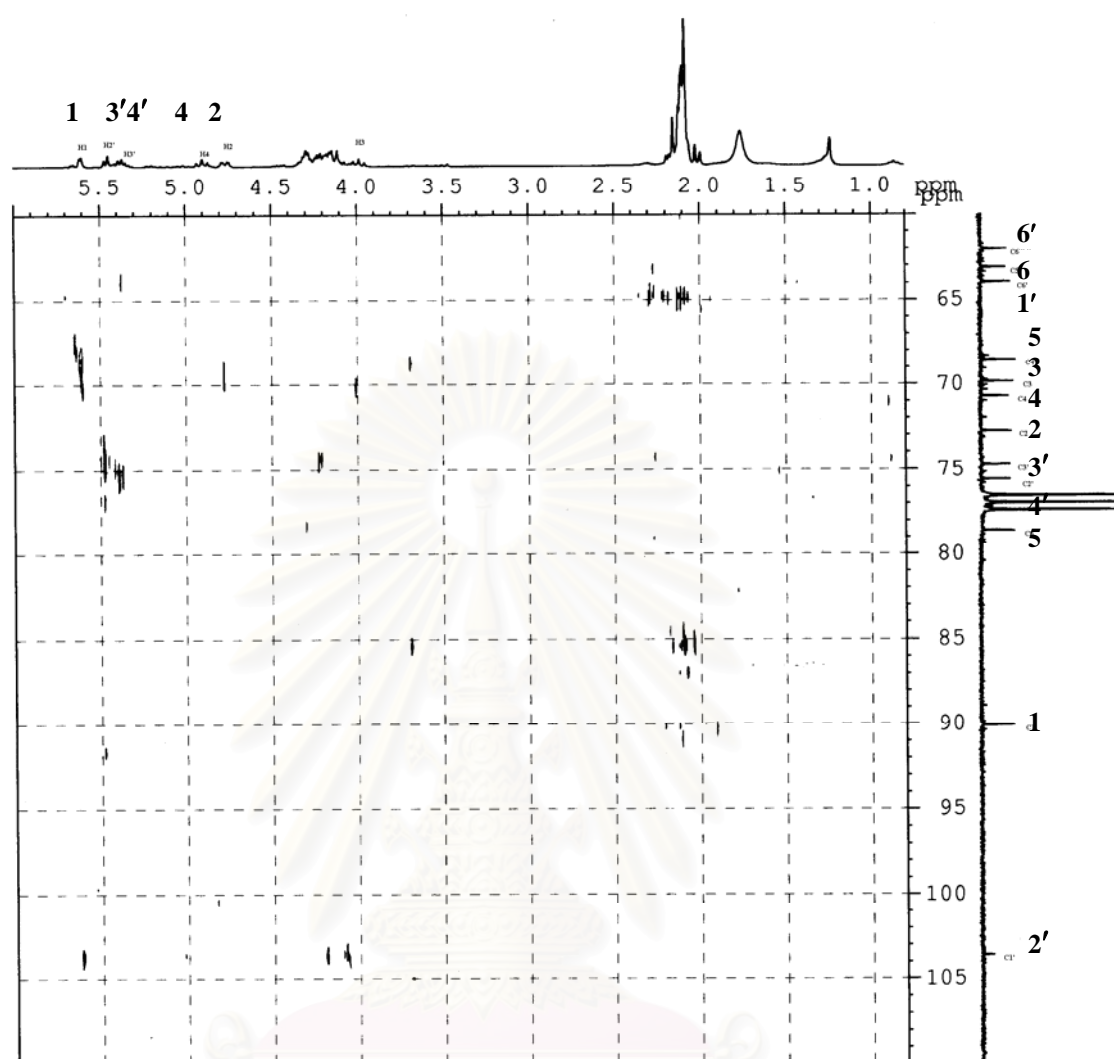
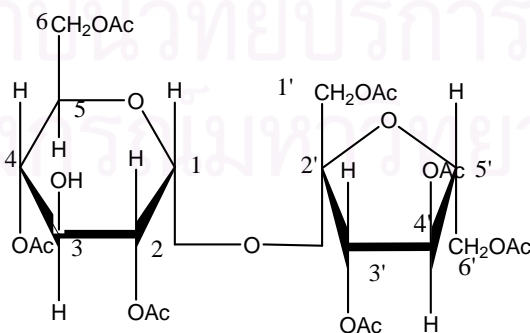


Figure 50 HMBC ($^nJ_{\text{H-C}} = 8 \text{ Hz}$) Spectrum of GP2 in CDCl₃



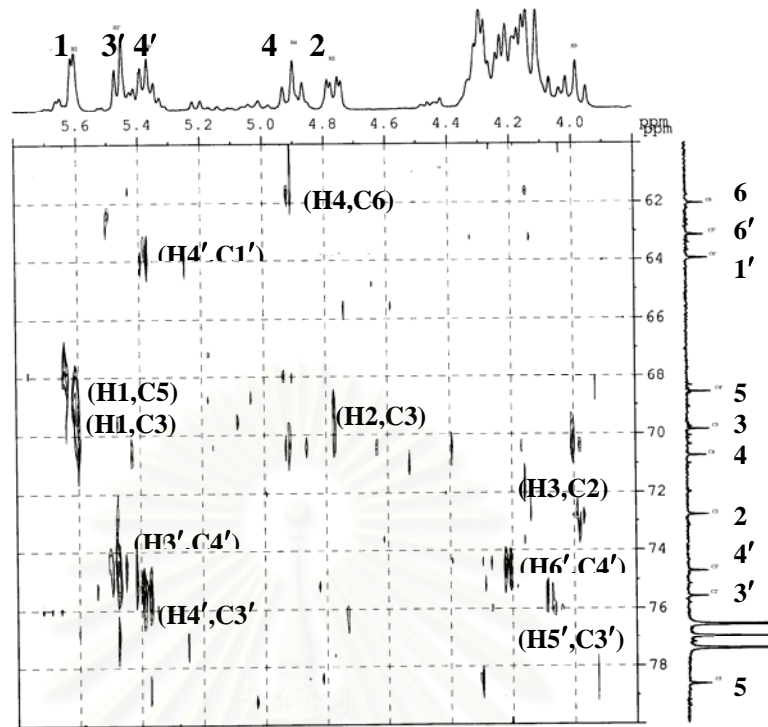
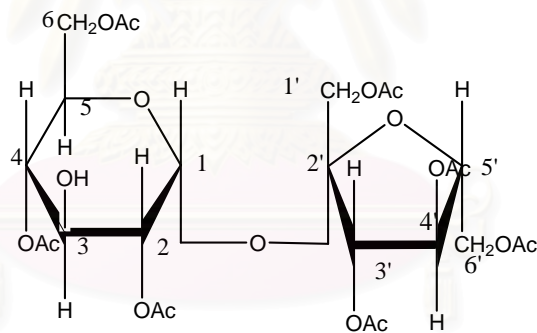


Figure 51 HMBC ($^nJ_{\text{HC}} = 8 \text{ Hz}$) Spectrum of GP2 in CDCl_3



สถาบันวิทยบริการ
จุฬาลงกรณ์มหาวิทยาลัย

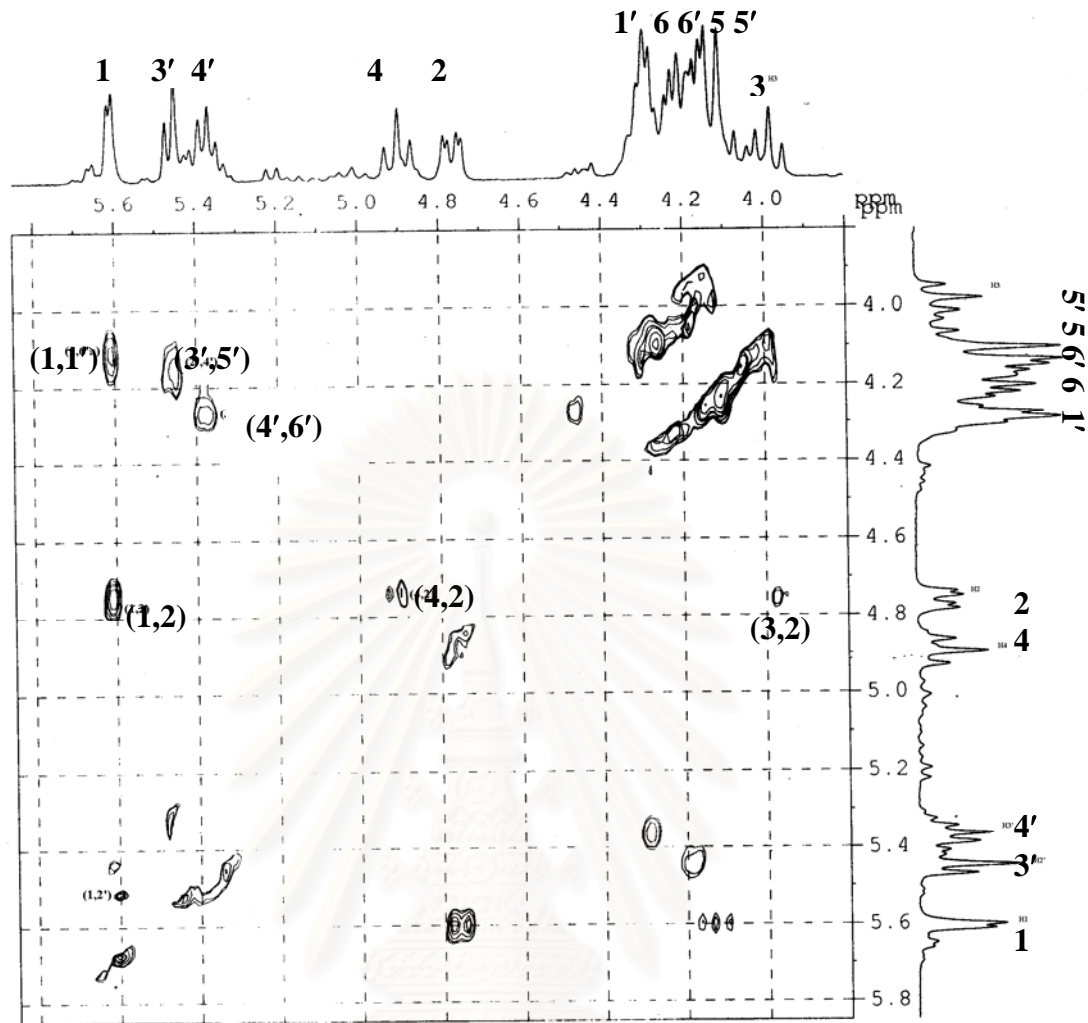
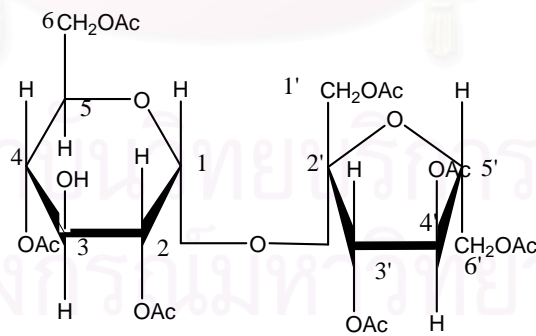


Figure 52 NOESY Spectrum of GP2 in CDCl₃



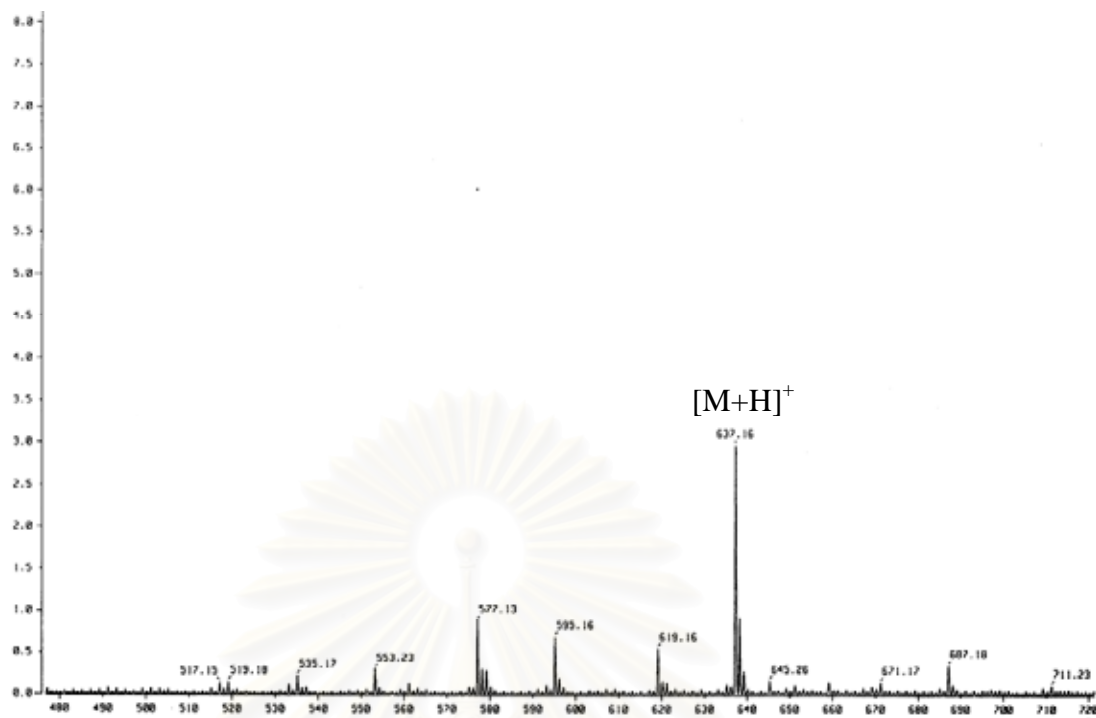


Figure 53 EIMS Spectrum of GP3

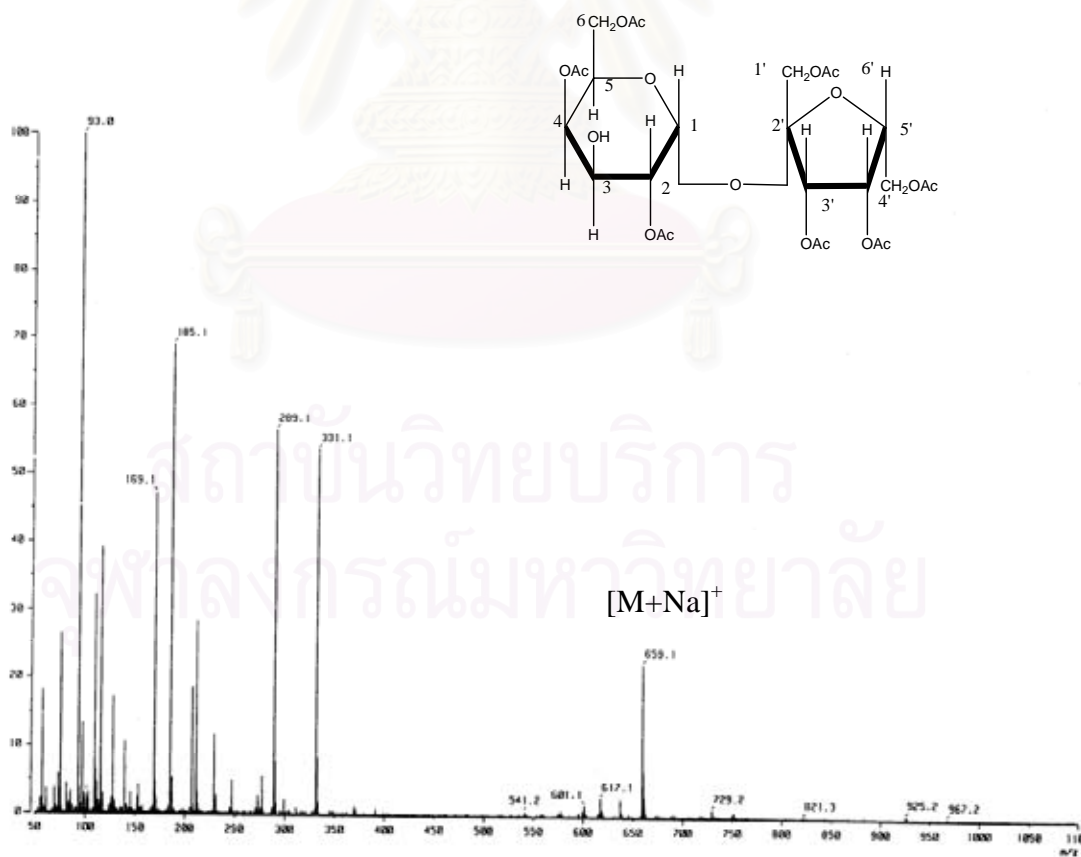


Figure 54 FABMS Spectrum of GP3

Figure 55 IR Spectrum (film) of GP3

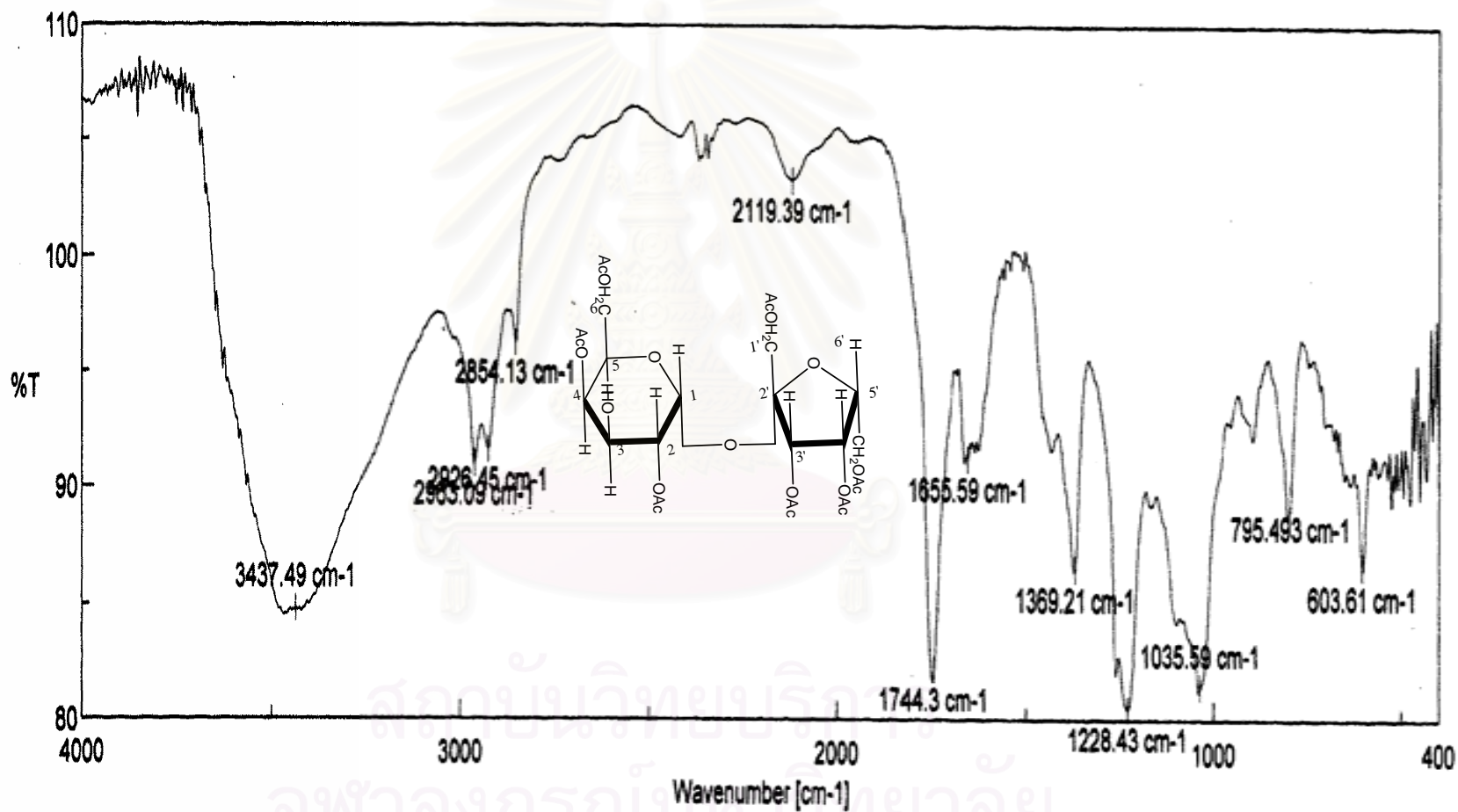


Figure 56 ^1H NMR (500 MHz) Spectrum of GP3 in CDCl_3

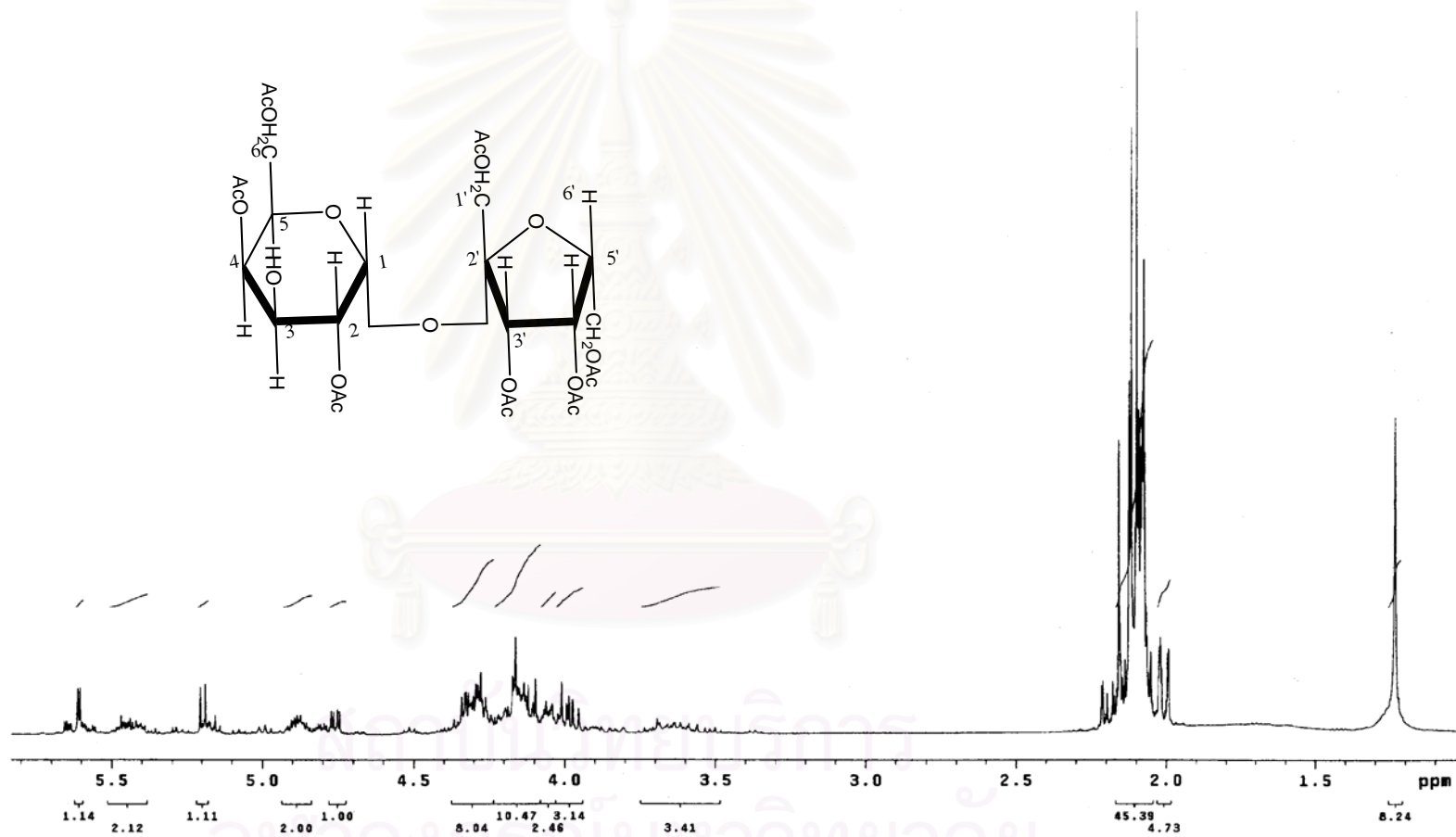


Figure 57 ^1H NMR (500 MHz) Spectrum of GP3 in CDCl_3

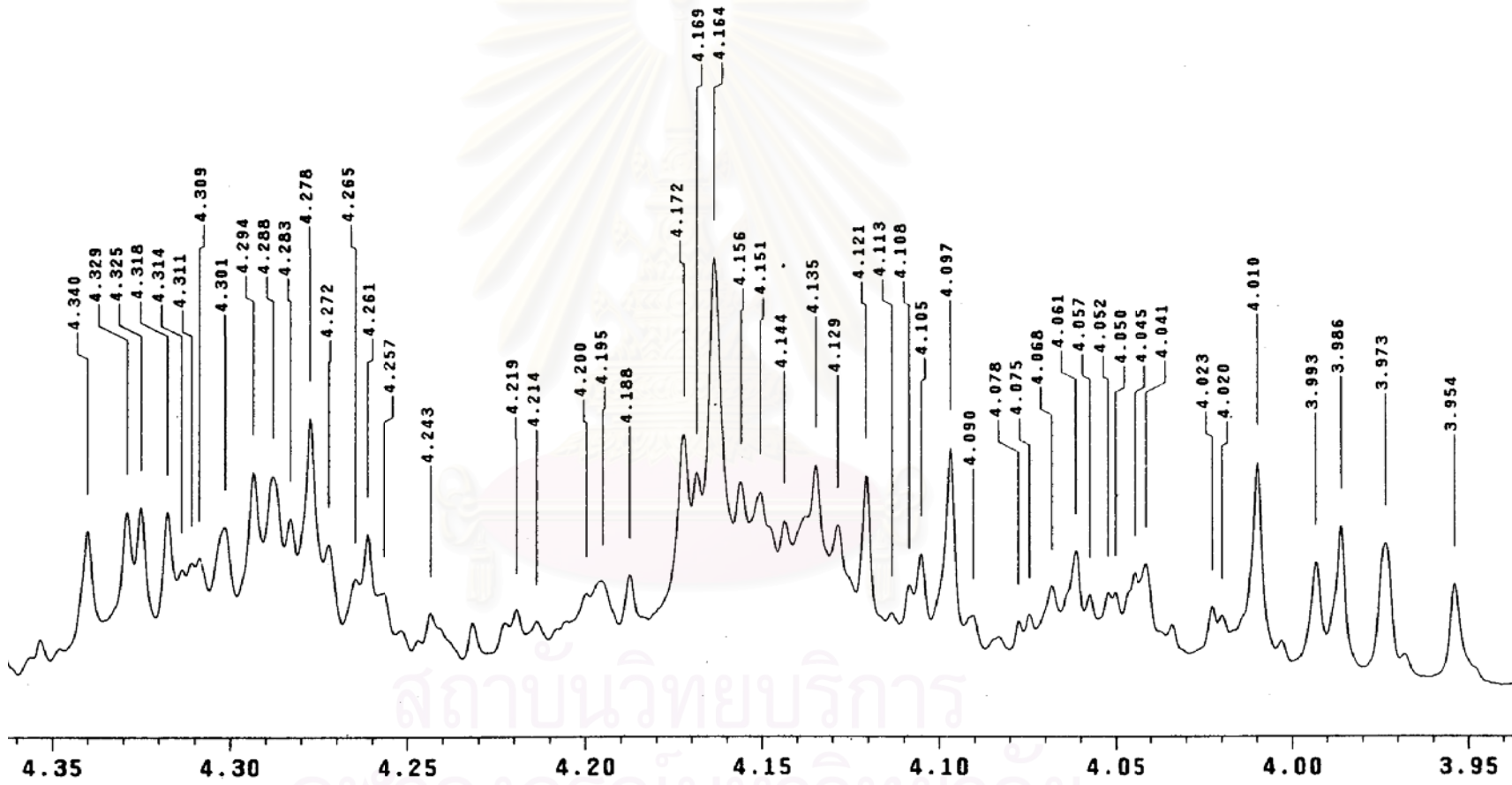


Figure 58 ^1H NMR (500 MHz) Spectrum of GP3 in CDCl_3

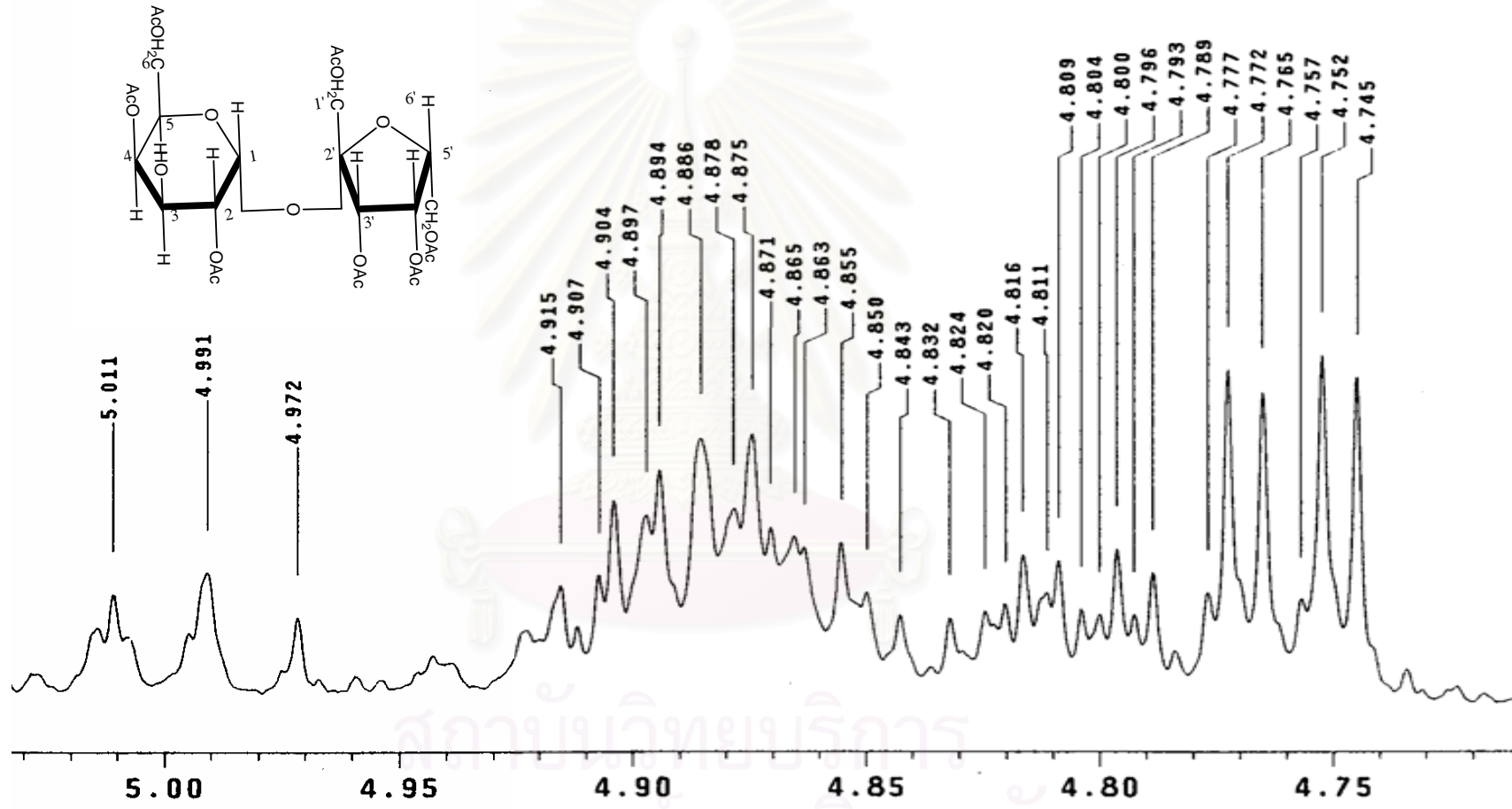
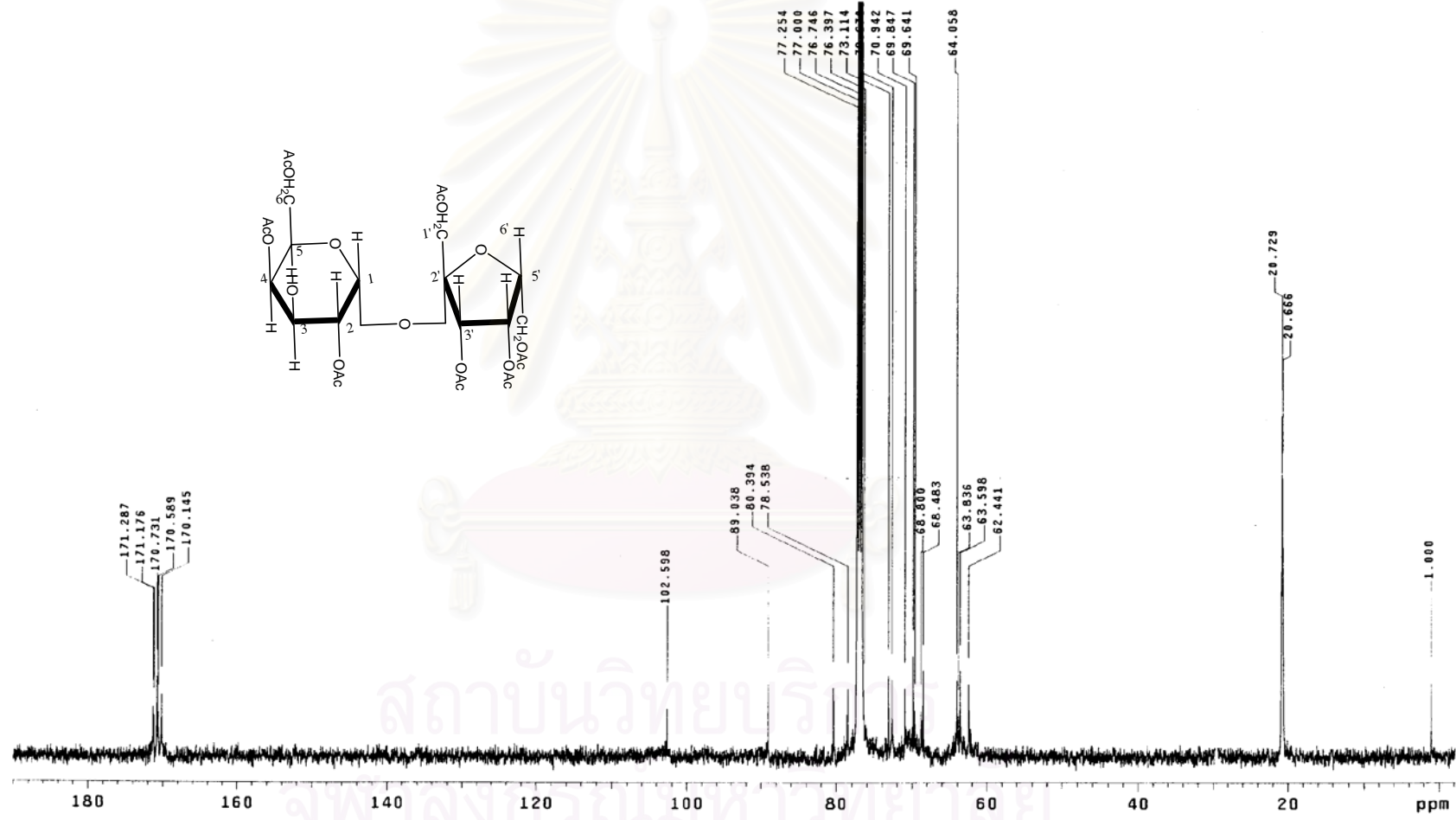


Figure 59 ^{13}C NMR (125 MHz) Spectrum of GP3 in CDCl_3



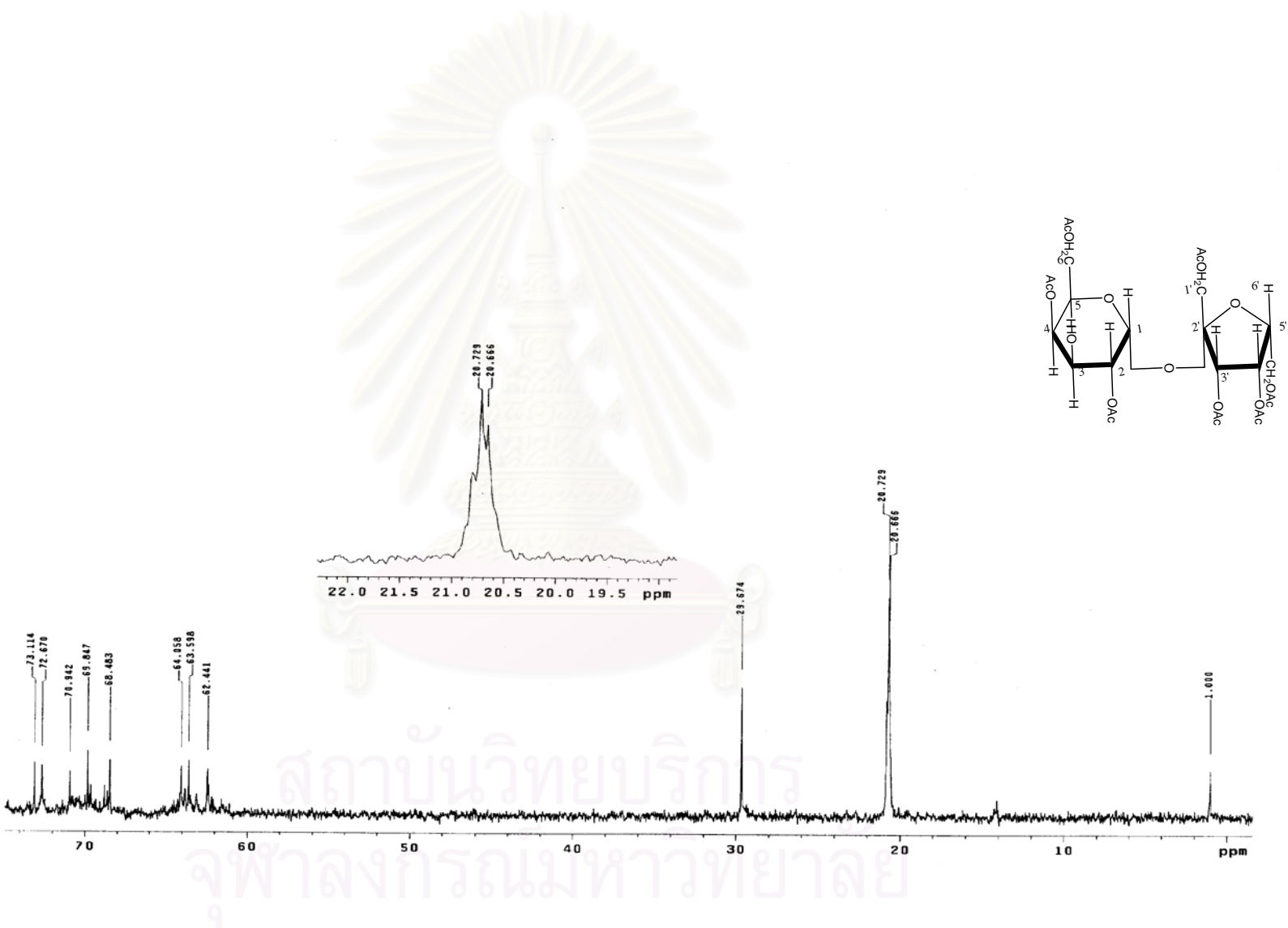
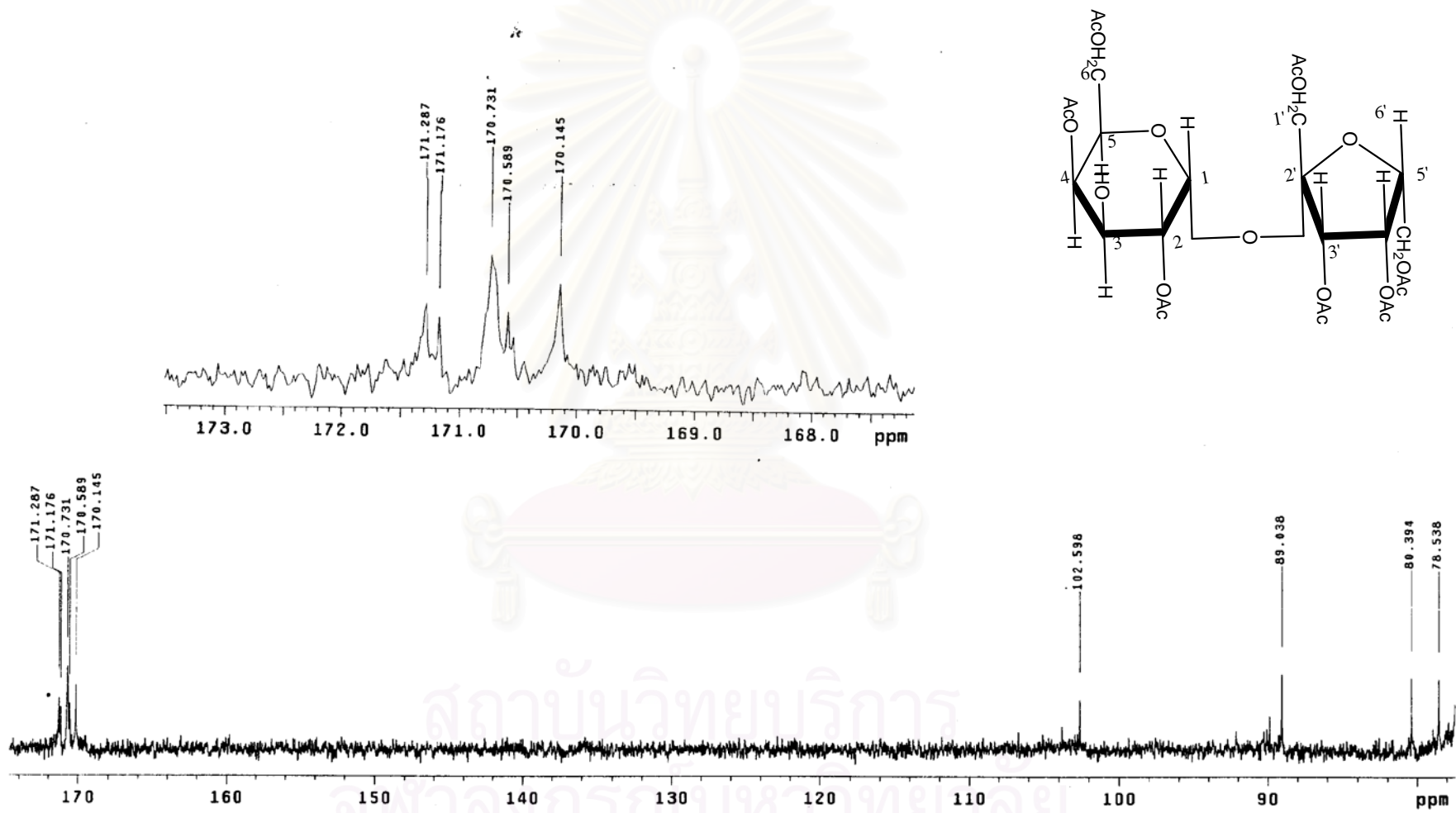


Figure 60 ^{13}C NMR (125 MHz) Spectrum of GP3 in CDCl_3

Figure 61 ^{13}C NMR (125 MHz) Spectrum of GP3 in CDCl_3



DEPT 135

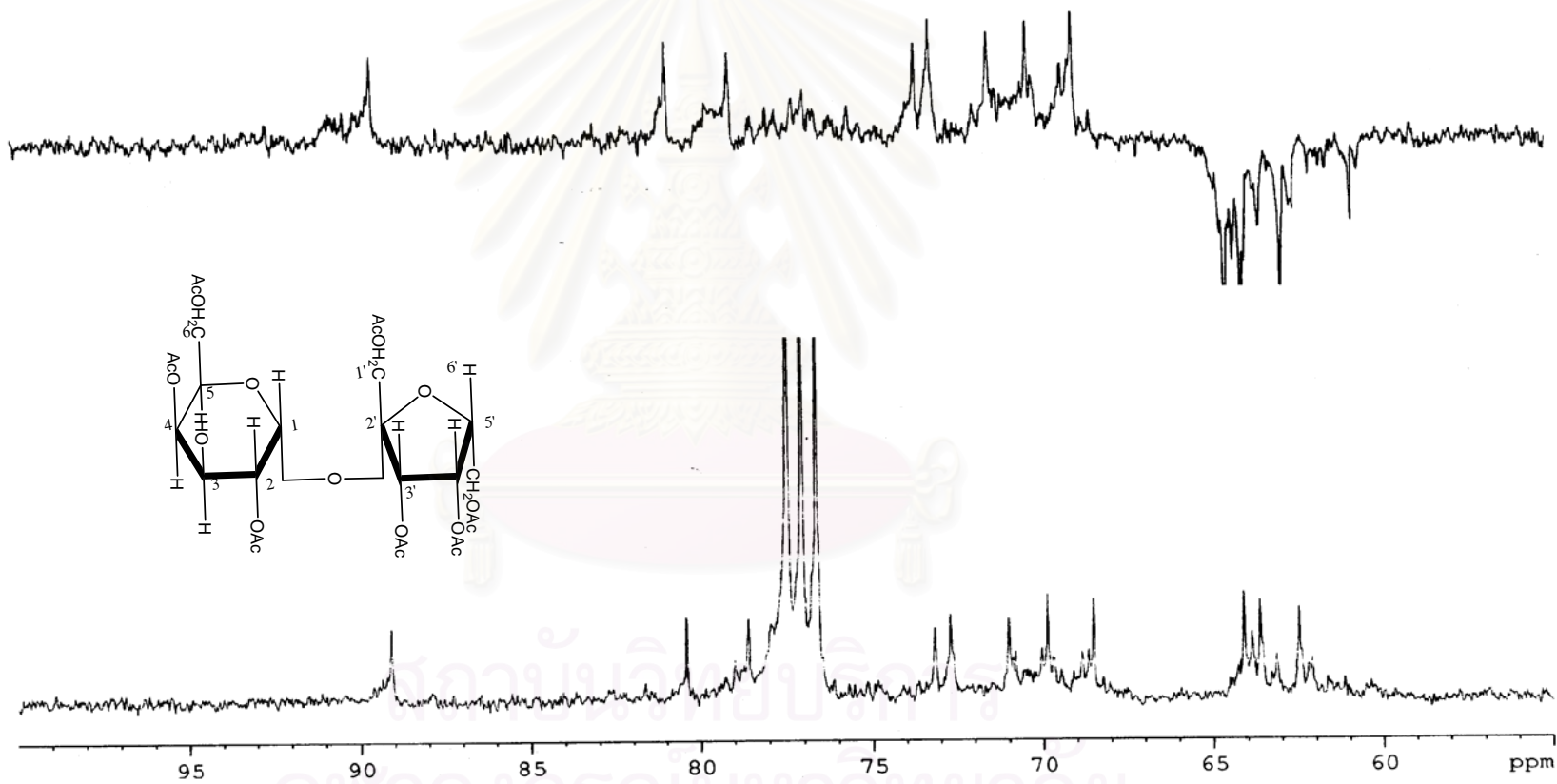


Figure 62 ^{13}C -DEPT (125 MHz) Spectrum of GP3 in CDCl_3

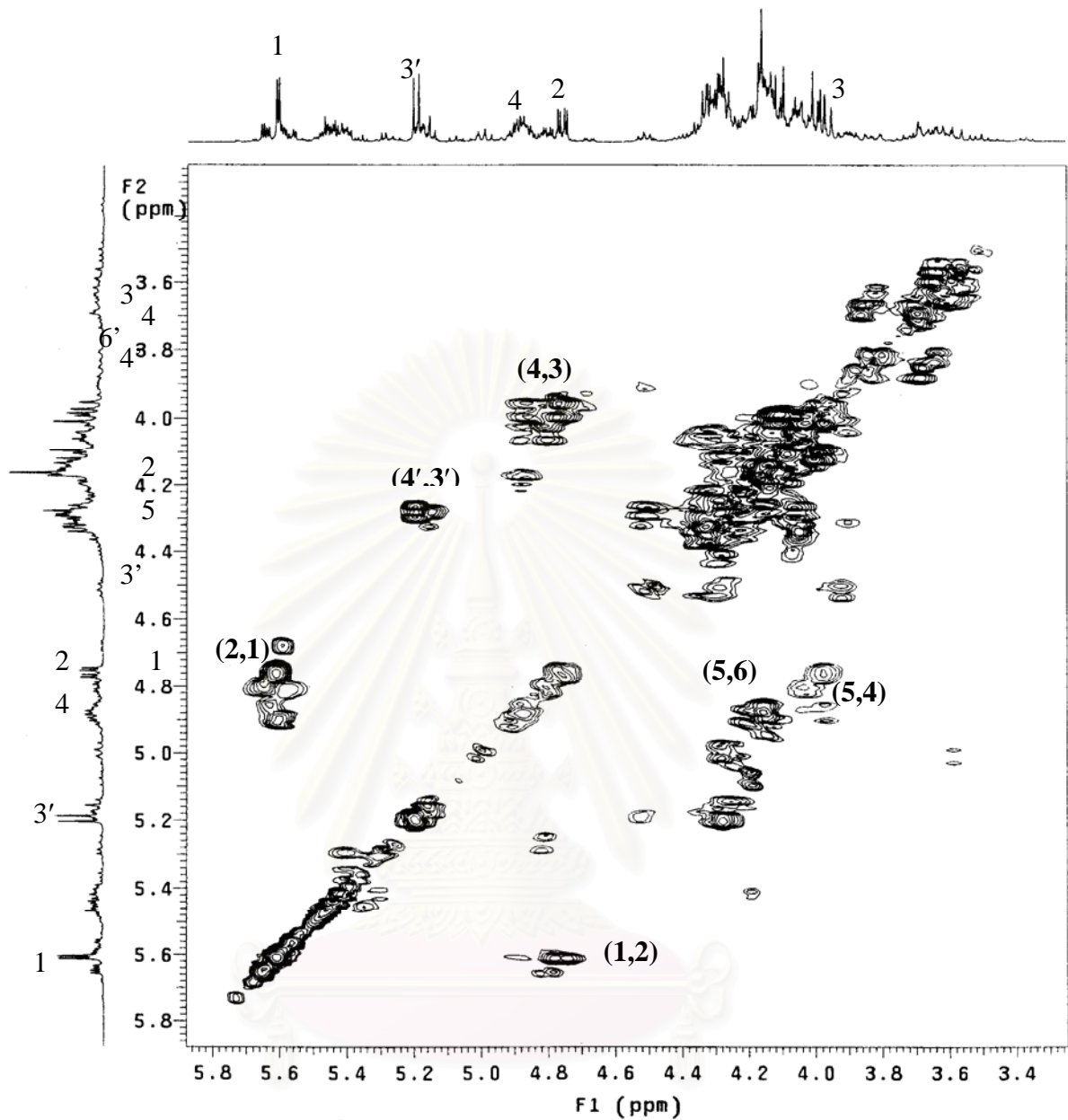
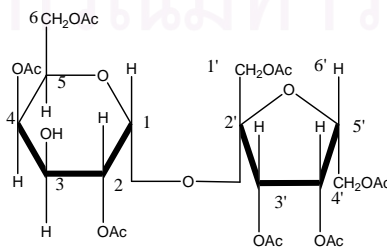


Figure 63 ^1H - ^1H COSY Spectrum of GP3 in CDCl_3



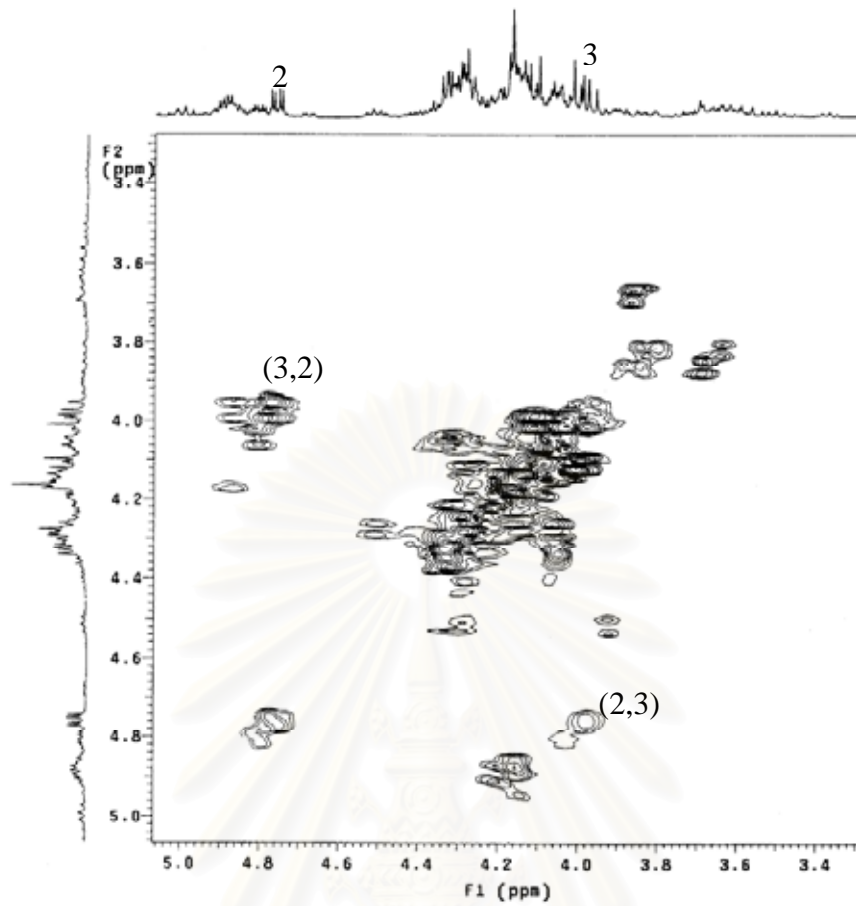
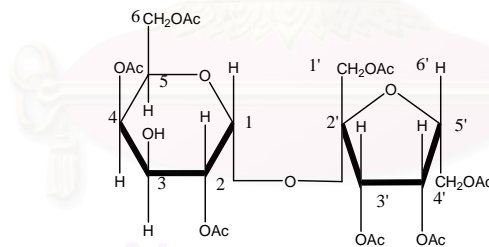


Figure 64 ^1H - ^1H COSY Spectrum of GP3 in CDCl_3



สถาบันวิทยบริการ
จุฬาลงกรณ์มหาวิทยาลัย

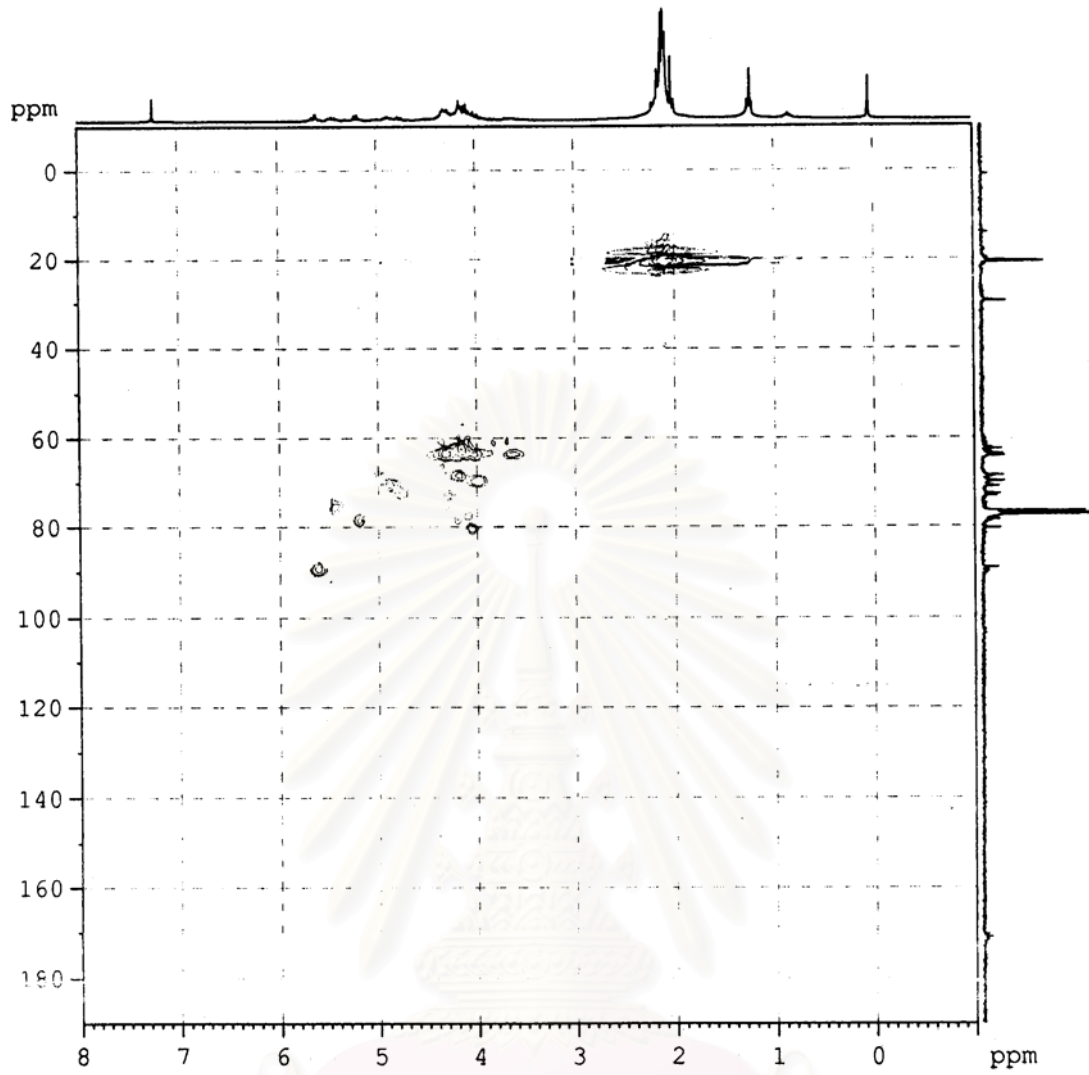
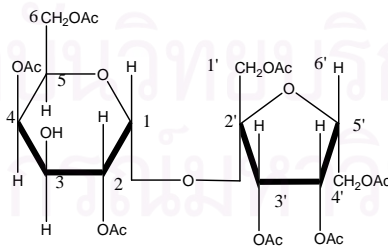


Figure 65 HMQC Spectrum of GP3 in CDCl₃



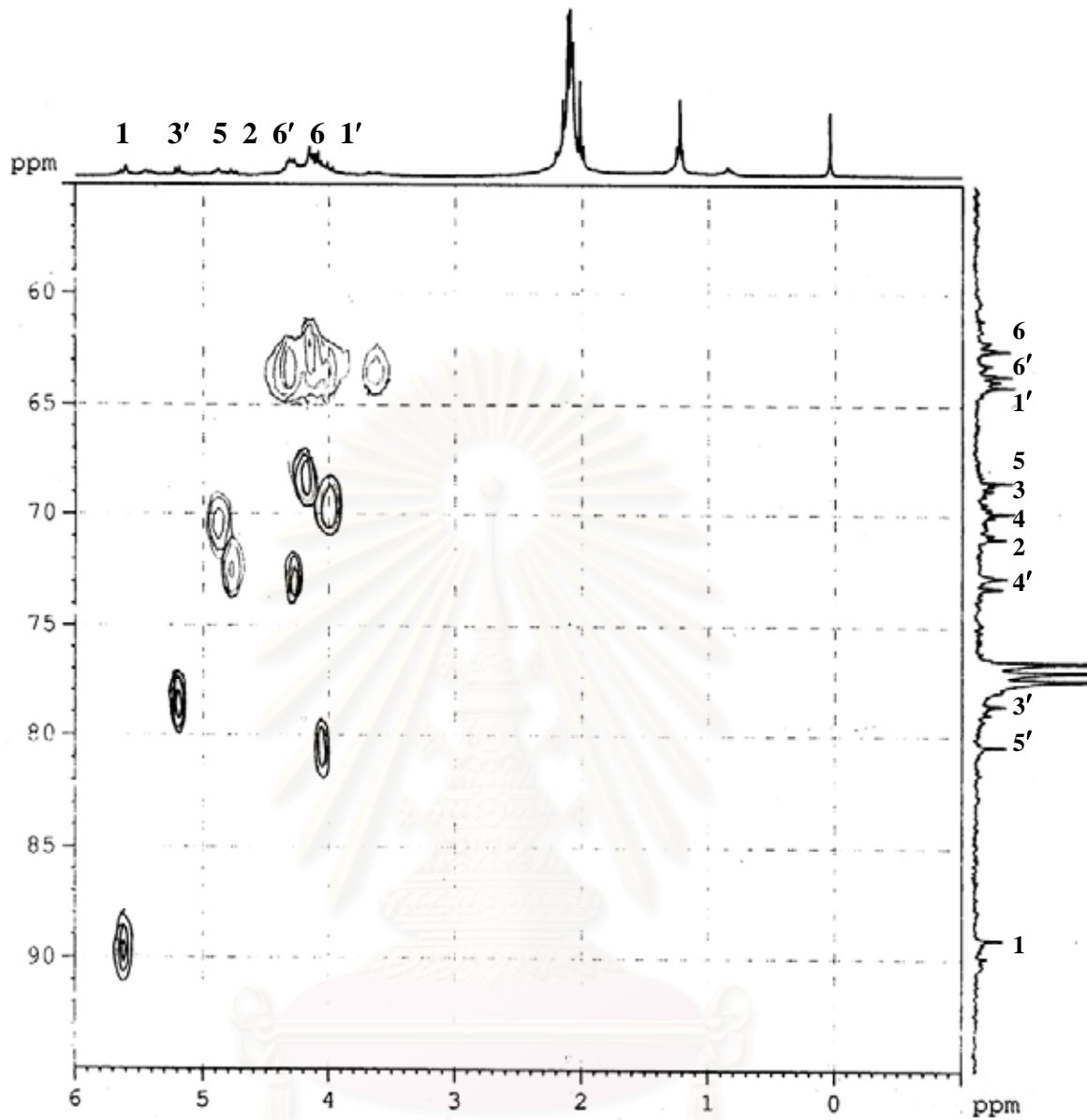
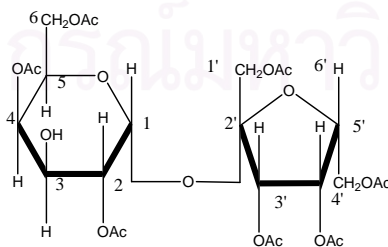


Figure 66 HMQC Spectrum of GP3 in CDCl_3



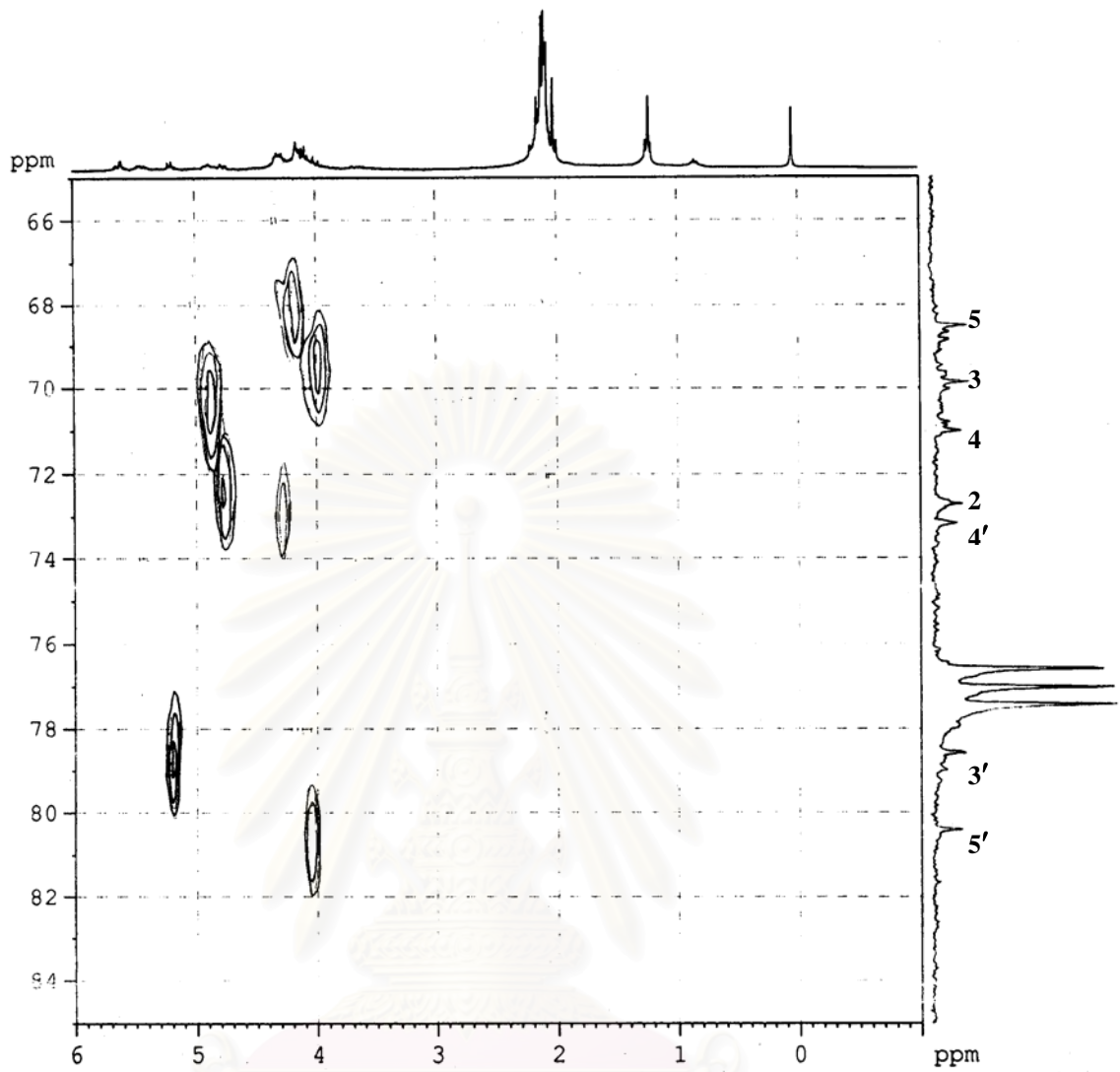
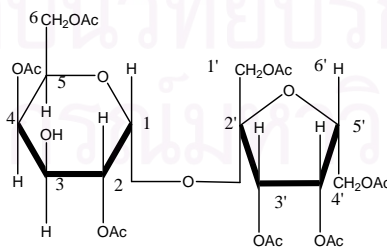


Figure 67 HMQC Spectrum of GP3 in CDCl_3



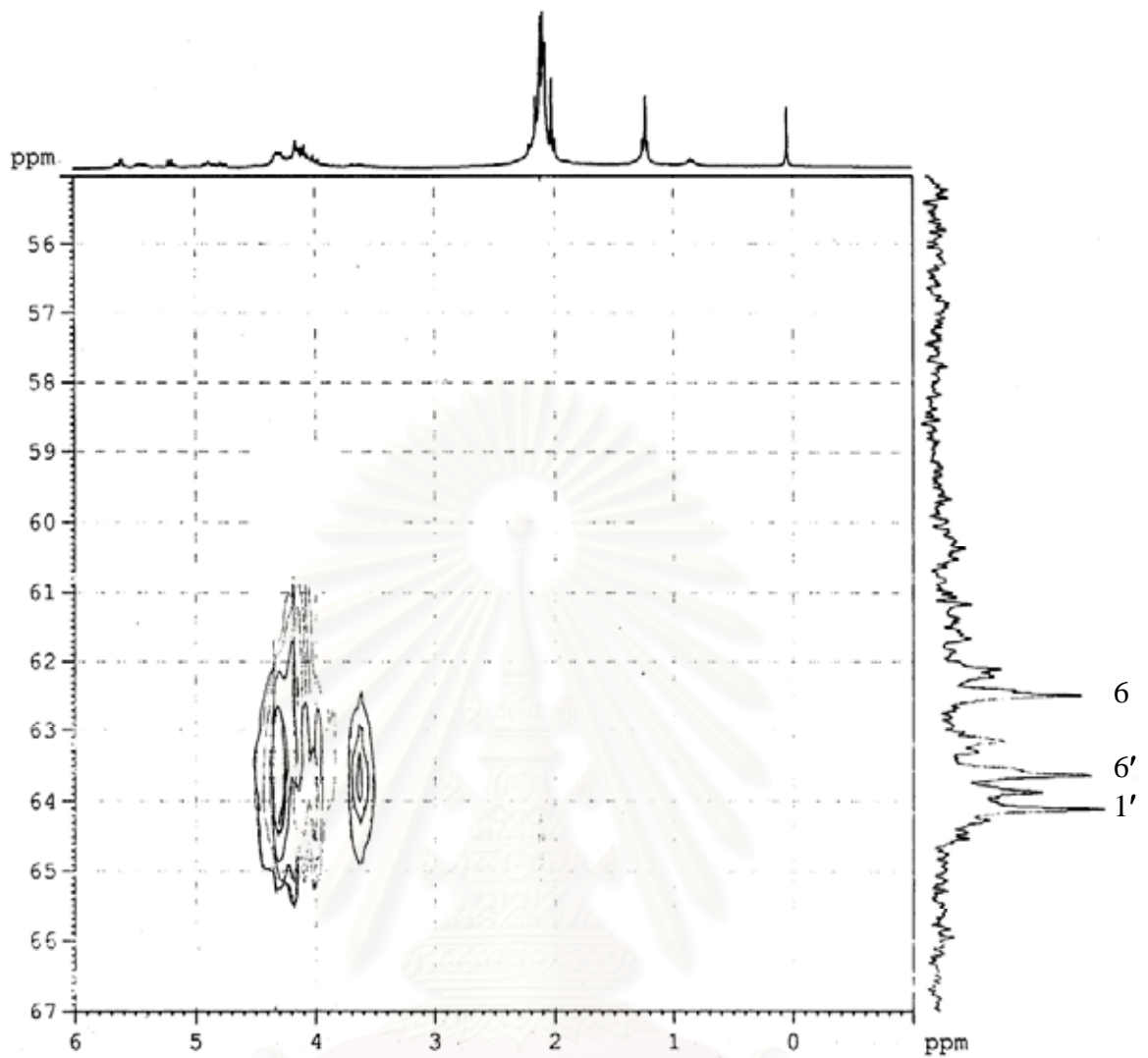
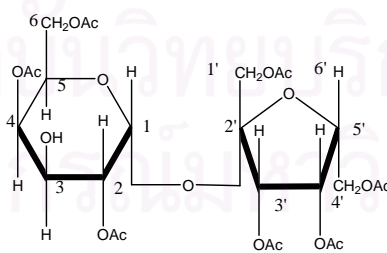


Figure 68 HMQC Spectrum of GP3 in CDCl₃



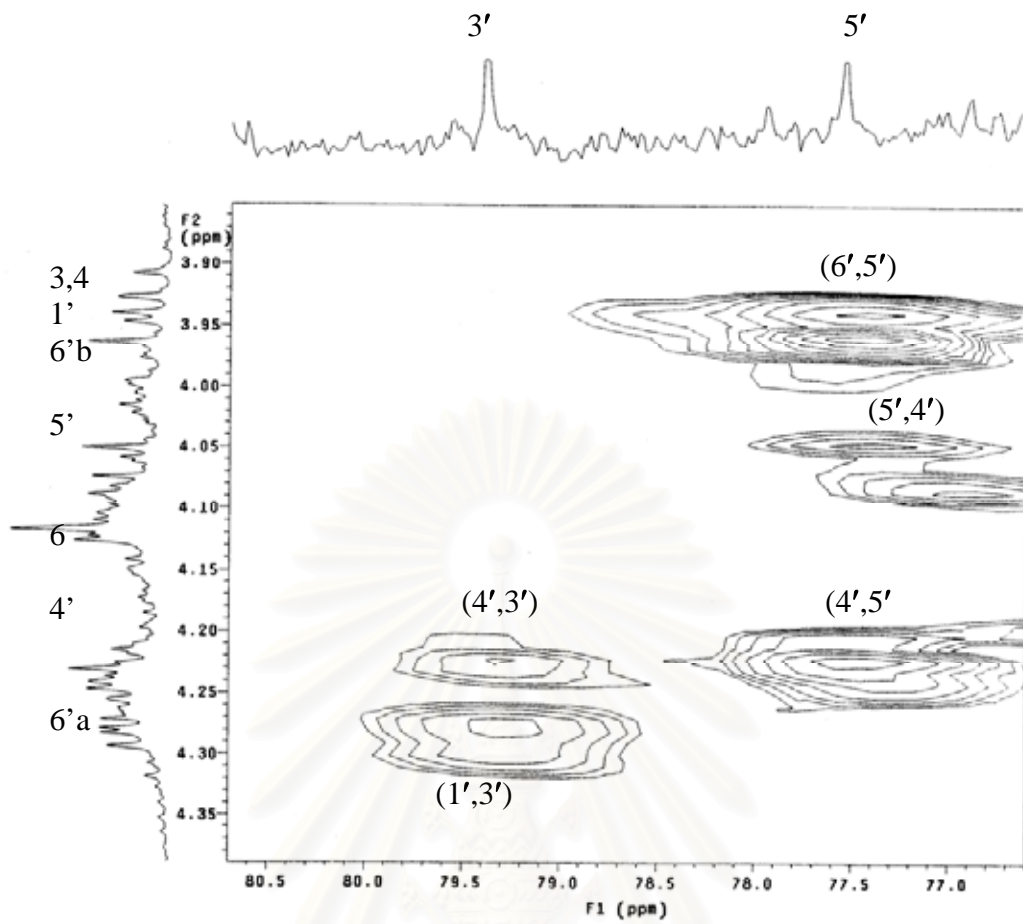
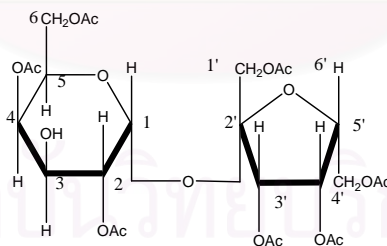


Figure 69 HMBC ($^nJ_{\text{HC}} = 8 \text{ Hz}$) Spectrum of GP3 in CDCl_3



สถาบันวิทยบริการ
จุฬาลงกรณ์มหาวิทยาลัย

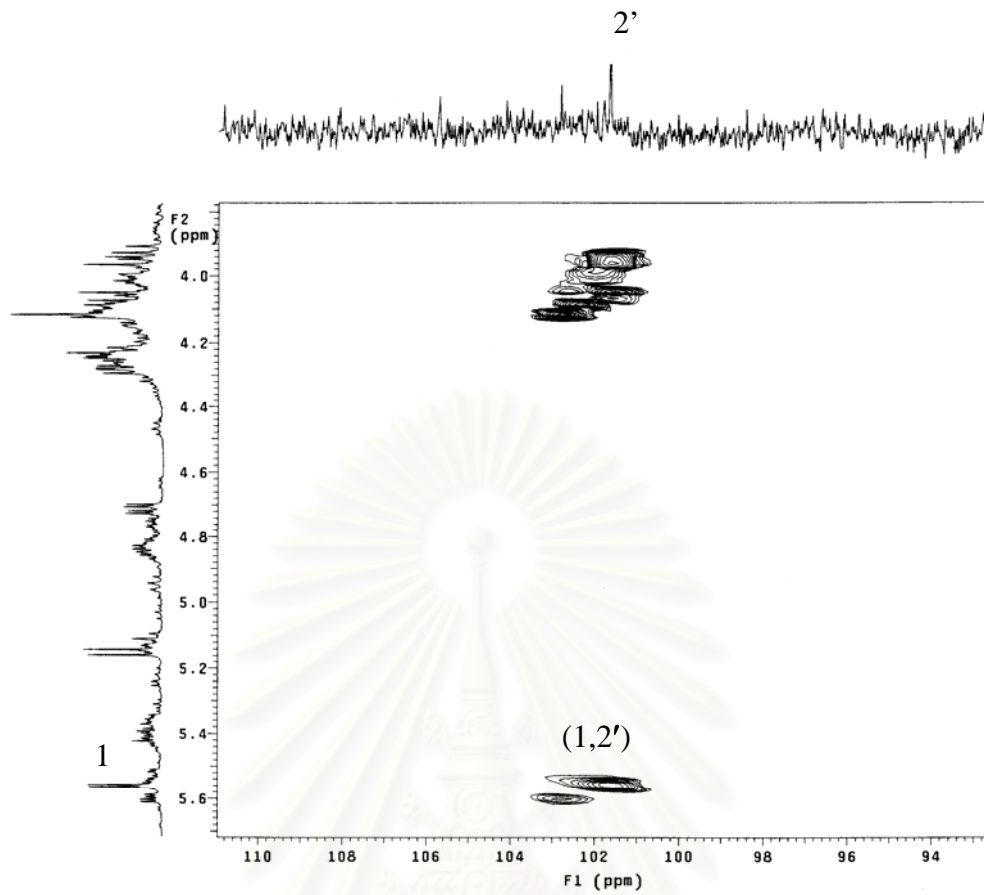
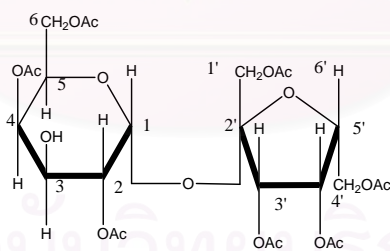


Figure 70 HMBC ($^nJ_{\text{HC}} = 8 \text{ Hz}$) Spectrum of GP3 in CDCl_3



สถาบันวิทยบริการ
จุฬาลงกรณ์มหาวิทยาลัย

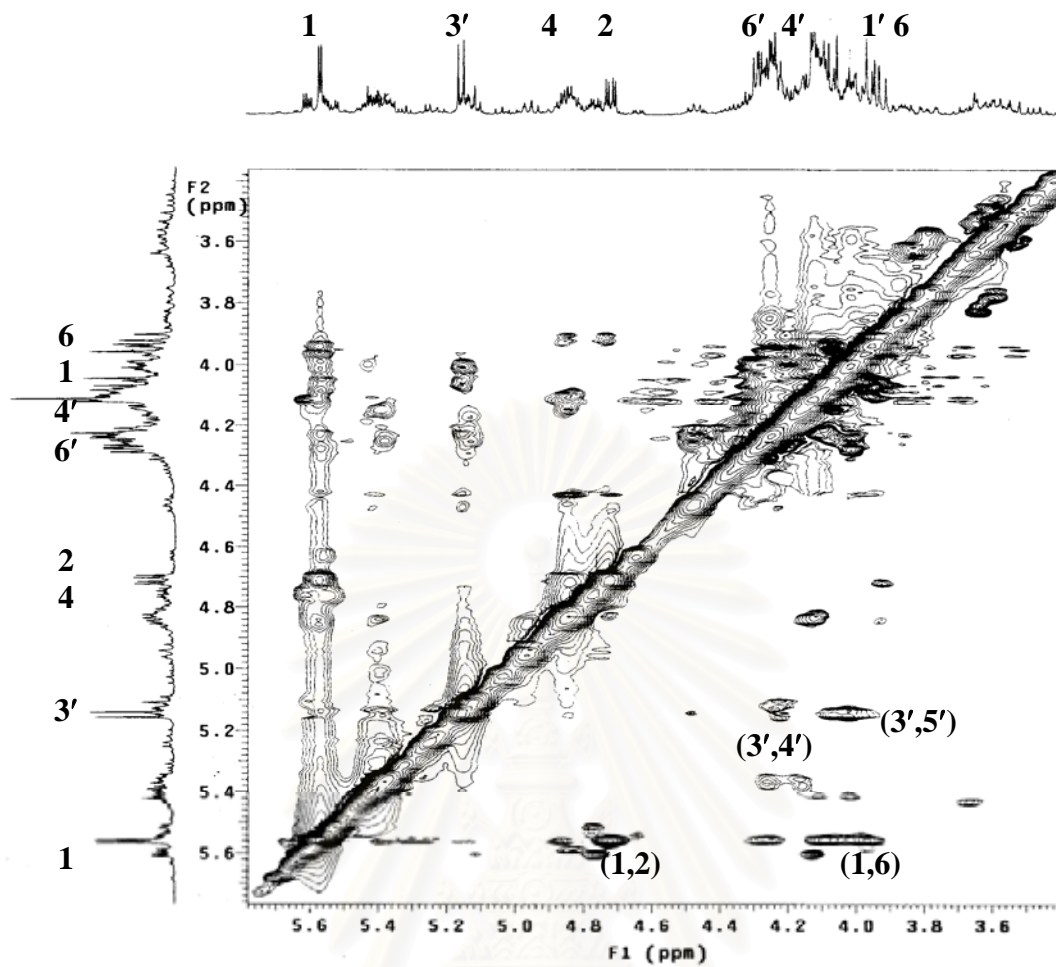
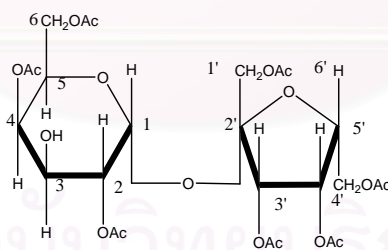


Figure 71 NOESY Spectrum of GP3 in CDCl₃



สถาบันวิทยบริการ
จุฬาลงกรณ์มหาวิทยาลัย

VITA

Ms. Jiranuch Mingmuang was born on February, 21st 1978 in Suphanburi province, Thailand. She received her Bachelor's degree of Science in Pharmacy in 2001 from Silpakorn Unniversity, Nakhon-pathom, Thailand. Since her graduation, she has been working as a pharmacist at the Institute of Medicinal Plant Research, Department of Medical Sciences, Ministry of Public health.



สถาบันวิทยบริการ
จุฬาลงกรณ์มหาวิทยาลัย